Dose intercomparisons between computer planning, *in-vivo* and phantom measurements for Iridium-192 HDR Brachytherapy

Freedom Hliziyo

HLZFRE001

MSc in Medicine, Medical Physics

Thesis presented in fulfillment of the requirements for the degree of Master of Sciences at the University of Cape Town.

Supervisor: Dr TC Kotzé

Department of Medical Physics

University of Cape Town

Co-supervisors: Mr C. Trauernicht & Ms H. Burger

Department of Medical Physics

University of Cape Town

May 2013

DECLARATION

I, the undersigned, hereby declare that the work contained in this thesis is my own original work and that I have not previously in its entirety or in part submitted it at any university for a degree.

Signature: Signed by candidate

Date: 17 May 2013

ABSTRACT

Abstract Title: **Dose inter-comparisons between computer planning, *in-vivo* and phantom measurements for Iridium-192 HDR Brachytherapy**

Introduction

During gynaecological high-dose rate (HDR) intracavitary brachytherapy (ICBT), *in-vivo* dosimetry is done to monitor the dose received by the bladder and rectum. This study was aimed at validating the need to do *in-vivo* dosimetry during ICBT. Thirty patients were recruited to participate in the study. Treatment setup data from the thirty patients was used to reproduce applicator and *in-vivo* diode treatment setups in a water phantom. Radiation doses administered to the patients were replicated in the water phantom to measure the doses at marked dose reference positions.

Method

Bladder identifying apparatus together with *in-vivo* bladder and rectal diode probes were inserted into the separate organs to measure the dose with the patient in the treatment setup position. Orthogonal x-ray images of the patient were taken and developed. International Commission for Radiological Units (ICRU 38) and American Brachytherapy Society (ABS) dose reference points recommendations were used to mark the bladder and rectal dose reference points onto the x-rays. On the same x-ray images, bladder and rectal diode dose points were also marked and then scanned into a treatment planning system (TPS). Patients were treated using optimized treatment plans and the dose registered by *in-vivo* dosimeters was recorded. For each treatment procedure, the applicator treatment setup was replicated in a water phantom and bladder and rectal diode dose measurements were done and recorded. Comparisons were made between the TPS planned doses, *in-vivo* and *in-vitro* doses for each treatment and patient.

Results

Thirty patients participated in the study. The ring and tandem applicator was used on 19 patients from whom valid data was drawn from 39 insertions. The vaginal cylinder and tandem combination (combo) was used on 11 patients from whom useful data was extracted from 11 insertions. The ratio of ICRU to *in-vivo* doses using the ring and tandem applicator were 1.4 ± 0.4 and 1.5 ± 0.4 for the bladder and rectum

respectively and correspondingly, 1.2 ± 0.5 and 1.8 ± 0.7 for the bladder and rectum when using the vaginal combo applicator. All in-vitro measurements closely confirmed the doses computed by the TPS and measured by the *in-vivo* diodes. For the rectum, *in-vivo* doses were higher than the TPS computed doses i.e. average ratio of TPS to *in-vivo* doses were 0.7 ± 0.1 and 0.8 ± 0.2 for the ring and tandem and vaginal combo applicators. The TPS planned doses closely compared to *in-vivo* doses for the bladder 1.1 ± 0.3 and 1.0 ± 0.1 for the ring and tandem and vaginal combo applicators. The variation in dose received by the bladder on separate ICBT insertions (intra-patient dose variation) calculated from TPS and *in-vivo* dose data was correspondingly 1.3 Gy and 0.6 Gy while for the rectum was 0.2 Gy and 0.5 Gy respectively. The random error associated with reproducing patient setups in the water phantom ranged from 0.1 Gy to 0.4 Gy for both bladder and rectum dose measurements. Paired sample T-test showed that TPS and *in-vivo* dosimetry had similar sample means and good correlation, i.e. $p = 0.00$ and average correlation coefficient > 0.75. Regression analyses of TPS against *in-vivo* doses showed scattered data plots with no linear relationship between data and relatively low R-squared values for plotted graphs, i.e. $R^2 \leq 0.60$.

Conclusion

Treatment planning using orthogonal radiographs and ICRU dose reference points to monitor doses received by organs at risk (OARs) is a fairly good method of verifying doses during ICBT. Bladder *in-vivo* dose measurements agreed with TPS doses corresponding to the 'setup point' in the patient for both the ring and tandem and vaginal combo applicators. Rectum *in-vivo* dose measurements were remarkably higher (by up to an average of 31%) compared to TPS planned doses. This may mean that the TPS underestimates the dose that the rectum receives during ICBT. *In-vitro* measurements confirmed the relationship between TPS planned doses and *in-vivo* measurements in the bladder and rectum for both the ring and tandem and vaginal cylinder applicators. Regression analysis cannot be reliably used to predict *in-vivo* and TPS planned doses. Therefore, individualized treatment plans must be done for each patient for each treatment. Computerised treatment planning and *in-vivo* dosimetry are separate complementary procedures that may be done simultaneously and independently to monitor the dose received by OARs during HDR brachytherapy.

ACKNOWLEDGEMENTS

I want to thank my supervisors for supervising my work and advising me throughout this research, especially Dr Tobie Kotze for his encouragement, Dr Leon Van Wijk and Chris Trauernicht for enduring long hours with me doing the practical work and for the advice, Jan Hough and Hester Burger for the constructive criticism and motivation and Dr Gerrie Maree for the support.

I would like to thank the mechanical workshop staff, Robin and Charlie, as well as Kobus Botha, Susan Tovey, Dr Alistair Hunter, C9 oncology nurses, radiology radiographers (Mrs Del Porto and Kashiefah), all medical physics interns and radiation oncology staff for assisting me in various ways to make this research possible.

I would like to thank the International Atomic Energy Agency (IAEA) for availing to me the opportunity to train and study Medical Physics at Charlotte Maxeke Johannesburg General Hospital, Groote Schuur Hospital and University of Cape Town in South Africa.

A big thank you goes to my wife Joyline for her love, understanding, endurance and encouragement and also to my son Tinotenda for his patience and being my inspiration. I am also grateful to my parents and in-laws for being there for me and my family all the way.

Finally I want to thank Jehovah God for giving me the inspiration to do this research and for making everything possible through His Son Jesus Christ, Amen.

CONTENTS

LIST OF FIGURES

LIST OF TABLES

CHAPTER 1 INTRODUCTION

1.1 Introduction

Brachytherapy comes from the Greek word βραχυς *brachys*, which means a short-distance, and is a form of radiotherapy in which a radioactive source is inserted into or close to a tumour. Brachytherapy is mainly used in combination with external beam radiotherapy (EBRT), chemotherapy and surgery; however, it can also be used alone. (Gerbaulet, et al., 2005) & (Anon., 2012). In brachytherapy, the radioactive source is encased in a thin titanium wire capsule which allows radiation to be emitted into the surrounding tissue and at the same time, protects against direct contact of the radioisotope with body tissue and interaction with bodily fluids. A desirable characteristic of brachytherapy sources is that they release short-range radiation that affects a localized region around the tumour volume. This limits unnecessary irradiation of normal healthy tissue and organs surrounding the tumour. Studies done to investigate the efficacy of brachytherapy have shown that treatment using brachytherapy is comparable to surgery and external beam therapy, or is enhanced when used adjuvant to surgery, and/or EBRT. (Viswanathan & Petereit, 2007) (Pickles, et al., 2009), (Haie-Meder, et al., 2009), (Battermann, et al., 2004) & (Galalae, et al., 2004).

1.1.1 History of Brachytherapy

In 1896 radioactivity was discovered by Henri Becquerel after a photographic film was accidentally exposed to uranium. Brachytherapy started as early as 1901, Pierre Curie postulated that it was possible to place a radioactive source inside a tumour. Danlos investigated this and found that the tumour shrunk as a result of the radiation. This gave birth to the practice of brachytherapy and in 1901 the first cancer treatments with radium were done. In 1901, Danlos and Bloc used radiation to treat lupus at the St. Louis Hospital in Paris, radium implants were done in the USA by Robert Abbe in 1905 at St Luke's and Memorial Hospital in New York, and in 1909 Finze in England

started to treat patients using radium (Gerbaulet, et al., 2005) & (Anon., 2012).

The use and development of brachytherapy decreased in the middle of the twentieth century because operators were exposed to radiation while manually handling radioactive sources during patient treatments. This challenge was overcome in the 1950s and 1960s with the use of new alternative radioactive sources, e.g. caesium and iodine, and the new design of equipment which provided shielding to the source and remote afterloading systems.

The development of afterloading systems with the capability to change source positions and dwell times has greatly enhanced the quality of treatments. Advances in medical imaging have also facilitated "more accurate definition of target volume and the localisation of adjacent normal tissue together with computerised dosimetry and better knowledge of the radiobiology involved", and have made brachytherapy much more accurate and safe (Gerbaulet, et al., 2005).

1.1.2 Types of Brachytherapy

There are four ways of describing brachytherapy and these depend on:

i. Source placement,
ii. Overall treatment duration,
iii. The dose rate, and
iv. Method of source loading.

1.1.2.1 Source Placement

- Interstitial brachytherapy is when radiation sources are placed inside the tissue or tumour, e.g. for treatment of the breast, skin and prostate.
- Contact /plesiobrachytherapy is when the radiation sources are placed close to or next to the tissue or tumour. Within contact brachytherapy there are four different types of brachytherapy, namely intracavitary, intraluminal, endovascular, and surface brachytherapy:

- Intracavitary brachytherapy is when radioactive sources are inserted into body cavities close to the tumour, e.g. in the cervix and nasopharynx .
- Surface brachytherapy is when radioactive sources are placed directly over the tissue to be irradiated, e.g. on the skin and soft tissue sarcoma.
- Intraluminal brachytherapy is when sources are inserted into a lumen, e.g. oesophagus and bronchus.
- Endovascular brachytherapy is when radiation sources are inserted into small or large arteries or veins. (Gerbaulet, et al., 2005) and (Podgorsak, 2005)

1.1.2.2 Overall Treatment Time

- Permanent implants are small radioactive sources that are encapsulated in very thin metal capsules, i.e. iodine seeds. The radioactive seeds usually have a short half-life and are implanted inside the tissue to irradiate the tumour over the lifetime of the source (Devlin, 2007). The radiation strength of the seeds is very low such that there is no afterloading required to place the seeds into the tissue.
- Temporary implants are placed inside the tumour site for a given amount of time until the prescribed dose is delivered after which they will be removed (Gerbaulet, et al., 2005). Caesium and iridium are the elements of choice for most temporary implants and they are placed into the tumour site in the patient using remote afterloading systems.

1.1.2.3 Dose Rate

- Low-dose rate brachytherapy systems will have radioactive sources which deliver dose rates of about 10 Gy per day, i.e. 0.4 – 2 Gy/hr.
- Medium-dose rate brachytherapy systems have radioactive sources which deliver dose rates of about 10 Gy per hour, i.e. 2 – 12 Gy/hr.
- High-dose rate brachytherapy systems have radioactive sources which deliver dose rates of about 10 Gy per minute, i.e. > 12 Gy/hr.

- Pulsed-dose rate (PDR) brachytherapy is another form of brachytherapy that uses an afterloading system with an Iridium-192 source. Ten minute-dose pulses are given are given each hour to achieve a dose equivalent of 60 cGy per hour. The optimization of the dose accomplished by this method is the same as that of HDR and the biological effect is the same as that obtained when using LDR (Devlin, 2007).

1.1.2.4 Method of Source Loading

- Hot loading is when the radioactive sources are loaded into the applicators before the applicator is inserted into/onto the patient.
- Afterloading is when the applicator is first placed into position and the radioactive sources will be loaded thereafter by hand or automatic remote afterloading (Gerbaulet, et al., 2005) and (Podgorsak, 2005).

1.2 Afterloading Devices

The careful, accurate and precise placement of applicators, guides, catheters or tubes into or next to tissues, in which radioactive sources will be loaded is called afterloading. Positioning of radiation sources is of utmost importance in brachytherapy. There are two types of afterloading, namely manual and remote afterloading systems.

1.2.1 Manual Afterloading

Manual afterloading is when the applicators, gutters, tubes, catheters, needles and the sources themselves are placed and loaded by hand.

1.2.2 Remote Afterloading

Remote afterloading systems move radiation sources from the source safe into applicators placed in or onto the patient. Current remote afterloader systems are capable of accurate and precise positioning of the source and retract the source back into the radiation safe after each treatment. The radioactive source is also retracted back to the source safe if a dummy source

released into the channel prior to treatment, encounters an uneven pathway, i.e. kinks along the source channel, or if a treatment room door with interlocks is opened, or when an emergency switch is activated. This method of administering radiation achieves good radiation protection, and with the help of good imaging modalities enables more accurate positioning of source applicators. Remote afterloading systems also allow users to change the source position and dwell times to achieve different dose distributions, thereby achieving individualised patient treatment (Gerbaulet, et al., 2005), (Devlin, 2007) & (Podgorsak, 2005).

1.3 Radiobiology Concepts of Brachytherapy

Dose distribution, treated volume, dose rate and treatment duration greatly determine the biological results of radiotherapy. The degree to which each of these aspects influence the outcome of radiotherapy is different for brachytherapy and external beam therapy. High doses are given in short times for a small number of fractions in brachytherapy. This is not applicable in external beam therapy since normal tissue cannot withstand such high doses due to the volume-effect relationship: small volumes of normal tissue (e.g. 1 – 2 cm^3) are capable of withstanding high doses of radiation that larger volumes would not withstand. This phenomenon may be explained as resulting from the nature of vascular supply which is arranged in three dimensions inside normal tissues (Gerbaulet, et al., 2005) and (Devlin, 2007). Similar radiobiology characteristics shown in continuous LDR, hypofractionated HDR and hyperfractionated PDR are also evident in normal fractionated external beam therapy. However, the major advantage of brachytherapy is the steep dose gradient as a function of distance from the source. Furthermore, radiobiologic dose sparing is also achieved due to the decrease of the dose and dose rate with distance (Gerbaulet, et al., 2005) and (Devlin, 2007).

Tumour repopulation, repair of sub-lethal damage, and the extent to which tumour re-oxygenation occurs, greatly influence the outcome of the treatment. Changes that may occur in the dose rate are the same as changes in dose

per fraction in external beam therapy. Dose rate plays an important part in influencing radiobiological systems. Outcomes of radiotherapy reduce as the dose rate reduces since there will be more repair of tumour cells (Devlin, 2007).

1.4 Properties of Brachytherapy Photon Sources

1.4.1 Practical Characteristics of Photon Sources

Radioactive sources used in brachytherapy are always enclosed in a thin metal capsule for purposes of:

- controlling the emission of radiation;
- giving source rigidity;
- containing other undesired types of radiation, i.e. α or β particles that may be released during source decay.

The metal capsule also serves to avoid direct contact of the radioactive source with tissue and also prevents the interaction of the radiation source with bodily fluids (Podgorsak, 2005). The desired radiation from a brachytherapy source is made up of the following:

- γ- rays, which constitute the fundamental part of the radiation produced;
- characteristic x-rays which are produced occasionally as a result of electron capture and intrinsic transformations that take place in the source;
- characteristic x-rays and bremsstrahlung that are produced in the capsule enclosing the source.

The selection of a radioisotope that releases a particular radiation of preference in brachytherapy is determined by a number of physical and dosimetry properties (Podgorsak, 2005), which are:

i. Energy of the photons, photon range in tissue and the amount of shielding required;
ii. Half-life;

iii. Half-value layer in lead and other shielding materials;
iv. Specific activity;
v. Source strength;
vi. Inverse square decrease in dose as a function of distance from the source.

Table 1.0 (see next page) gives a list of the properties of radioisotopes most used in brachytherapy.

1.5 Gynaecological High-Dose Rate Brachytherapy

This research is concerned with gynaecological high-dose rate (HDR) brachytherapy, which is a form of intracavitary brachytherapy. Cancers of the uterine cervix, uterine body and vagina are usually treated using intracavitary brachytherapy. A variety of applicators can be used for insertions in gynaecological brachytherapy. A chosen applicator for a particular patient is placed into the body cavity and images of the patient are taken with the applicators in place in order to determine the position of the applicators relative to the tumour. Modern image guided radiotherapy (IGRT) remote afterloaders allow guided placement of applicators to the region of interest close to the tumour. After correct placement and positioning of the applicators, radioactive sources will move into specified positions (dwell positions) for predetermined dwell times to achieve a dose distribution to adequately cover the tumour during treatment. Caesium-137, Iridium-192 and recently Cobalt-60 are commonly used for treatment of gynaecological cancers.

1.5.1 Side Effects

External beam radiotherapy followed by intracavitary HDR brachytherapy has become the standard treatment for gynaecological malignancies (Gerbaulet, et al., 2005). However, patients who have undergone the treatment regime may suffer from bladder and rectum early and late complications as side effects of the treatment due to the closeness of these organs to the sources of radiation during intracavitary brachytherapy (Gerbaulet, et al., 2005), (Wang, et al., 1997) and (Pötter, et al., 2000). Recent studies have revealed that there

is an insignificant difference in the occurrence of complications in patients who receive either LDR or HDR brachytherapy (Viani, et al., 2009).

Table 1.0: Properties of radioisotopes used in brachytherapy (Podgorsak, 2005).

Radioisotope	Average photon energy (MeV)	Half-life	HVL in lead (mm)	$\Gamma_{AKR}{}^{b,d}$ $\left(\frac{\mu Gy^{-}m^{2}}{GBq.h}\right)$	$\Lambda^{c,d}$ $\left(\frac{cGy.h^{-1}}{cGy.cm^{2}.h^{-1}}\right)$
Cobalt-60	1.25	5.26 years	11	309	1.11
Caesium-137	0.66	30 years	6.5	77.3	1.11
Gold-198	0.41	2.7 days	2.5	56.2	1.13
Iridium-192	0.38	73.8 days	3.0	108	1.12
Iodine-125	0.028	60 days	0.02	-	-
Palladium-103	0.021	17 days	0.01	-	-

Where $\Gamma_{AKR}{}^{b,d}$ is the air kerma rate constant and Λ is the dose rate constant.

Table 1.1 Possible complications after LDR or HDR brachytherapy (Devlin, 2007)

Acute	Late
Urine perforation	Proctitis
Vaginal laceration	Ulceration of the bladder or rectum
Fever	Fistula
Thrombotic events	Stricture
Anaesthesia related nausea	Vaginal stenosis

Table 1.1 above shows the complications that can arise from either LDR or HDR brachytherapy.

HDR brachytherapy is used at most centres, since it facilitates treatment for many patients on any single day to achieve the same results as LDR brachytherapy (Viani, et al., 2009). There are two categories of factors that contribute to radiotherapy-induced toxicity: radio-brachytherapy techniques and doses, and/or non-irradiation techniques, e.g. surgery, concomitant chemotherapy and diabetes (Gerbaulet, et al., 2005). This research is interested in complications that may be attributed to radiation and will look at methods of dosimetry used to measure and monitor the doses that the organs at risk (OARs) receive during intracavitary HDR brachytherapy.

1.6 Dissertation Aims

The aim of this thesis is to introduce and evaluate a reliable method to perform *in-vivo* dosimetry on patients undergoing intracavitary HDR brachytherapy as part of treatment for gynaecological malignancies at Groote Schuur Hospital, Cape Town. The doses to patients' critical organs, i.e. the bladder and rectum are going to be computed using a treatment planning system (TPS), which will derive information from orthogonal films. In-vivo dose measurements in the bladder and rectum will be made in patients on a separate treatment day. A water phantom with accessories to mount patient applicators and *in-vivo* probes will be made to reproduce the treatment set-up

of patients and dose measurements will be made in water. Comparisons will be made between the values of dose computed from the TPS, *in-vivo* dose measurements in patients and measurements made in water for the dose received by the bladder and rectum during gynaecological intracavitary brachytherapy. Mathematical analysis of the computed and measured values will be made to investigate the relationship between these values. The investigator will compare computed with measured values to ascertain whether the treatment planning system gives a true reflection of the actual dose received by the OARs during treatment. Evaluation of doses measured in patients and doses measured in a water phantom will be compared to establish if the inhomogeneities present in patient anatomies should be taken into account when computing dose to critical organs.

CHAPTER 2 LITERATURE REVIEW

2.1 Sources of Radiation

Radiation used for medical purposes is sourced either from radioactive materials or from x-rays produced through the *bremsstrahlung* process. Radioactive substances are the main source of radiation used for brachytherapy procedures, although there is advanced on-going research of employing bremsstrahlung techniques to produce low energy x-rays to be used in brachytherapy. This research will cover radiation derived from radioactive isotopes since the research was done using Iridium-192.

2.1.1 Radioactivity

Radioactivity was discovered by Antonio Henri Becquerel in 1896 and is defined in general terms as the random and spontaneous decay of unstable nuclei in elements, producing radiation in the process. The radiation produced may be in nature of particles, electromagnetic radiation or a combination of both (Khan, 2010). Rutherford and Soddy in 1902 and later Bateman in 1910, came up with laws that characterize the exponential disintegration of radioactive substances with time (Podgorsak, 2005).

A typical radioactive decay involves an arbitrary parent nucleus P that decays with a decay constant into a stable daughter nucleus D (Podgorsak, 2005):

$$\mathrm{P} \xrightarrow{\lambda_p} \mathrm{D} \qquad \ldots (2.1)$$

At any time t, there will be $N_p(t)$ number of parent nuclei which will be decaying according to the mathematical relationship:

$$N_p(t) = N_p(0)e^{-\lambda_p t} \qquad \ldots (2.2)$$

$N_p(0)$ being the original number of nuclei at the beginning of the decay, i.e. time $t = 0$. Another radiation describing term, activity A, was introduced in

1962 by the International Commission on Radiological Units (ICRU, 1962). The latest definition of activity (ICRU, 1980) is:

" The activity *A* of an amount of radioactive nuclide in a particular energy state at a given time is the quotient of dN by d*t* where dN is the expected value of the number of spontaneous nuclear transitions from that energy state in the time interval d*t*."

i.e. $$A = {}^{dN}/_{dt} \quad \ldots (2.3)$$

Therefore, the parent nuclei activity $A_p(t)$ at time *t* is:

$$A_p(t) = A_p(0)e^{-\lambda_p t} \quad \ldots (2.4)$$

Where the activity at the beginning of the disintegration when *t* = 0 is $A_p(0)$. Another important radioactive measurement unit is the half-life $t_{1/2}$, which is defined as the time taken for either the number of nuclei or the activity to decay to half the initial value (Khan, 2010):

$$N_p\left(t = t_{1/2}\right) = \frac{1}{2} N_p(0)e^{-\lambda_p t_{1/2}} \quad \ldots (2.5)$$

i.e. $$t_{1/2} = \frac{\ln 2}{\lambda_p} \quad \ldots (2.6)$$

2.1.2 Photon Beams

A beam of radiation, either x-rays emanating from a target or γ-rays from a radioactive source, consists of many photons, possibly of different energies (Khan, 2010). The photon fluence (Φ) represents the number of photons dN that are incident on a hypothetical sphere having a crossing-sectional area da, i.e.:

$$\Phi = {}^{dN}/_{da} \quad \ldots (2.7)$$

2.2 Interactions of Ionizing Radiation

Photons are known as indirectly ionizing radiation, since charged particles, i.e. directly ionizing particles are produced when photons pass through a medium. A beam of photons, i.e. x- or γ-rays, traversing through matter often transfers energy to the medium. Usually, electrons are emitted from the absorbing medium as a result of the energy transfer. These secondary electrons release their energy by effecting further ionization and excitation of atoms with which they collide as they traverse through the medium. (Khan, 2010). When radiation is incident on body tissues it may produce ionization and excitation of atoms within the tissue, resulting in enough energy being deposited within the cells and thus incapacitating their ability to reproduce. When photons interact with matter there are three main processes that produce secondary high-speed electrons in the absorbing medium (Khan, 2010):

i. Photoelectric effect;
ii. Compton effect; and
iii. Pair production

2.2.1 Photoelectric Effect

Photons with low energies interact with matter predominantly by the photoelectric effect. The photoelectric effect involves interaction between a low energy photon and an atom and does not occur between a photon and a free electron. All the energy from the incident photon is absorbed in the atom and an electron is ejected in the process. The ejected electron takes up the energy of the photon E minus the binding energy E_{shell} of the electron, giving the electron kinetic energy T_e (Baltas, et al., 2007).

$$T_e = E - E_{shell} \quad \ldots (2.8)$$

The probability of photoelectric effect occurring is highest for K-shell electrons, i.e. approximately 80 % of the interactions involve K-shell electrons. The probability for photoelectric effect occurring for L- and M-shell electrons drops very sharply from the K-shell. Photoelectric attenuation also depends heavily

on the atomic number of the absorbing medium that can be approximated by the mathematical equation:

$$\tau/\rho \propto Z^3 \quad \ldots (2.9)$$

The dependence of photoelectric effect on the atomic number of the absorbing material is exploited in diagnostic radiology where the different Z of tissues, e.g. bone, muscle, fat and adipose tissue magnifies the differences in x-ray absorption, which results in a well defined topographic anatomical image (Khan, 2010).

2.2.2 Compton Effect

Compton scattering (incoherent scattering) occurs when a photon collides with a free electron and there is an inelastic collision. The photon imparts some of its energy to an atomic electron which scatters away from the atom, while the photon is deflected with less energy at an angle to its direction of incidence (see Fig 2.1). If the electron is assumed to be at rest and a free electron, then the energy of the scattered photon in relation to the scattering angle θ is given by (Baltas, et al., 2007)

$$E_{sc} = E \frac{1}{1+\left(E/m_e c^2\right)(1-cos\theta)} \quad \ldots (2.10)$$

where the energy of the photon at incidence is E, the rest energy of the electron is $m_e c^2$, and T_e is the kinetic energy imparted to the recoil Compton electron:

$$T_e = E - E_{sc} = \frac{\left(E/m_e c^2\right)(1-cos\theta)}{1+\left(E/m_e c^2\right)(1-cos\theta)} \quad \ldots (2.11)$$

The energies of the recoil electron T_e and the scattered photon E_{sc} are determined by the scattering angle and the incident photon energy as shown in equations 2.10 and 2.11 above. Compton interaction relies on the number of free electrons per unit mass of absorbing material and does not depend on the atomic number Z of the material. The Compton effect also depends on the energy of the incident photon, i.e. the energy of the incident photon must be

comparatively larger than the binding energy of the electron for Compton scatter to take place.

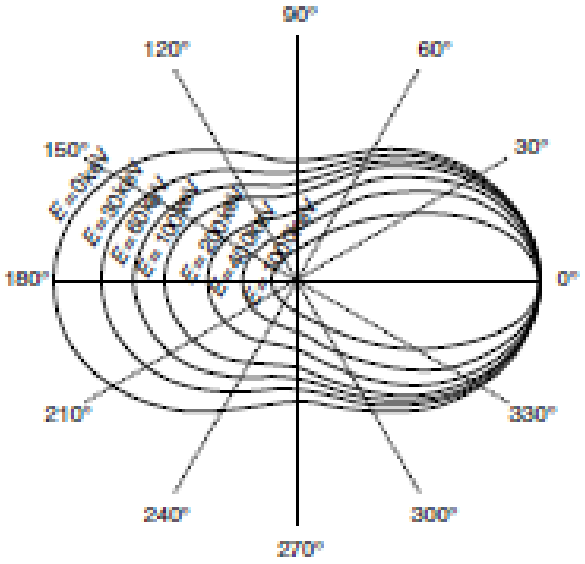

Figure 2.1 Angular distribution of photons with incident energies of up to E = 1 MeV scattered by a free electron (Baltas, et al., 2007)

2.2.3 Pair Production

Pair production can occur when photons with energies greater than 1.022 MeV traverse through matter. During pair production, the photon is involved in intense electromagnetic interactions with an atomic nucleus such that all of the photon's energy is absorbed and an electron and positron pair is created (Khan, 2010). A photon with an energy equivalent to 1.022 MeV has sufficient energy to produce the electron and positron pair since the rest mass energy of the electron is 0.511 MeV and the incident photon energy is enough to produce a positron and an electron pair (see Fig 2.2 below). The positron which was produced during pair production loses its energy as it moves in the absorbing medium by ionization, excitation and bremsstrahlung. Somewhere along the way, the positron will interact with a free electron and create two annihilation photons with energies of 0.511 MeV each. The two photons produced are emitted in opposite directions as a result of conservation of momentum during the process (Khan, 2010). When a photon traverses

through matter, the probability of pair production occurrence is proportional to the square of the atomic number of the absorbing medium.

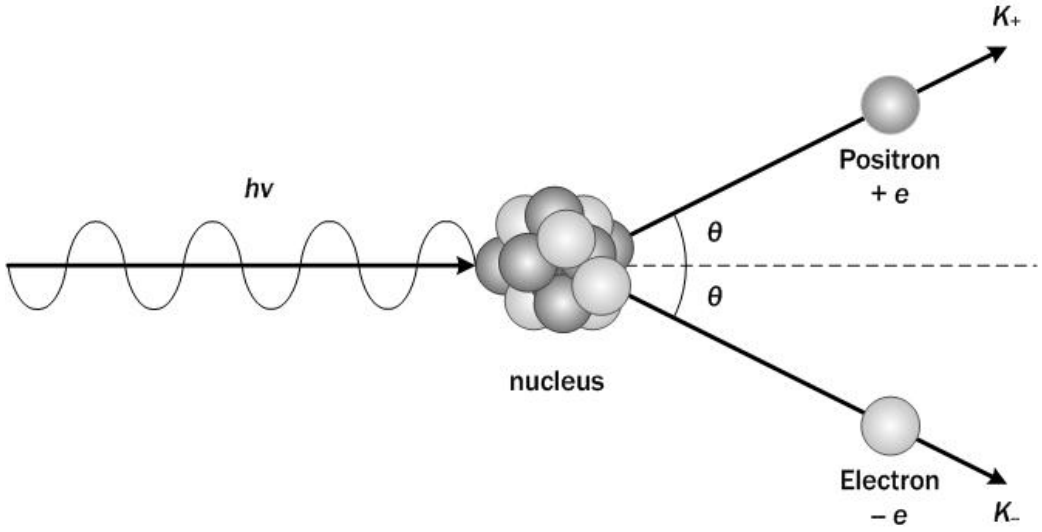

Figure 2.2 Formation of electron pair in pair production (Wikidot, 2012)

In brachytherapy the most common interactions are as a result of either the photoelectric or Compton effects. This is as a result of the 'intention' of brachytherapy and therefore the energies of the gamma sources of radiation selected for use in brachytherapy.

Photons react with matter either by photoelectric, Compton or pair production processes, while charged particles, i.e. protons, electrons, α-particles and nuclei, produce ionization and excitation when they traverse through a medium (Khan, 2010). The particles experience radiative loss of energy (bremsstrahlung) following collisions between the particle and the nucleus. Scattering of particles also happens and this is accompanied by a minimal loss of energy. During ionization, the rate at which the particle loses energy is proportional to the square of the particle's charge and inversely proportional to the square of its speed. This means that the ionization or dose released into the medium (absorbed dose) increases as the particle's velocity decreases (Khan, 2010).

2.3 Exposure

Since the inception of the use of radiation in medicine, radiation workers have always been conscious of the necessity to measure patient response to radiation in terms of the quantity of radiation and duration for which the radiation was administered (Godden, 1988, p. 3). Holzknecht was the first to try to estimate dose measurements in 1902. He observed that a fused mixture of potassium chloride and sodium carbonate changed colour as a function of time of radiation exposure. Numerous efforts have been made since then to try to measure patient dose by means of radioactive substance used, activity, ionization produced in air (exposure), energy absorbed by tissue (absorbed dose), a combination of two or all of these methods (Godden, 1988). The various methods used to measure radiation caused a lot of misunderstanding until in 1956, the ICRU came up with a definition of the roentgen in terms of the exposure dose based upon the capability to ionize. The definition of exposure X, is defined (ICRU, 1980) as:

"*The exposure X is the quotient of dQ by dm where the volume of dQ is the absolute value of the total charge of the ions of one sign produced in air when all electrons (negatives and positives) liberated by photons in air of mass dm are completely stopped in the air*."

i.e. $$X = dQ/dm \text{ C·kg}^{-1} \quad \ldots (2.12)$$

where the unit of exposure is the roentgen (R), which is:

$$1 \text{ R} = 2.58 \text{ X } 10^{-4} \text{ C·kg}^{-1}$$

2.4 Absorbed Dose

In 1904 Beclere discovered the importance of measuring radiation absorbed in tissues in radiology and in 1950 the ICRU acknowledged the need to look into how ionising radiation is related to biological effects produced by the radiation. During that time a term relating the dose to the amount of energy

deposited per unit mass (ergs) was formulated and absorbed dose was defined (ICRU, 1954):

Absorbed dose is the energy imparted per unit mass to matter by ionizing radiation at a specified point.

The unit of absorbed dose is the rad where:

$$1\,rad\ =\ 100\,ergs/gram$$

Absorbed dose is also defined (ICRU, 1980) as the quotient of dE by dm where dE is the mean energy released by ionising radiation into the medium of mass dm, i.e.

$$D\ =\ dE/dm$$

The special name for the unit of absorbed dose is the gray (Gy) where

$$1\,Gy\ =\ 1\,J\cdot kg^{-1}\ ,$$

or, from first principles

$$1\,Gy\ =\ 100\,rad.$$

Absorbed dose in brachytherapy is obtained from a combination of the exposure due to a given activity of a radionuclide and a factor relating exposure to the actual absorbed dose (Godden, 1988). A factor W_{air}/e relates the energy released by an exposure of radiation to the absorbed dose in air, where W_{air} is the energy necessary to create an ion pair in air (Godden, 1988). Therefore, an exposure X of radiation creates an absorbed dose in air D_{air}, i.e.

$$D_{air}\ =\ X\ (W_{air}/e) \qquad \ldots (2.13)$$

For any medium, energy absorbed per unit mass is proportional to the mass energy absorption coefficient (μ_{en}/ρ). Therefore, the relationship between the absorbed dose in the medium, D_{med} and absorbed dose in air D_{air}, is given by:

$$D_{med} = D_{air}[\mu_{en}/\rho]_{air}^{med} \qquad \ldots (2.14)$$

The term $[\mu_{en}/\rho]_{air}^{med}$ gives the ratio of mass energy absorption coefficient for the medium to the absorption coefficient of air. Replacing D_{air} by the term in equation (2.13) above, equation (2.14) becomes

$$D_{med} = X\,(W\mathrm{air}/e)[\mu_{en}/\rho]_{air}^{med} \quad \ldots (2.15)$$

From W_{air}/e = 33.85 J·C^{-1} (ICRU, 1979), the exposure can expressed in terms of the SI units of C·kg^{-1}

$$D_{med} = (33.85[\mu_{en}/\rho]_{air}^{med})X \text{ J kg} \quad \ldots (2.16)$$

and,

$$D_{med} = (0.873[\mu_{en}/\rho]_{air}^{med})X \text{ cGy} \quad \ldots (2.17)$$

when exposure is expressed in terms of roentgens (R).

The absorbed dose in tissue is now obtained from the kinetic energy released per unit mass (kerma). This theory was initiated (ICRU, 1962) to bring to light that transfer of energy to matter from indirectly ionizing radiation happens in two stages (Godden, 1988). The first stage involves transfer of energy from indirectly ionizing particles, i.e. photons and neutrons, by different interactions (photoelectric effect, Compton effect, pair production, etc.) to secondary charged particles (electrons). Secondary charged particles transmit their energy to the medium via ionization and excitation (Podgorsak, 2005).

Kerma is the mean energy transmitted from indirectly ionizing radiation to charged particles in the medium dE_{tr} per unit mass by dm, where $dE_{tr}$is the sum of initial kinetic energies of all charged ionizing particles:

$$K = dE_{tr} / dm$$

Under conditions of electronic equilibrium, secondary charged particles experience a gradual decrease in speed as they traverse through matter, resulting in the loss of most of their energy to the medium (Godden, 1988).

The energy transferred to the medium, i.e. absorbed dose D_{air}, is related to the kerma K_{air} , by the mathematical equation :

$$D = K\,(1 - g) \qquad \ldots (2.18)$$

where g represents the fraction of secondary charged particle energy lost in producing bremsstrahlung. Therefore, for a particular air kerma K_{air}, the absorbed dose in air D_{air} is specified as:

$$D_{air} = K_{air}\,(1 - g) \qquad \ldots (2.19)$$

From equations (2.14) and (2.19) the dose imparted to a medium is expressed in terms of kerma as:

$$D_{med} = K_{air}\,(1 - g)[\mu_{en}/\rho]_{air}^{med}$$

Also,

$$\mu_{en}/\rho = (\mu_{tr}/\rho)(1 - g)$$

where the mass energy transfer coefficient is μ_{tr}/ρ, this means

$$D_{med} = K_{air}\,(\mu_{en}/\rho)(\mu_{tr}/\rho)$$

In brachytherapy g is less than 0.5%, meaning

$$(\mu_{en}/\rho)_{air} \approx (\mu_{tr}/\rho)_{air}$$

Therefore,

$$D_{med} = K_{air}[\mu_{en}/\rho]_{air}^{med} \qquad \ldots (2.20)$$

For photons with energies between 200 keV and 2 MeV, $[\mu_{en}/\rho]$ is equivalent to the numerical value 1.11 in water (Godden, 1988). Therefore, the absorbed dose of most radionuclides used in brachytherapy (except Iodine-125) is given by:

$$D_w = 1.11 \cdot K_{air} \qquad \ldots (2.21)$$

2.5 Biological Effects of Radiation

Secondary electrons produced from interactions of photons with matter release energy as they are slowed down when traversing through the medium. This energy is absorbed in the surrounding tissue and the outcome produced by absorption of ionizing radiation in a population of cells can be classified into three ways, namely:

1. Ionisation may occur outside the critical region resulting in **no damage** to the cells;
2. Ionisation may occur within the critical region such that enough energy to damage the cell may be deposited within. The cell loses its ability to reproduce and this is known as **lethal damage**;
3. Partial ionisation may take place within the cell's critical region inflicting damage without necessarily killing the cell, i.e. **sub-lethal damage**. The cell may retain enough capability to repair itself and experience total recuperation from the effects of radiation.

The extent to which cell damage occurs is dependent on the amount of dose administered (Godden, 1988). In brachytherapy, dose is administered in a number of fractions sufficient to destroy the malignant cells, while at the same time allowing sufficient time between each fraction to facilitate normal tissue cell repair. Continuous low-dose-dose rate irradiation may be regarded as equivalent to a vast number of small fractions. From this knowledge, this means that repair of sub-lethal damage increases with reduction in dose rate up to a point where all the sub-lethal damage is repaired and at this point the dose rate effect no longer applies, i.e. the death rate per cell cycle is the same as the birth rate (Godden, 1988). Dose rates currently used for brachytherapy treatments are sufficient to hamper cell division while killing more tumour cells than normal tissue for the same dose.

Low-dose rate (LDR) brachytherapy has been widely accepted to produce favourable therapeutic outcomes due to the following reasons (Godden, 1988):

i. As a result of the sharp dose gradient around sources, the tumour is subjected to a higher dose rate and subsequently more radiation, with less dose being delivered to the surrounding normal tissue.
ii. The range of dose rates enables the repair of sub-lethal damage to occur during the treatment.
iii. The low oxygen enhancement ratio (OER) gives advantages to brachytherapy.

2.6 High-Dose Rate versus Low-Dose Rate

At many centres, treatment of patients is done using HDR brachytherapy sources as opposed to using LDR brachytherapy. Numerous research has been done to compare clinical outcomes of HDR and LDR brachytherapy (Tamaka, et al., 2012), (Wang, et al., 2010), (Stewart & Viswanathan, 2006), (Hareyama, et al., 2002), (Kim, et al., 2001). However, there seems to be no binding universal agreement on this issue based on clinical data outcomes, i.e. overall survival rates and early and late tissue complication rates. Most centres use HDR because of a number of reasons that include the capacity to treat more patients, convenience of treatment on an outpatient basis, minimal exposure to staff etc (see Table 2.1).

2.7 Iridium-192

Iridium-192 was first used in brachytherapy by Ulrich Henschkle in 1958. Initially it was in the form of seeds, but these were replaced by iridium wires which were started to be manufactured in the early 1960s and these were used in the Paris System developed at the Institut Gustave Roussy (Godden, 1988). Iridium-192 has virtually replaced Radium-226 as the radionuclide of choice for many brachytherapy applications. It has a high specific activity, making it possible to supply sources of different activities up to hundreds of GBq's.

Iridium-192 decays 95% through β^- particles to the 3rd and 4th excited states of Platinum-192. ^{192}Pt further de-excites to the stable state of ^{192}Pt by emission of several γ-rays (Baltas, et al., 2007).

$$^{192}_{77}Ir \rightarrow {}^{192}_{78}P_t + {}^{0}_{-1}e + \gamma \qquad \ldots (2.22)$$

The β-rays emitted have energies of 530 keV and 670 keV, while γ-rays released in achieving stable status are of 370 keV average energy (Godden, 1988).

2.8 Intracavitary Brachytherapy

Intracavitary brachytherapy is when radioactive sources are placed inside natural body cavities to administer a radiation dose for therapeutic purposes. Since the inception of brachytherapy at the beginning of the 20th century, brachytherapy techniques have been used to treat many lesions, e.g. cancers of the bladder, anus, rectum, antrum, oesophagus, nasopharynx and auditory tube. However, the most common use of brachytherapy has been in the treatment of gynaecological malignancies (Godden, 1988). Gynaecological brachytherapy enables placement of radiation sources in close proximity to the tumour, allowing a high radiation dose to be delivered to the neoplasm while sparing normal surrounding tissue as a result of the steep dose gradient of brachytherapy radiation. This characteristic also means that for large tumours, brachytherapy alone is not sufficient to achieve curative intent. It has almost become standard practice for the treatment of gynaecological malignancies to combine intracavitary brachytherapy (ICBT) with external beam radiotherapy (EBRT). Numerous research has been done which established that tumour control rates achieved using EBRT and ICBT are considerably enhanced than with EBRT alone (Viswanathan & Petereit, 2007). ICBT may be administered before, during the course of, or after EBRT (Godden, 1988). The clinical outcome of brachytherapy partially depends on the proficiency and expertise of the radiation oncologist.

Table 2.1 Comparison between high-dose rate and low-dose-rate brachytherapy (Stewart & Viswanathan, 2006)

	Advantages	Disadvantages
Low-dose rate	• Approximately 100 years of data available, • Doses are standardised, • Treatment plans are standardised, • Treatment plans are standardised, • Two insertions at maximum	• Inpatient treatment, • Staff are exposed to radiation, • Source strength a limiting factor, • Availability of sources is limited, • General or spinal anaesthesia required, • Patient has long bed rest, . anticoagulation required, . constipating medication needed, . pain control required for the patient.
High-dose rate	• Outpatient treatment, • Time of administration is short, • Source strength is standard, • Sources are easily available, • Conscious sedation using IV is possible, • Reassessment of tumour size possible with multiple fractions, • Normal tissue dose optimization possible, • Minimal exposure to staff, • Board stabilizes applicator during treatment	• High risk of errors: . Intensive quality assurance required, . Intensive maintenance needed, . Intensive physician/physicist time required, • Number of treatment fractions is more than two, • Treatment to be done on insertion day, • Capital costs are high, • Caution to be exercised when treating large tumours, • Caution needed to monitor normal tissue dose.

It is crucial that applicators are placed accurately and precisely in order to maintain the reproducibility of the treatment setup and achieve local tumour control and reduction in morbidity. Technical adequacy of the implant or applicator also plays a pivotal role in establishing local tumour control (Viswanathan & Petereit, 2007). The basic equipment and facilities required to administer HDR ICBT are an adequately radiation shielded procedural room where applicator insertion and the treatment procedure are carried out, an HDR remote afterloader, imaging equipment for planning, i.e. anterior – posterior (AP) and lateral (LAT) x-ray images, computed tomography (CT),or magnetic resonance imaging (MRI), as well as treatment planning software. In this research images were acquired using conventional x-ray equipment and treatment planning was done using AP and LAT x-ray radiographs only.

Patients receive spinal anaesthesia on their first insertion, where manual examination of the vaginal vault and rectum is done simultaneously. Manual examination is done to establish the following (Viswanathan & Petereit, 2007):

- the size of the tumour,
- the size of the cervix,
- to assess the visible vaginal and cervical extent of the disease and determine the visibility of the cervical ostium,
- the nature of the tumour, i.e. whether it is exophytic, endocervical, symmetrical or eccentrically placed,
- the extent of the disease in the vagina, e.g. are the fornices palpable,
- to assess if EBRT caused fibrosis or narrowing of the vagina that will probably further deteriorate with brachytherapy,
- to assess if the vagina is large enough to allow sufficient packing,
- the visibility and palpability of the ostium,
- mobility of the uterus,
- the state of the uterus, i.e. anteverted or retroverted,
- to determine the curvature of the tandem that will optimize the uterine position in order to minimize dose to the bladder and rectum.

The radiation oncologist takes into account all of the above factors before the insertion of radiation sources in order to determine the best applicator to use.

With the patient in the lithotomy position, patient movement is minimised by strapping the legs to holders on the treatment couch. Magnification rings or magnification reconstruction apparatus are put on the surface of the patient's skin and then an applicator of choice is inserted into the patient. A Foley catheter with a balloon is inserted into the bladder via the urethra and 7 ml of contrast liquid is allowed into the balloon. A rectal retractor and gauze packing are placed in the vaginal vault under the applicator (when feasible). These devices serve to push the rectum away from the radiation.

2.8.1 Imaging

When satisfactory patient setup geometry has been achieved, a set of oblique orthogonal, AP and lateral x-rays are obtained in order to plan the insertion. The image typically shows the whole system including bony anatomic landmarks. The images and the geometry of the implant are critically analyzed and the process repeated if the images are not satisfactory. If a CT scan is used, it is possible to generate lateral and AP digitally reconstructed radiographs (DRR's). A Foley catheter with balloon is inserted into the bladder and filled with fifty millilitres of contrast before scanning. The radiation oncologist can scroll through the CT images, which makes identification of perforations possible. Detection of a perforation warrants removal of the applicator, which can then be reintroduced into the cervix using ultrasound guidance to guarantee positioning in the centre of the uterus. The use of CT scans enables delineation of the bladder, rectum, sigmoid and tumour volume, which facilitates assessment of dose to these structures using dose volume histograms (DVH) (Viswanathan & Petereit, 2007). Magnetic Resonance Imaging (MRI) enables outstanding soft tissue visualization and contrast, which facilitates accurate contouring of the OARs and the tumour volume and is recommended (Gerbaulet, et al., 2005) and used at some centres for imaging in treatment of gynaecological malignancies. However, constraints

related to cost and large patient volumes limit the availability and accessibility of MRI to most patients at most centres worldwide.

2.8.2 Dose Specification

In the early 1900s when brachytherapy commenced, there was a lack of comprehensive knowledge about the biological effects of treatment using radiation. However, beginning from the 1920s and early 1930s, better understanding and new scientific methods were developed and implemented, particularly at the Radiumhemmet in Stockholm (Stockholm system in 1929, 1935) and at the Curie Foundation in Paris (Paris system in 1929). In the 1930s at the Christie Hospital, Manchester, Todd and Meredith modified the Paris system and established the most widely used brachytherapy technique in the world (Godden, 1988). Todd and Meredith calculated the dose to various regions of the pelvis in roentgen, as opposed to calculating the dose in milligram hours (mgh) of radium. They defined a series of points that are anatomically similar from patient to patient, at which the exposure dose should be stated and measured. The points were chosen in such a way that they were independent of small alterations in applicator position.

Table 2.2 Tandem and ovoid dose points ((ICRU-38, 1985)

Point A (right or left)	2 cm along the axis of the central tube from the lower end and 2 cm from it laterally, i.e. for the ring and tandem applicator, point A is positioned at 2 cm away from the central tandem and 2 cm above the ring.
Point B (right or left)	2 cm superior to the ring or ovoid and 5 cm laterally from the midline.
ICRU Rectum	5 mm below the vaginal wall/speculum, radiopaque gauze packing, rectal retractor or most posterior ovoid position.
ICRU Bladder	• On Anterior-Posterior radiograph - center of Foley bulb, • On lateral radiograph – lowest mid position on Foley bulb.

Todd's work proved that the limiting radiation dose was the dose to the region where the uterine vessels cross the ureter, i.e. the 'paracervical triangle', and not the bladder or the rectum**.**

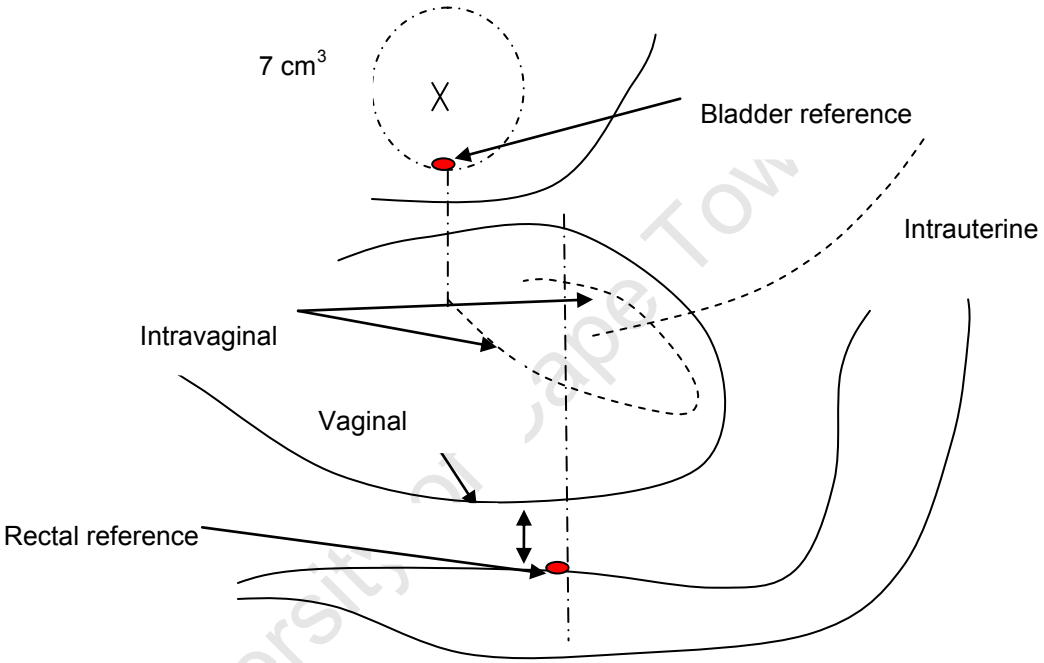

Fig 2.3: Localization of bladder and rectum points from (ICRU, 1985)

This gave birth to the designation of Point A for specifying dose and the system of radiation sources planned was intended to deliver a constant dose rate to identified points close to the cervix, regardless of any difference in the size and shape of the uterus and vagina. At first this point was defined as lying "2 cm lateral to the uterine canal and 2 cm from the mucous membrane of the lateral fornix of the vagina in the plane of the uterus" (Godden, 1988). Point A is now identified as being at 2 cm along the axis of the central tube

from the lower end and 2 cm from it laterally, i.e. for the ring and tandem applicator, point A is positioned at 2 cm away from the central tandem and 2 cm above the ring. Another reference point, Point B, was also formulated and was defined as being 5 cm away from the midline and 2 cm from the mucous membrane of the lateral fornix, see table 2.3 and fig 2.3 earlier, and figs 2.4 (a) and (b) below.

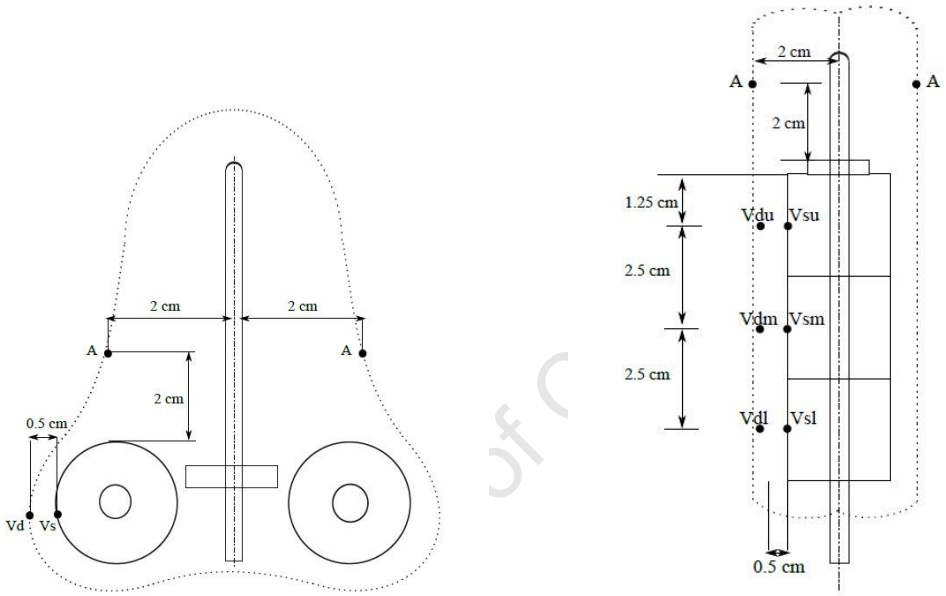

Figure 2.4: (a) Manchester/Fletcher and Fig 2.4 (b) Cylindrical applicator (redrawn from (Gerbaulet, et al., 2005))

Point B was formulated in order to determine the dose in the region close to the pelvic wall near the obturator node and assess the lateral spread of the effective dose (Godden, 1988).

2.8.3 Computerised Treatment Planning

Treatment planning and dosimetry in brachytherapy is not at the same level as that of external beam therapy. (Williamson, 1988) researched and reported on the possible reasons why treatment planning systems in brachytherapy

have lagged behind those in external beam therapy. The reasons he gave are listed below:

- Difficulties were experienced in defining the dose specification of the target volume and organs at risk,
- There was lack of resources and problems of artefacts produced when CT images were acquired with applicators inside the patients,
- High dose gradient in brachytherapy,
- The heavy dependence on point dose calculations derived from radiographic information rather than from volumetric prescription for dosimetric calculations,
- The absence of calculation algorithms which incorporate accurate corrections for tissue inhomogeneities, inter-source effects and complex shielding applicators,
- The reliance on retrospective clinical data for prescriptive and acceptable tolerance doses.

However, accuracy in brachytherapy has advanced in recent years owing to a renewed interest in brachytherapy dosimetry and also due to the following (Venselaar, et al., 2004):

- The availability of remote afterloading which uses HDR, LDR and PDR sources,
- Increased accessibility of CT scan data,
- Volume definition using MRI,
- Dose calculation using Monte Carlo techniques,
- Availability of real-time dosimetric and biologic optimisation,
- Use of low energy gamma ray sources.

Specification of source strength in treatment planning systems is internationally recommended to be in units of reference air kerma rate, K_R, which can be traced to an Accredited Calibration Laboratory in documentation. Calculations within the treatment planning system (TPS) rely on interpolations from a table of dose in water stored for each source (i.e. a dose rate table). The dose rate tables consider the sources to be of cylindrical

symmetry and that the space in which the calculations are made is water equivalent. The tables do not take into account the different heterogeneities and modifications for inter-source effects and applicator attenuation. The sources and dose points are reproduced in 3D space and then the co-ordinates are transposed into the dose rate table co-ordinate system. Interpolation and renormalization is done and the dose at a particular point is obtained by summation of contributions of all individual sources, i.e. all the dwell positions of one source. Most TPS systems use dose rate tables derived from the American Association of Physicists in Medicine Task Group Report No. 43 (Nath, et al., 1995), AAPM TG 43 formalism.

2.8.4 AAPM TG 43 Formalism

This formalism considers the dose distribution to be cylindrical. A polar co-ordinate system with the source centre as the origin and an angular origin in the longitudinal axis of the source describes the geometry as shown below.

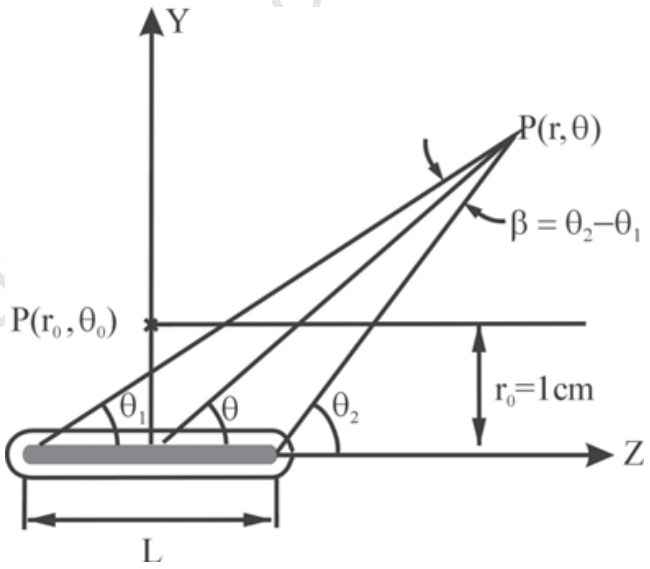

Fig 2.5 Radial and rectangular co-ordination with reference from the source (Nath, et al., 1995).

The dose at point P(r,θ) can be written as:

$$D(r,\theta) = S_K \, \Lambda t \frac{G(r,\theta)}{G(r_0,\theta_0)} g(r) F(r,\theta) \quad \ldots (2.24)$$

where,

r is the radial distance from the source's centre in the same plane as the axis;

θ is the polar angle;

S_K is the air kerma strength;

Λ is the dose rate constant;

t is the exposure time;

$G(r,\theta)$ is the geometry factor which takes into consideration the spatial distribution of the active material in the source;

$F(r,\theta)$ is the anisotropy function which gives the angular dependence of absorption and scatter of the photons inside the core and encapsulation; and

$g(r)$ gives the radial dose function which incorporates the distance dependence of absorption and scatter in water along the transversal axis, i.e. for the angle $\theta = {}^{\pi}/_{2}$. (r_0,θ_0) is an angle situated at 1 cm away from the centre of the source, i.e. for r_0 = 1 cm and $\theta_0 = {}^{\pi}/_{2}$.

Λ is the dose rate constant and is the dose rate to water,1 cm to the transverse axis of a unit air kerma strength source in water,

$$\Lambda = \overline{\left[\frac{\mu_{en}}{\rho}\right]}_{air}^{m} \varphi(r_0) G(r_0,\theta_0) \quad \ldots (2.25)$$

where,

$\overline{\left[\frac{\mu_{en}}{\rho}\right]_{air}^{m}}$ is the term representing the ratio of mass energy absorption coefficients in medium m and in air,

$\varphi(r)$ amalgamates the attenuation of primary photons, together with effects of scattered photons in the medium,

$G(r_0, \theta_0)$ is a geometry factor that gives the spatial distribution of the active material in the source,

$g(r)$ gives the dose gradient along the axis of the source and together with effects of absorption and scatter in water.

$$g(r) = \frac{\varphi(r)}{\varphi(r_0)} \qquad \ldots (2.26)$$

The term $g(r)$ is also affected by filtration of photons by the encapsulation and source materials (Nath, et al., 1995).

2.9 Adverse Side Effects

The most common side effects after treatment of gynaecological malignancies usually involve the bowel and urinary tract. Table 1.1 gives a summary of the acute and late complications that may occur in patients after receiving radiotherapy as treatment for gynaecological cancers.

Radiotherapy-induced toxicity may either be attributed to brachytherapeutic techniques and doses or other radiotherapy independent factors, i.e. surgery, concomitant chemotherapy, diabetes, HTA, etc. (Gerbaulet, et al., 2005). This research will consider those factors which are attributed to irradiation. The following factors influence the occurrence of complications in radiotherapy treatment of gynaecological malignancies.

1. **Total Dose:** The total radiation dose, i.e. by external beam irradiation of the whole pelvic region and by intracavitary brachytherapy, greatly influences the occurrence of side effects (Perez, et al., 1991) and (Perez, et al., 1999). There is a significant increase in the occurrence of side effects when total doses of greater than 80 Gy are given.
2. **Volume:** Occurrence of complications in combined external irradiation and intracavitary brachytherapy is also closely related to the total irradiated volume. There is a considerable increase in the volume receiving more than 60 Gy when patients receive more than 30 Gy of external beam radiotherapy (Esche, et al., 1987).
3. **Brachytherapy technique:** It was discovered that the use of certain applicators was associated with a higher likelihood of occurrence of complications (Perez, et al., 1999). However, techniques were developed (Barillot, et al., 2000) and can now be used to reduce complications after receiving radiotherapy treatment for gynaecological cancers.
4. **Dose rate:** It has been argued by many authors that low-dose rate brachytherapy produces better results and less complication rates than high-dose rate brachytherapy (Haie-Meder, et al., 1993) and (Newman, 1996). However, this issue has been a source of controversy up to now (Stewart & Viswanathan, 2006). (Stewart & Viswanathan, 2006) suggest that LDR may be preferable for large, bulky tumours at the time of brachytherapy, while on the other hand, they recommend that satisfactory tumour shrinkage should have occurred before HDR is administered and cautious monitoring of dose to normal tissues should be done. An extensive study by (Wang, et al., 2010) concluded that "there was no significant difference between HDR and LDR when considering overall survival, disease-specific survival, relapse-free survival, local control rate, recurrence and metastasis and treatment related complications for patients with clinical stages I, II and III. Therefore we recommend the use of HDR for all clinical stages of uterine cervix cancer."

2.10 *In-vivo* Dosimetry

Radiotherapy aims to administer a lethal dose to the primary tumour volume (PTV), while surrounding normal tissue and organs receive the least possible dose. Numerous experiments and clinical studies have shown that small changes in dose of between 7 % and 15 % can reduce local tumour control (Dutreix, 1984). The International Commission on Radiological Units (ICRU, 1976) recommends that the difference between the prescribed and delivered dose should not exceed 5 % in order to maintain local tumour control. Uncertainties in the dose delivered in radiotherapy arise from each step executed in the treatment process, i.e. from treatment planning itself until treatment is administered. Therefore, the American Association of Physicists in Medicine (AAPM) (Kutcher, et al., 1994) and (ICRU, 1976) recommend *in-vivo* dosimetry to be done on patients.

In-vivo dosimetry is a tool to measure the radiation dose delivered to patients during radiotherapy. The aim of in-vivo dosimetry is to compare dose measurements with the dose values specified by the radiation oncologist and the dose values calculated by the TPS. This exercise is done to verify that:

- 'what is prescribed is what is delivered',
- ' what is treated is that which is intended to be treated',

In other words, *in-vivo* dosimetry serves to 'verify',

i. output and performance of the treatment equipment ;
ii. patient set-up;
iii. the dose calculation algorithm and to determine the effect of changes in body shape, size and density on the dose calculation procedure;

In-vivo dosimetry is not only intended to verify the dose delivered to the target volume, but also to monitor dose to organs at risk (e.g. bladder, rectum, bowel), or in circumstances in which it will be difficult to predict the dose (e.g.

when using non-standard source-to-skin distances in external beam radiotherapy) (Podgorsak, 2005). Practising *in-vivo* dosimetry helps to:

i. decrease the risk of occurrence of serious radiation accidents;
ii. guarantee that patients are treated as planned;
iii. comply with laws and regulations governing the practice of radiotherapy in South Africa, i.e. The Hazardous Substances Act, 1973 (Act 15 of 1973) and Regulations (No R1332 of 3 August 1973) governing the safe use of medical x-ray equipment in South Africa.

2.10.1 *In-vivo* Dose Measurement Techniques

Semiconductor detectors (silicon diodes) and thermoluminescent detectors (TLDs) are the most commonly used types of detectors for *in-vivo* measurements. There is a wide variety of dosimetry systems that can also be used to perform *in-vivo* measurements, e.g. film, gel dosimeters, ionization chambers, electronic devices (e.g. metal oxide semiconductor field effect transistors (MOSFETs)) and alanine (Podgorsak, 2005). However, in this research, silicon diodes were found to be best adapted to perform intracavitary *in-vivo* dose measurements and therefore were used in this research.

2.10.2 Silicon Diodes

Characteristics of silicon diodes that make them the detector of choice for *in-vivo* dosimetry include high spatial resolution, high sensitivity, absence of external bias, small size and the utility of making real-time measurements (Podgorsak, 2005). Silicon's density and the relatively low average energy it needs to make a carrier pair produces radiation induced current densities approximately 18,000 greater than those produced in air. This means that small volumes of silicon (typically $10^{-2} \sim 10^{-1}$ mm^3) generate a considerable amount of current (Yorke, et al., 2005).

There are two types of silicon diodes, i.e. n-type or p-type silicon, that rely on minority carriers being holes or electrons respectively (Huyskens, et al., 2001). Fig 2.6 below shows how a p-type silicon radiation detector works. At the junction between the separate p-type and n-type regions, there is a lack of free charge carriers. A potential of approximately 0.7 V exists over the depletion area when the detector is made to operate at zero external voltage. This causes the charge carriers produced by the radiation to be carried away into the crystal body.

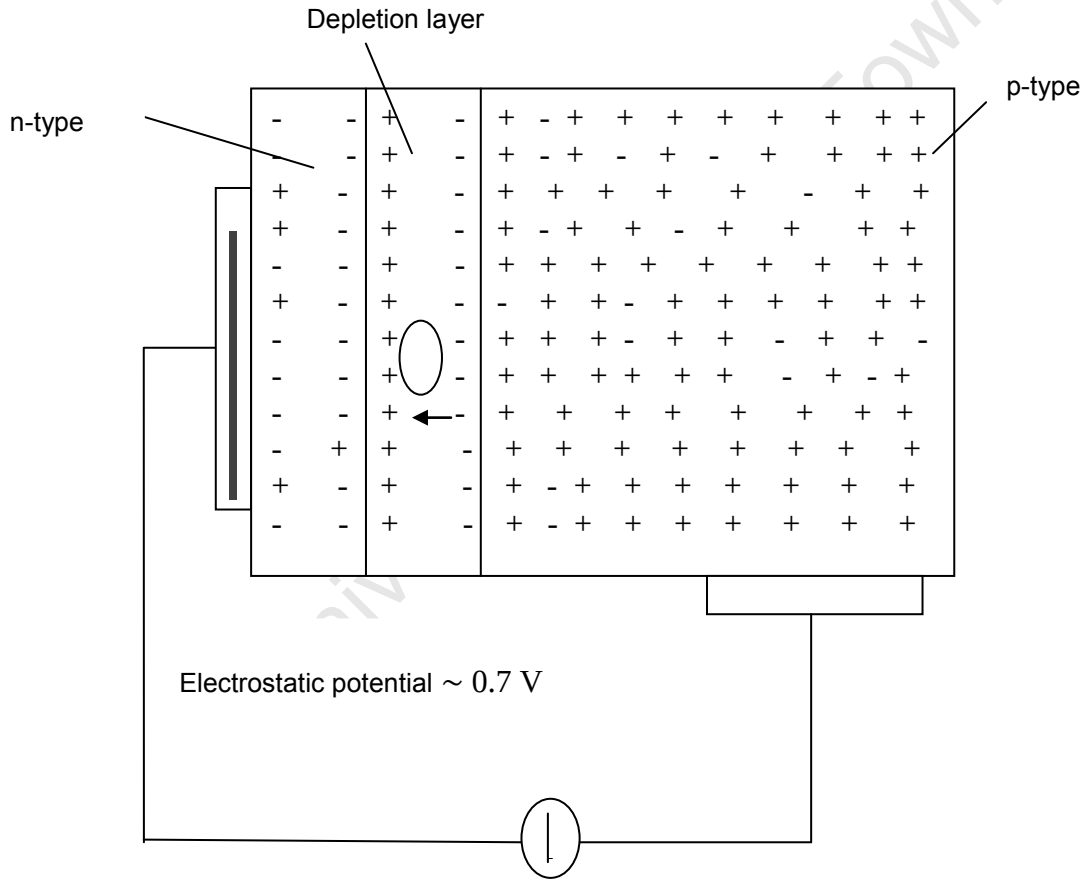

Figure 2.6: Schematic drawing of a p-type silicon radiation detector (Huyskens, et al., 2001).

The diode is asymmetrically doped, i.e. there is heavier doping of the n-type region compared to the p-type region. This means that the charge flow produced by the irradiation almost entirely consists of electrons (in a n-type diode the induced charge flow would mostly consist of holes).

The diode signal is reduced as a result of some electrons being trapped by defects in the crystal lattice. In n-type diodes, holes are more susceptible to be trapped in crystal lattice defects and this greatly influences the detection capacity of the diode (Huyskens, et al., 2001).

The lifetime of the charge carriers and the quantity of the recombination centres in the crystal determine the sensitivity of the detector. Diode detectors have small sizes and high spatial resolution which make them very useful in measuring dose in steep dose gradient regions, for instance, the area around a brachytherapy source. Below are some of the desirable characteristics of diode detectors (Wilkinson, 2010):

i. Small size and weight.
ii. Mechanically stable and generally having good reproducibility.
iii. Provide real–time dose read outs.
iv. Diode production costs are relatively low.
v. Detectors show little radiation field perturbation.

Diode detectors are very useful in *in-vivo* dosimetry, but they have the following limitations (Wilkinson, 2010):

i. Diodes exhibit an angular (directional) dependence which is dependent on the shape and size of the diode, and how the diode is set up relative to the direction of the source of radiation.
ii. Diode detectors show a temperature dependence, i.e. diode response varies with temperature.
iii. Diode detectors also show energy dependence, i.e. the diode response varies with energy of the incident radiation.
iv. Diode detectors exhibit reduced sensitivity with accumulated dose over time consequent to continuous usage.

Diode detectors have been in use clinically in gynaecological brachytherapy for some time now and (Wäldhausl, et al., 2005) carried out an extensive *in-vivo* dosimetry study using diodes involving 55 ICBT applications on patients. Diodes used in that study, i.e. PTW diode probes, are identical to the diodes that were also used in this study. Bladder and rectum doses computed by the TPS and doses measured by the diodes showed differences ranging from -27 % to +26 % for the bladder and -31 % to +90 % for the rectum. Another study carried out by (Hassouna, et al., 2011) reported that the ratio of the ICRU reference point dose to the diode dose was 1.2 ± 0.5 for the bladder and 1.7 ± 0.5 for the rectum. In the study by (Wäldhausl, et al., 2005), they also evaluated the characteristics of the PTW diodes for reproducibility, linearity, angular, energy and temperature dependence and discovered a ± 7 % uncertainty in measured dose.

CHAPTER 3 IN-VIVO DOSIMETRY MEASUREMENTS

3.0 Introduction

HDR Brachytherapy has experienced rapid technical advances in treatment planning and dose delivery systems over the last decade. However, the accuracy of these systems still requires independent checking to prevent potential dose errors (Qi, et al., 2007). The need and necessity for in-vivo dosimetry was discussed in the previous chapter and this chapter will describe how an *in-vivo* dosimetry system was set-up for use during HDR brachytherapy for gynaecological malignancies at Groote Schuur Hospital, Cape Town.

3.1 Calibration and Reference Dosimetric Quantity of a HDR Source

Source strength of a brachytherapy source is expressed in terms of:

i. Activity of the source, A;
ii. Apparent activity;
iii. Equivalent mass of radium in milligrams;
iv. Air kerma strength , S_k.

Air kerma strength is the American Association of Physicists in Medicine (AAPM) recommended reference dosimetric quantity. S_k is derived from exposure rate ($\dot{X}$) obtained at 1 m distance from the source in free air (Khan, 2010).

$$S_k = \acute{K} d_{ref}^2 \quad \ldots (3.1)$$

where the air kerma rate $\acute{K}$, is obtained at a reference distance d_{ref}, and d_{ref}= 1 m. ^{192}Ir sources are calibrated in terms of exposure rate at 1 m in *open-air scatter-free* geometry at primary standard dosimetry laboratories (PSDLs). Clinical calibrations for brachytherapy sources are supposed to be traceable to appointed PSDLs or secondary standard dosimetry laboratories

(SSDLs). Calibration of brachytherapy sources in hospital settings is performed in well chambers with calibration factors obtained at PSDLs or SSDLs. In this study, the ^{192}Ir source was calibrated in a well chamber and in a standard *in-air* jig. The measured values are compared with the 'decayed' values of the reference source air kerma strength provided on an accompanying source calibration certificate, measured at the secondary standard laboratory at PTW-Freiburg, Germany.

Stability Check

A stability check of the Farmer type ionization chamber was performed in a long life Strontium-90 source.

Tolerances

The tolerance for the stability check is 1 %. Deviations of check values beyond 1 % warrant investigation and documentation.

3.1.1 In-Air Calibration of ^{192}Ir Sources

The in-air measurement technique determines the source strength in terms of the air kerma rate at a certain distance, from which the reference air kerma rate is then worked out (Venslaar, et al., 1994). In this study a 0.6 cc PTW Farmer ionisation chamber, type 31002 and accompanying electrometer, PTW UNIDOS, with calibration factors traceable to PTW-Freiburg, Germany, were used to calibrate the ^{192}Ir source. Recommendations for the calibration of ^{192}Ir HDR sources (Venselaar, et al., 1994) urge the use of a thimble chamber together with its build-up cap during source calibration. The build-up cap serves to contain contaminating electrons emanating from the ^{192}Ir source encapsulation. The in-air calibration was done in a dedicated jig which provides reproducible repositioning of the ionisation chamber and source catheters (see figures 3.1 (a), (b) and 3.2 below) (Venselaar, et al., 1994, p. 6).

The measurements were done at a distance of 100 mm. Time intervals of 600 s were used to obtain the measurements. The reference air kerma rate Ḱ ($cGy.h^{-1}$) was obtained using the following formulas and relationships.

$$\acute{K}_{ref} = \frac{M.N_k.\Pi f_i.d^2}{t} \quad \ldots (3.2)$$

where

$$M = M_{uncor}.\rho_t.\rho_p.\rho_{hum}.\rho_{ion}.\rho_{pol}.\rho_{nu} \quad \ldots (3.3)$$

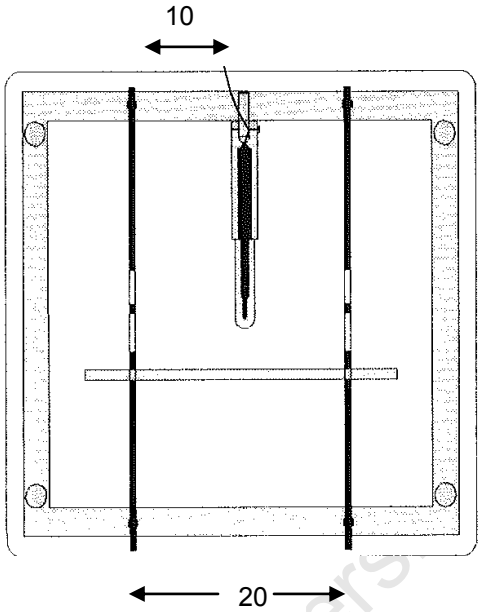

Figure 3.1(a): Birds eye view of jig

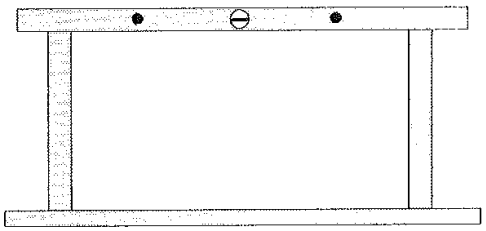

Figure 3.1(b): Side view of jig

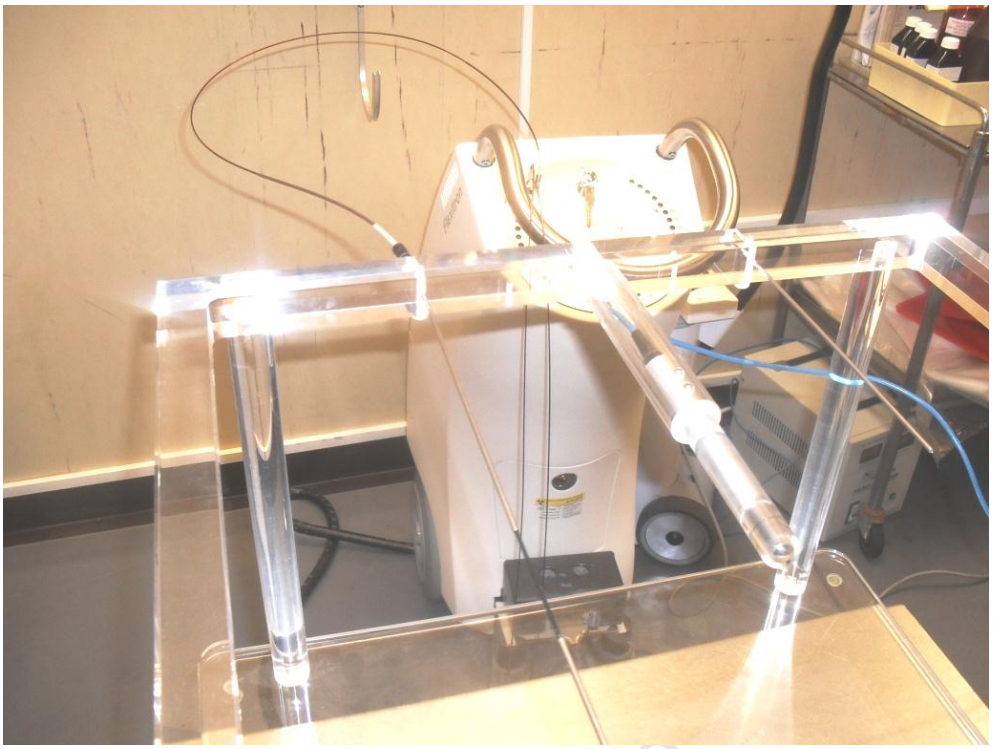

Figure 3.2: In-air calibration setup at Groote Schuur Hospital, Cape Town

where

M is the corrected reading from the instrument for the time period t;

M_{uncor} is the uncorrected reading from the instrument;

ρ_t is the air temperature correction factor as a function of the reference temperature at which the calibration factor N_k was determined;

ρ_p is the air pressure correction factor as a function of the reference air pressure at which the N_k was determined;

ρ_{hum} is the air humidity correction factor;

ρ_{ion} is the ion recombination factor; (1.000)[1]

ρ_{pol} is the correction factor for polarity effects; (1.000)[1]

ρ_{nu} is the correction factor that takes into account the dose non-uniformity over the chamber wall and is calculated from data given by (Kondo & Randolph, 1960); (1.006)

N_k (μGy per unit reading) is the air kerma calibration factor for the ^{192}Ir gamma-ray spectrum for the ionization chamber;

where,

$$\Pi f_i = f_{tr} \cdot f_{rs} \quad \ldots (3.4)$$

f_{tr} is the correction factor for source transport time for (t > 600 s or 0.1667 h) (1.0)

f_{rs} is the correction factor for room scatter for a wall to chamber distance of 0.5 m or more (0.999)

and where,

d is the source-to-chamber axis distance for the jig relative to the 1 m reference distance. (0.100)

t is the total exposure time (in hours) of the measurement with the source at its position in the catheter. (0.1667)

[1] Are values obtained for the specified measurement conditions and may change under different measuring conditions. Performing the measurements at a distance of 100 mm allows omission of the effect of air attenuation since it amounts to a very small correction when applied to measurements done at such small distances.

The air kerma strength $S_{k'}$ is then calculated from the air kerma rate from the relationship shown below,

$$S_{k'} = \acute{K} d_{ref}^2 \quad \text{(cGy/h m}^2\text{)} \quad \ldots (3.5)$$

Where $\acute{K}$ is the air kerma rate at a reference distance d_{ref}, d_{ref} = 1 m.
The air kerma strength is the standard measurement used to specify the source strength in source ordering, dose computation, treatment planning and implant description (Bochud, et al., 2005).

3.1.2 Calibration of ^{192}Ir Sources in a Well Chamber

Performing relative source strength measurements of ^{192}Ir sources in a Well chamber, i.e. the redundancy standard, is standard practice at the hospital. The calibration serves to confirm the source strength indicated on the

accompanying calibration certificate (reference), measured at the SSDL at Nucletron, in the Netherlands. The well chamber used at the hospital is a PTW Well chamber type 077.091 shown in Figure 3.2 (a) below.

This is a dedicated well chamber for calibration of ^{192}Ir sources. A typical schematic diagram of a well-type chamber is shown in Figure 3.3 (b).

The source is *stepped*-into the well chamber at specified distances and constant time intervals to locate the highest reading point. Several readings are taken at this point and the average reading is used to calculate the air kerma rate as shown in equation 3.6.

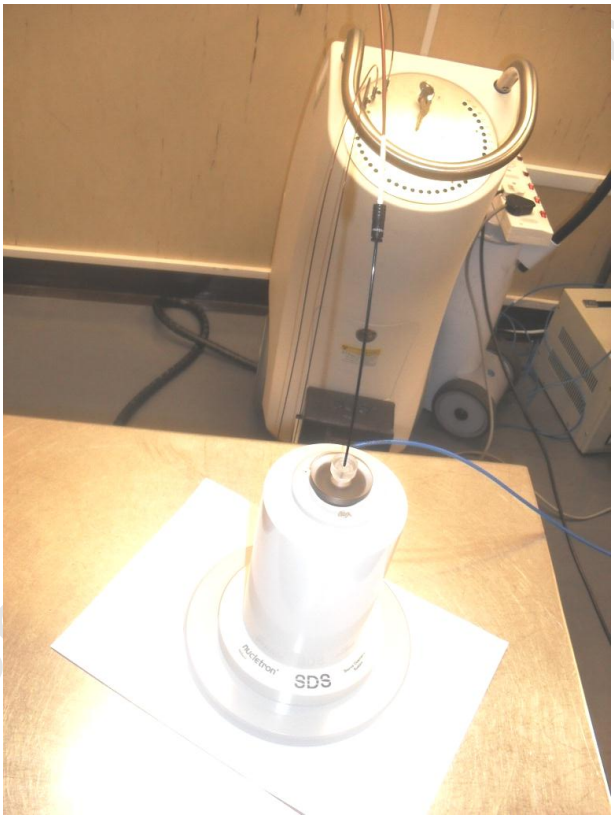

Figure 3.3: (a) Measuring ^{192}Ir source strength using a PTW Well type Chamber

$$\acute{K}_{ref} = \frac{M.N_k.f_{tr}}{t} \quad \text{... (3.6)}$$

where,

$\acute{K}_{ref}$ is the reference air kerma rate of the source;

M is the electrometer reading;

N_k is the calibration factor of the well chamber;

f_{tr} is the correction factor for source transport time;

t is the exposure time of the measurement with the source at the maximum reading position inside the well chamber.

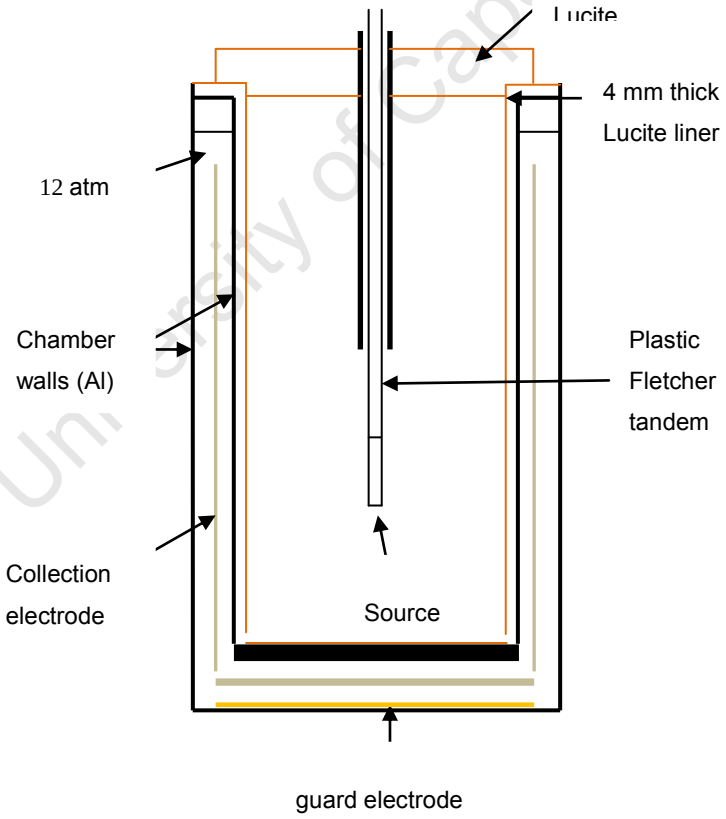

Figure 3.3 (b) Capintec Model CRC-10 dose calibrator (Khan, 2010)

Since the well chamber is a sealed chamber, there is no need for temperature and pressure corrections. The air kerma strength is calculated from the air kerma rate using equation 3.2 above.

3.1.3 Uniformity with Vendor Reference

Reference air kerma values obtained at the hospital are compared with the vendor-supplied values. A deviation within 3 % between the two values is considered as acceptable and the vendor reference air kerma values are used in determining patient treatment times. If the discrepancies are more than 3 %, investigations to find possible reasons are made and if the discrepancies remain, then a report is made to the vendor.

3.1.4 Uniformity of Measurements at the Hospital

For redundancy measurements done at any time at the hospital, the air kerma strength measured using the local standard is compared with the redundancy standard. The vendor reference value is used without investigation for differences in values less than 3 %. If the difference is greater than 3 %, then this warrants investigation.

3.2 Rectum and Bladder Dosimeters

Semiconductor dosimeter probes manufactured by PTW-Freiburg were used to measure doses received by the bladder and rectum in this study. The semiconductor diodes are covered with waterproof encapsulation and are custom made for ease of insertion into the organs.

The rectum probe (T9112) has five independent diodes that measure the dose at different points along the rectum. T9113 is a single diode bladder probe that is used to measure doses in the bladder.

The diodes generate a current when exposed to ionizing radiation. A dosimeter (PTW Vivodos Electrometer) connected to the probes measures the current and converts the current to dose. Online measurements for individuals are viewed and stored on a computer using a software program called MultiSoft.

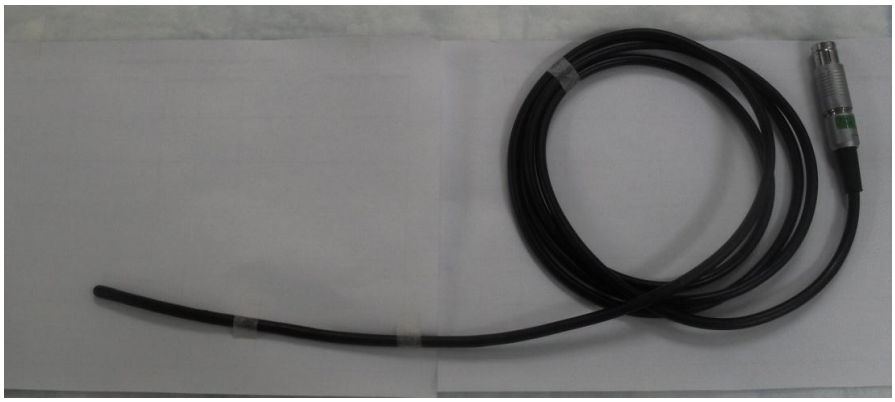

Figure 3.4 (a) : T9112 rectum probe

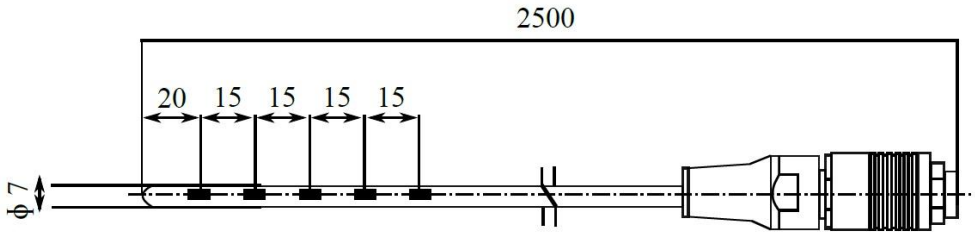

Figure 3.4 (b) : T9112 rectum probe

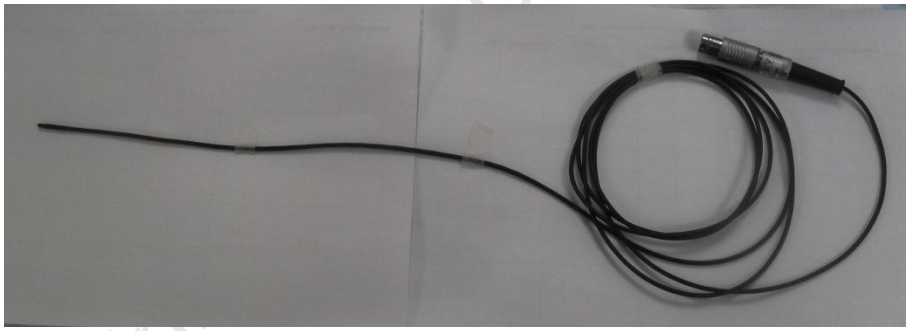

Figure 3.4 (c) : T9113 bladder probe

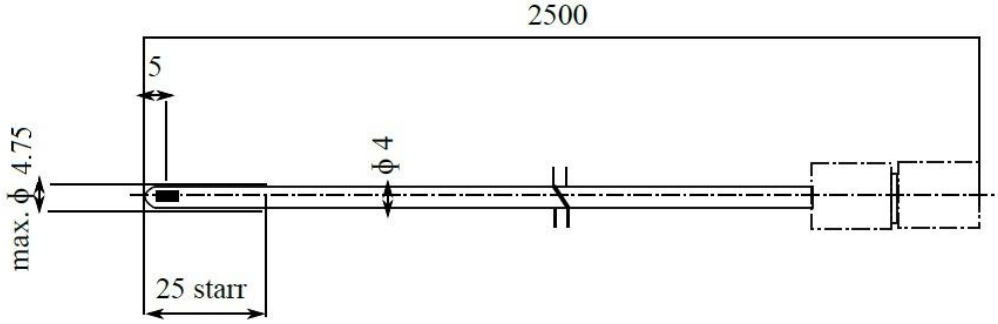

Figure 3.4 (d): T9113 bladder probe

3.3 Calibration of Semiconductor Probes

Calibration of semiconductor probes is carried out in a custom-made afterloading cylindrical PMMA calibration phantom (type 9193), manufactured by PTW-Freiburg, Germany. There is a central slot for placement of the ^{192}Ir source and on a circle of radius 8 cm; it has four holes that are situated 2 cm from the edge of the phantom.

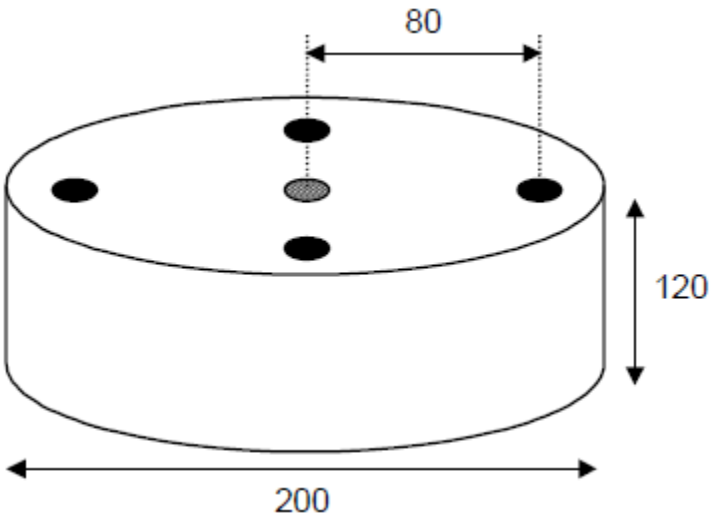

Figure 3.5 (a): Afterloading calibration PMMA phantom (Bochud, et al., 2005)

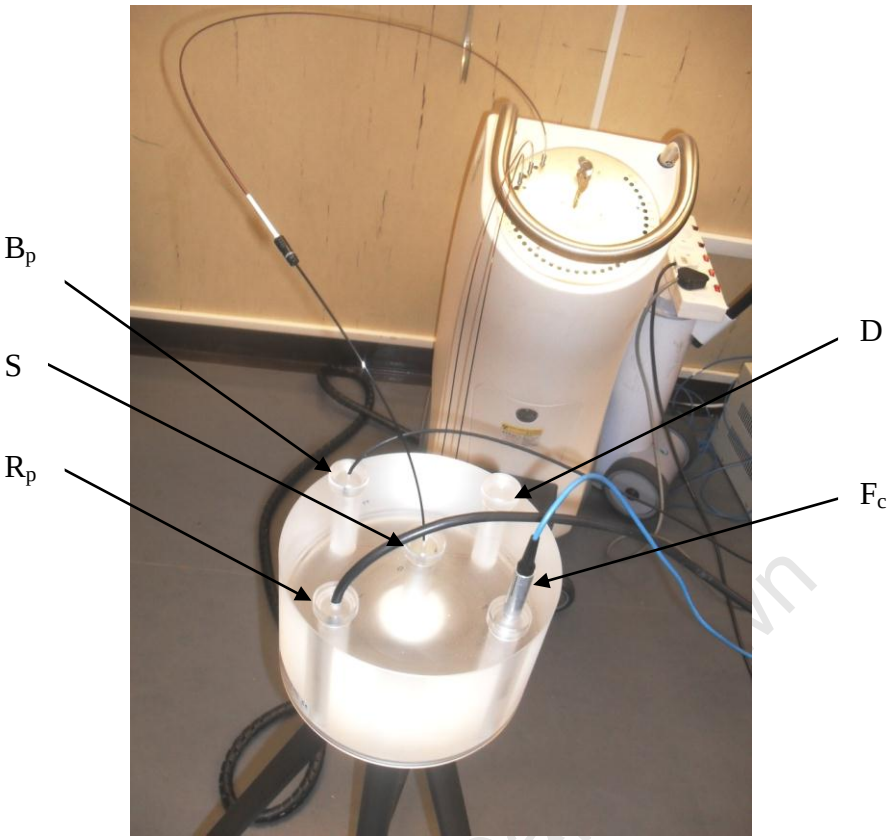

Figure 3.5 (b): PTW Type 9193 Phantom connected to Flexitron Remote Afterloader

where,

B_p is the bladder probe,

S_c is the ^{192}Ir source catheter,

R_p is the rectum probe,

F_c is the PTW Farmer chamber, and

D is the dummy plug.

These holes are positioned at 0°, 90°, 180° and 270° into which detectors, i.e. a thimble ionization chamber, bladder and rectum probes, are placed using appropriate plugs as shown in Figs 3.5 (a) and (b). The phantom also functions as a redundancy standard for calibration of source strength for

brachytherapy sources. Closing unused holes in the phantom during source calibration achieves equal scatter of radiation within the phantom.

Calibration of the semiconductors is done against the redundant thimble chamber with calibration factors traceable to the PTW-Freiburg SSDL in Germany. The thimble chamber was calibrated in a Cobalt-60 beam and a 100 kV beam.

3.3.1 Air Kerma Strength Calculation from Air Kerma Measurements

Dose measurements performed by a thimble chamber calibrated in terms of air kerma in Cobalt-60 radiation is given by:

$$S_k = \{k_{a\to p}.k_r\,.k_{zp}\}.k_\lambda\,.N_K\,.k_\tau\,.k_{pT}\,.M \quad \ldots (3.7)$$
$$= 0.00760$$

where,

N_k is the air kerma calibration factor for Cobalt-60 radiation [µGy/readout unit];

$k_{a\to p}$ is the perturbation factor from air to PMMA environment ($k_{a\to p}$ = 1);

k_r is the inverse square law correction factor ($k_r = 8/100)^2$ = 0.0064;

k_{zp} is the geometry correction factor for the PTW - type 9193 cylindrical PMMA phantom;

k_{zp} = 1.187 ± 0.012 (Bochud, et al., 2005, p. 14). k_{zp} also contains the volume correction factor for the PTW 31002 thimble chamber at a distance of 8 cm;

k_λ is the correction for the instrument response in ^{192}Ir radiation. k_λ is calculated from the instrument specifications. For an instrument with a response of 1.00 in ^{60}Co radiation, k_λ is the extrapolated response calculated between ^{60}Co and the highest x-ray energy available assuming the mean energy of ^{192}Ir to be 380keV (k_λ =1);

k_{pT} is the air density correction factor = $\left(\frac{T_{ph}+273.15}{293.15}.\frac{1013.25}{P}\right)$, where T_{ph} is the phantom temperature [°C] and p is the air pressure [hPa];

k_T is the time correction factor $\left(\frac{60}{\tau}\right)$, where τ [min] is the measurement time;

$\{k_{a\to p}.k_r\,.k_{zp}\}$ = 0.00760 for all measurements made in the phantom (Bochud, et al., 2005).

3.3.2 Air Kerma Calculation from Absorbed Dose to Water Measurements

An ionization chamber calibrated in absorbed dose to water in ^{60}Co radiation can also be used to determine the air kerma strength S_k [µGy/hm^2].

$$S_k = \left\{\frac{1}{1-g_w}.\frac{(\mu_{en}/\rho)_a}{(\mu_{en}/\rho)_w}\,.k_{w\to p}\,.k_r\,.k_{zp}\right\}.k_\lambda\,.N_w\,.k_\tau\,.k_{pT}\,.M \qquad \ldots (3.8)$$

$$= 0.00684$$

where,

M is the instrument reading [readout unit];

N_w is the absorbed dose to water calibration factor performed in ^{60}Co radiation;

$k_{w\to p}$ is the perturbation factor from water to PMMA environment ($k_{w\to p}$ =1.00);

$(\mu_{en}/\rho)_a$ and $(\mu_{en}/\rho)_w$ are the mass energy absorption coefficients for air and water respectively. [$(\mu_{en}/\rho)_a$ / $(\mu_{en}/\rho)_w$ = 0.899];

g_w is the relative energy lost through bremsstrahlung (g_w = 0.001).

All the other factors are the same as given in equation 3.7 above (Bochud, et al., 2005).

The ^{192}Ir source was calibrated in the phantom using the two methods mentioned above and the average of three measurement runs was taken and compared with vendor supplied reference air kerma strength (see source certificate in Appendix 1). The result was found to be within 3 % of the standard and was considered as a valid air kerma strength value for that date.

A complete *in-vivo* dosimetry measurement set consists of a Well chamber, afterloader phantom T9193 with accessories, PosiCheck T43006 (for

checking source positioning), Vivodos AL Dosimeter, MultiSoft Software, single semiconductor T9113 bladder probe, five-diode semiconductor T9112 rectum probe, and a detector connection box to connect the detectors to the dosimeter. Since this system was brand-new and was set up for the first time, the semiconductor probes, i.e. the bladder and rectum diodes had no calibration factors. The MultiSoft software program allows calibration of the semiconductor probes and enables viewing and documentation of dose measurements on a computer monitor.

3.3.3 Calibration using MultiSoft Software

The MultiSoft software was installed on one of the treatment planning computers. The semiconductor probes had no calibration factors and they had to be cross-calibrated using an ionization chamber. The bladder and rectum probes, as well as the source catheter and a dummy plug were placed in the T9193 phantom as shown in Fig 3.5 (b). The T9193 phantom places the source, bladder diode, rectum diode number 3 and the active measuring volume of the ionization chamber at the same measuring point. The detectors were exposed to a previously determined (reference) dose or air kerma value. The MultiSoft program was set to calibration mode, the dose was measured for the specified time, and calibration factors for the bladder diode and central rectum detector were computed. The software program automatically takes into account the differences in distance from the source to the other rectum diodes and simultaneously computes the respective calibration factors for the diodes. These calibration factors were then saved into the software program and computer. The semiconductor detectors were then ready to perform dose measurements. The detectors were exposed to the reference dose and the dose measured by the bladder diode and central diode of the rectum probe was compared with the dose registered by the ionization chamber. The calibration procedure was repeated until the dose registered by the ionization chamber, bladder diode and central diode of the rectum probe were identical. Identical dose measurements of the respective detectors confirm the acquisition of correct calibration factors for the bladder and rectum detectors.

The calibration factors were saved for future use and at this point the bladder and rectum probes were ready for use in patients.

The calibration procedure is a continuous exercise repeated periodically with time since the semiconductor detectors change their characteristics after cumulative exposure to high radiation doses. The change in calibration factors is a function of applied dose and energy and occurs gradually over time with increased use of the detectors.

3.3.4 Pilot Study in Phantom

After the bladder and rectum probes were calibrated, a pilot study was carried out in a Rando phantom. The Rando phantom provides an adequate radiation scatter medium that is tissue equivalent, satisfying ICRU Report No.44 requirements (ICRU-44, 1989).

Method

- The Rando phantom was set up together with a reconstruction box on a patient treatment bed.
- A standard Smit applicator (5 cm active length) and bladder probe were inserted into two separate holes in the phantom as shown in Figs. 3.6 (a) and (b) above.
- Anterior-posterior and lateral radiographs were taken and the central point of the bladder diode was marked as a dose control point on the x-ray images.
- The radiographs were scanned into the TPS and a 2 Gy dose was prescribed to ICRU (ICRU-38, 1985) point A.

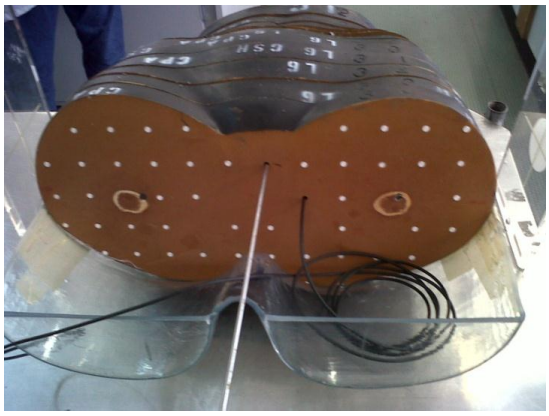

Figure 3.6 (a) Setup for dose measurement in Rando phantom (front view)

Figure 3.6 (b) Setup for dose measurement in Rando phantom (side view)

- The TPS computed the dose that the bladder was going to receive and the plan was transferred to the treatment machine for activation of an exposure.
- The Rando phantom was irradiated with a prescribed dose of 2 Gy to point A and the dose registered by the bladder probe was recorded.
- The dose measured by the bladder diode in Rando was compared with the TPS calculated value and was found to be within 3 %.

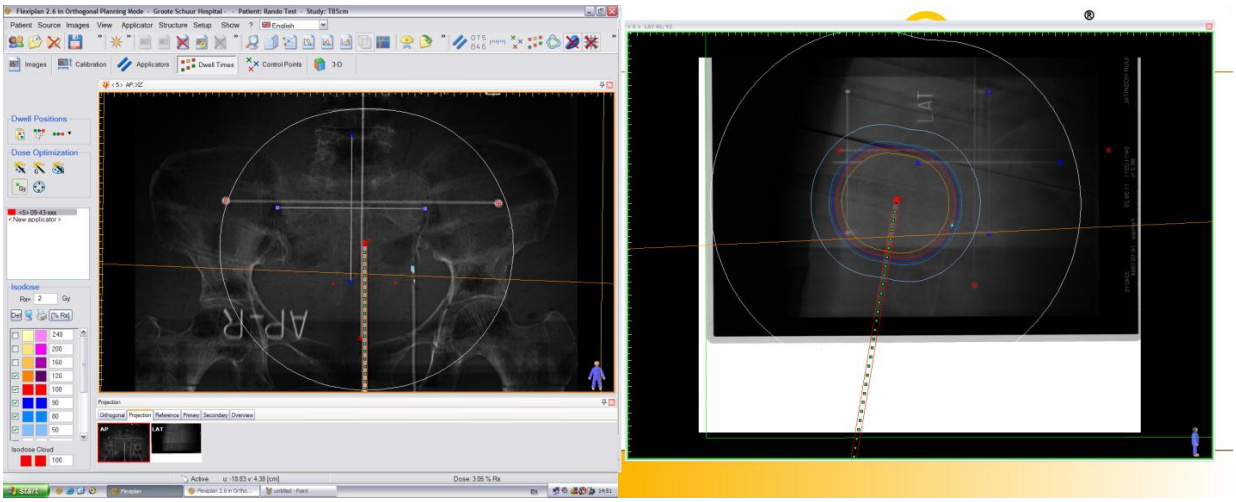

Figure 3.7: Flexiplan treatment plan for a radiation dose of 2 Gy to point A in Rando

The method was repeated a number of times with the bladder probe at different positions. The results obtained were within 3 % of each other and this confirmed that the bladder probe was calibrated correctly. The rectum probe could not fit into the diode holes in the Rando phantom. However, from the in-phantom source and detectors calibration procedure, it was concluded that the rectum probe was also calibrated correctly.

3.4 Dose Measurements in Patients

3.4.1 Background

The process of setting up a patient for treatment, identification and selection of appropriate applicators for use and dose prescription for the ICBT procedure is discussed in the previous chapters. Currently at Groote Schuur Hospital (GSH), Flexiplan, a treatment planning software (TPS) program, is used to compute doses received by the bladder and rectum during ICBT. The procedure for obtaining the dose to the OARs is as follows:

- Contrast liquid is injected via a catheter into a Foley balloon inserted in the bladder and a rectal retractor (which serves to push away the

rectum from the applicator and serves as a rectal marker) is placed inside the vaginal cavity.

- Anterior-posterior and lateral orthogonal radiographs are taken with the applicator and markers in position.
- A Radiation Oncologist identifies the International Commission on Radiological Units Report No. 38 (ICRU-38, 1985) and American Brachytherapy Society (ABS) (Nag, et al., 2000) dose reference points for the bladder and rectum and marks the points on the radiographs.
- The marked radiographs are then scanned and digitized into the Flexitron TPS program on a treatment planning computer.
- The TPS will produce a dose distribution of the setup showing the type and size of applicator used, as well as the position of the ICRU and ABS reference points relative to the sources of radiation and the alignment of the applicator in the cavity. The ICRU reference point A is prescribed to receive 100 % of the dose and the bladder and rectum reference points should each receive at most 70 % of the prescribed dose.

This method is the only method that is in use to obtain values of the dose received by the rectum and the bladder during gynaecological brachytherapy at GSH. However, previous investigators recommend that it is good practice to carryout *in-vivo* dosimetry measurements to complement the dose computations by the TPS (Hassouna, et al., 2011) and (Wäldhausl, et al., 2005).

3.4.2 *In-vivo* Measurements in Patients

After successful commissioning of the *in-vivo* dosimeters (a detailed procedure of commissioning of *in-vivo* dosimeters was done by (Wilkinson, 2010)), seeking and obtaining ethics approval, a protocol was followed in selecting participants and carrying out the study. The main aim of the study was to compare doses computed by the TPS with *in-vivo* and *in-vitro* dose measurements.

In order to achieve this, additional to the protocol of using ICRU (ICRU-38, 1985) and ABS (Nag, et al., 2000) dose reference points for computing dose received by the rectum and bladder during ICBT described in section 3.5.1 above, the following procedures were done:

- The bladder and the rectum diodes were marked as dose control points on the orthogonal images.
- The TPS computed dose that was supposed to be registered by the semiconductor detectors and the approved treatment plan was transferred to the treatment computer and machine for treatment.
- The patient was treated and the dose received by the bladder and rectum was measured by the *in-vivo* dosimetry system.
- The measured in-vivo measurements were recorded and compared with the TPS computed doses.

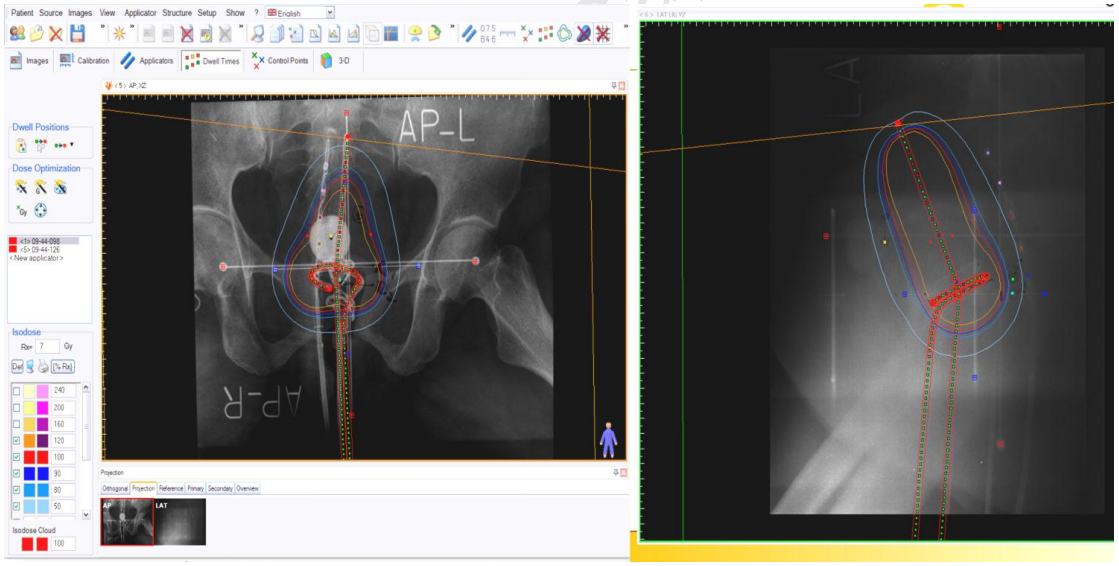

Figure 3.8: A standard treatment plan for a 30 mm diameter ring - 70 mm intrauterine tube (Tandem) Fletcher applicator.

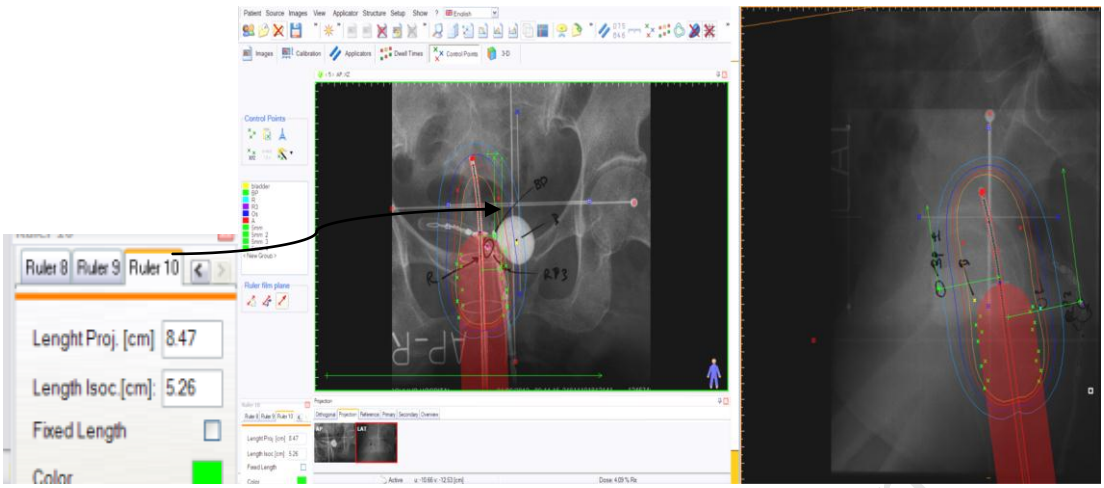

Figure 3.9: A typical cylinder and tandem combo applicator showing how coordinates for the diode measuring points are obtained

3.4.3 Dose Measurements in a Water phantom (*In-vitro* Measurements)

The treatment applicator setup was replicated in a water phantom based on previous work that was done to analyse rectum doses during HDR brachytherapy (Huh, et al., 2007). Water was chosen to be the perfect tissue-equivalent material and a motorised PTW 3D MP3 water tank was used as the phantom satisfying the definition of a phantom, i.e.

"*A body phantom is generally composed of various tissue substitutes simulating the human body or a part of the body with respect to size, shape, position, mass density and radiation interaction*", (ICRU, 1989).

The bladder and rectum diode probes were separately mounted and positioned in the water tank using the motorised apparatus usually used for positioning ion chambers in calibration of external beams (see Figs 3.10 (a),(b) and (c)). Distances between the diodes and particular applicator 'reference' points were measured from AP and lateral x-ray images on the TPS using a calibrated ruler. Diode measuring-point coordinates were used to position the bladder and rectum probes relative to the applicator in a water

tank. A PTW MP3 3D water tank with 0.1 mm measuring capability functioned as a phantom in which dose measurements were made.

The dimensions of the PTW MP3 tank are 600 mm x 600 mm x 408 mm = 0.14688 m^3 and this is equal to a full patient radiation scatter volume. Therefore, the MP3 tank was filled up every time *in-vitro* measurements were made. The bladder and rectum probes were secured to custom-made acrylic rods using ordinary thin masking tape to provide rigidity and ease of positioning. The motorised ruler on the MP3 tank was used to position the bladder and rectum probes.

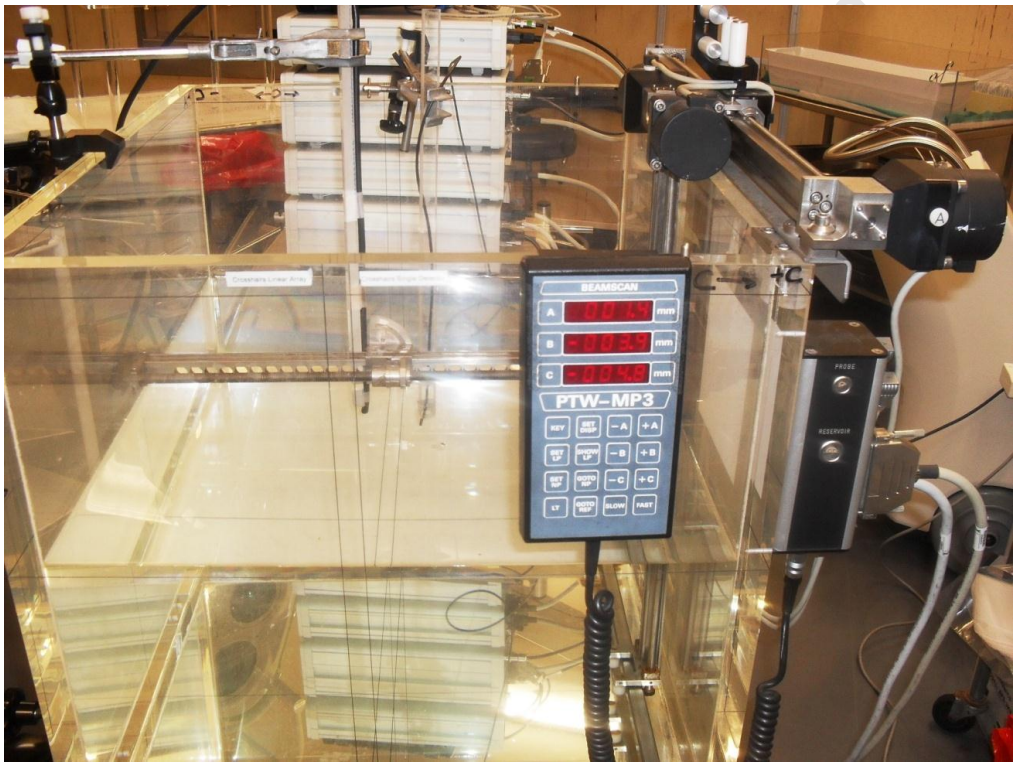

Figure 3.10 (a): PTW MP3 water tank with apparatus for *in-vitro* dose measurements

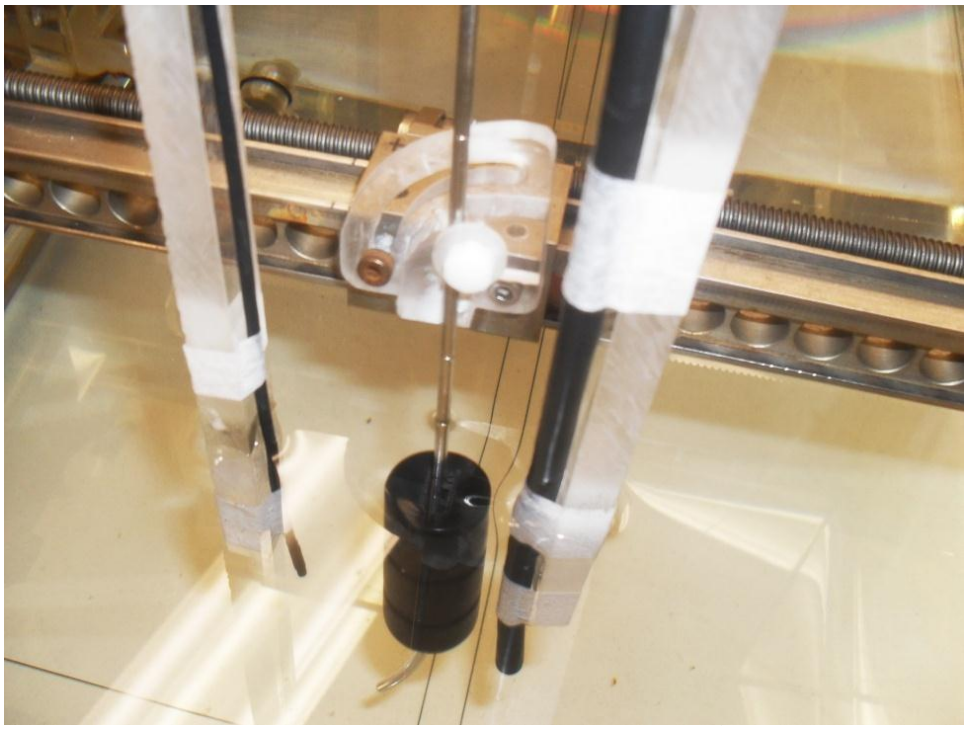

Figure 3.10 (b): Cylinder and tandem combo setup in PTW MP3 tank

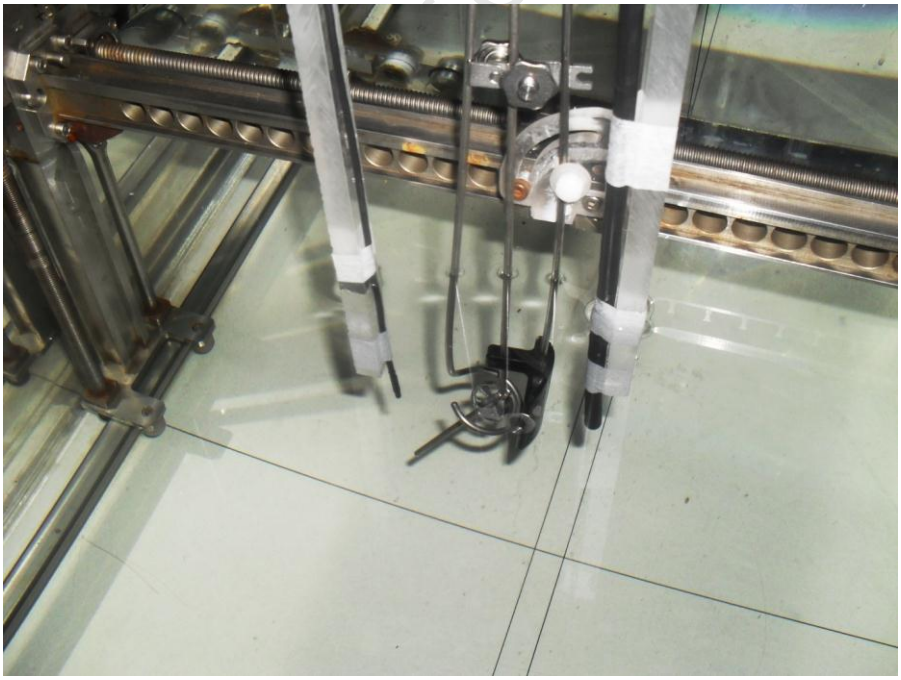

Figure 3.10 (c): Fletcher (ring and tandem) applicator showing adjustable acrylic adapter

The acrylic adapter served to accurately position the applicator and minimized additional radiation scatter that was produced in the measuring setup. There were no x-ray radiographs taken in this procedure and positioning of the diodes was critical to reproducing the patient treatment setup in the water phantom.

Distances between diodes and particular applicator ‘reference’ points were measured using calibrated rules in the x,y and z directions from the AP and lateral x-ray images on the TPS as shown in Fig 3.9 above.

For *in-vitro* measurements, the ‘treatment’ position of the applicator in water was regarded as the origin i.e. (0, 0, 0).For each diode position, x,y,z coordinates were reproduced in water by moving the applicator in x,y,z directions to position the diode in water. Diode ‘measuring-point’ coordinates were used to position the bladder and rectum probes relative to the applicator in the water tank.

When a satisfactory setup was achieved in the water phantom, a specified patient dose was delivered and the dose measured was recorded. The procedure was repeated several times in water for each patient treatment and the average recorded and compared with the TPS computed and *in-vivo* measured doses.

CHAPTER 4 RESULTS

4.1 Measurements

In calibrating the diode probes used for all measurements in the research, a traceable reference dosimetric quantity had to be used to provide reliable traceability reference for the calibration factors of the diode probes. The source air kerma strength was used as the reference dosimetric quantity that provided reference to the calibration of the source strength done at the Secondary Standard reference laboratory at Nucletron in the Netherlands.

Measurement of the source air kerma strength was carried out in-air using a jig, in a phantom and repeated in a Well chamber. The results were compared with the value of the source air kerma strength provided on the source certificate (see Chapter 3, section 3.1 for measurement procedure). The in-air method of calibration used a 0.6 cc PTW 31002 Farmer type chamber. Temperature and pressure corrections were done for every measurement and recorded. On the first day of carrying out measurements, the $K_{T,P}$ was obtained from an average atmospheric pressure of 1014.8 *kPa* and 23.5 ^{0}C temperature:

Average temperature = 23.5 ^{0}C

Average Pressure = 1014.8 kPa

From

$$K_{T,P} = \left(\frac{1013,3}{P}\right) X \left(\frac{273.2+T}{273.2+20}\right) \quad \ldots (4.1)$$

$$= \left(\frac{1013.3}{1014.8}\right) X \left(\frac{273.2 +23.5}{273.2+20}\right)$$

$$= \underline{1.011}$$

This temperature and pressure correction factor was used to correct all the dose measurements that were done on that particular day.

4.2 Stability Check

The dosimeter, i.e. the PTW Farmer chamber and electrometer combination may not be stable due to environmental or voltage and current fluctuations. A stability check is done to verify the stability of the dosimeter by checking it against a stable long half-life Strontium-90 source whose activity is known and documented. The first step that was done each day for verifying the stability of the measuring instrument was to obtain the temperature and pressure correction factor, $K_{T,P}$. A typical stability check calculation done on the 24th of January 2012 is shown below. The $K_{T,P}$ was calculated as shown above in section 4.1:

The PTW Farmer chamber (without cap) was put inside a Strontium-90 source to measure the activity of the strontium against the known decayed value of the strontium as shown in Figure 4.1. Three measurements of the source dose rate were done for one minute each (see Table 4.1 below).

Table 4.1: Stability check measurements

Readings	R_1	R_2	R_3	R_{Av}	R_{cor}
[$\cdot 10^{-2}$ Gy·min^{-1}]	3.745	3.744	3.744	3.744	3.785

where R_{cor} is corrected for temperature and pressure i.e.

$$R_{cor} = R_{Av} \; X \; K_{T,P} \qquad \ldots (4.2)$$

The reference dose rate, R_{ref} of the Strontium-90 source for that particular day was retrieved from the electrometer and was found to be:

$$R_{ref} = 3.768 \cdot 10^{-2}\ \mathrm{Gy} \cdot \mathrm{min}^{-1}$$

The dosimeter stability was calculated using equation 4.3 below:

$$\text{Dosimeter stability} = \left(\frac{\text{Rcor} - \text{Rref}}{\text{Rcor}}\right) X\ 100\% \quad \text{... (4.3)}$$

$$= \left(\frac{3.785 - 3.768}{3.785}\right) X\ 100\%$$

$$= \underline{0.45\%}$$

Stability values that fall within 1 % confirm that the dosimeter is stable and values above this threshold may warrant further investigations to be done in order to rectify any problems and maintain equipment stability within the 1 % limit.

Figure 4.1 shows a picture of the set-up to do a stability check.

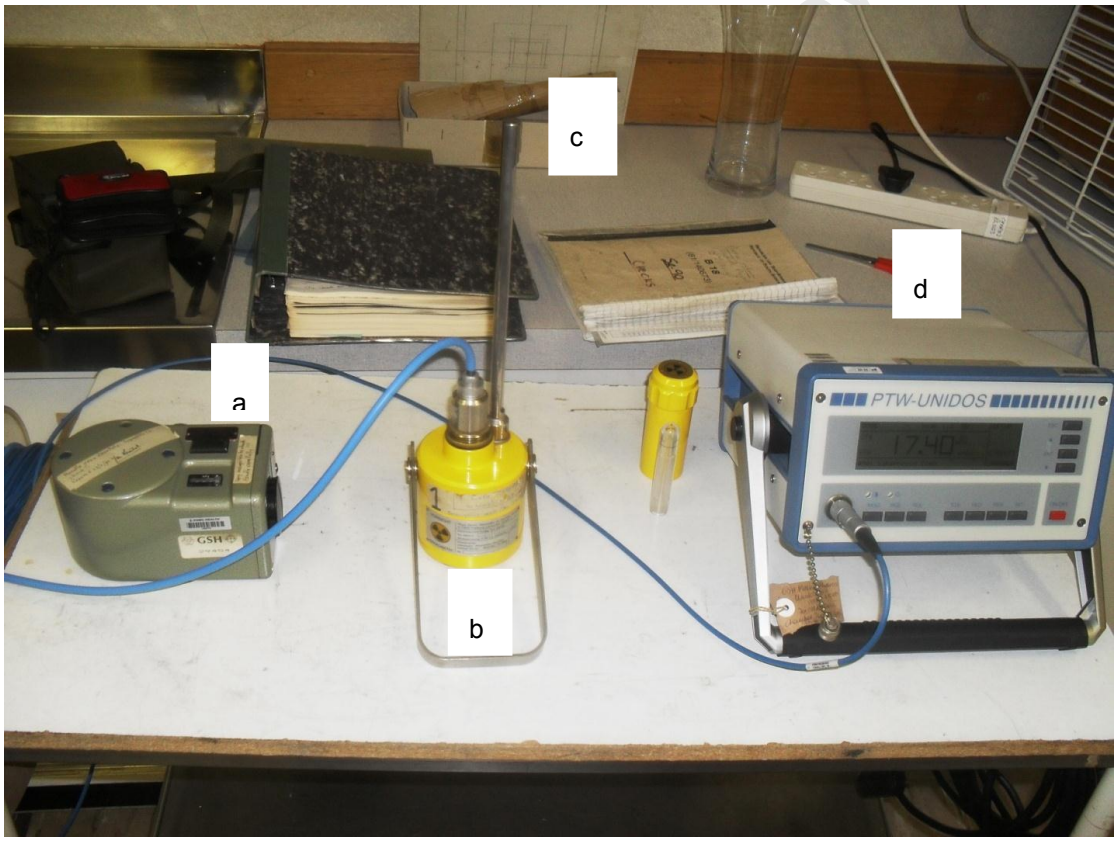

Figure 4.1: Experimental setup for performing a dosimeter stability check

where,

a is a army type barometer,

b is the Strontium-90 check source with the PTW Farmer chamber inserted,

c is a thermometer measuring the temperature of the environment inside the check source,

d is the electrometer and Farmer chamber cable .

4.3 In-Air Calibration

The ^{192}Ir source strength was determined using a custom made in-air jig (see Figs 3.1(a), (b)and 3.3). In general, for each source strength measurement, the reference air kerma rate, $\acute{K}$ (cGy.h^{-1}) was calculated from which the source strength, $S_{k'}$ (cGy/h m^2) was then obtained. After setting up the in-air source calibration setup as shown in Figs 3.1 and 3.2, several exposures were done with the source on either side of the ion chamber. The duration of each exposure was 600s and the measurements obtained are shown below. Two sets of air kerma strength were calculated using the in-air method as follows:

Table 4.2: Measurements obtained using the Air kerma strength calibration factor

Readings	R_1	R_2	R_3	R_4	R_{Av}
Charge (nC)	72.732	72.699	72.792	72.789	72.753

The air kerma strength was calculated using equations 3.2, 3.3 and 3.5 in the previous chapter i.e.

$$\acute{K}_{ref} = \frac{M.N_k.\Pi f_i.d^2}{t},$$

where,

$$M = M_{uncor} \cdot \rho_t \cdot \rho_p \cdot \rho_{hum} \cdot \rho_{ion} \cdot \rho_{pol} \cdot \rho_{nu} \ ,$$

and the air kerma strength,

$$S_{k'} = \acute{K} d_{ref}^2$$

With all the symbols in the above equations representing the same properties and values given in section 3.1 of the previous chapter, and the temperature and pressure correction calculated as from equation 4.1 above.

$$S_{k'} = \frac{(72.753nC \cdot 1.011 \cdot 1 \cdot 1 \cdot 1 \cdot 1.006 \cdot 4.914\ X\ 10^7\ \cdot 1 \cdot 0.999 \cdot (0.10)^2}{0.1667}$$

$$= \mathbf{21.790\ cGy\ h^{-1}.\ m^2}$$

Repeating the same experiment under the same conditions, the air kerma strength was obtained again using the absorbed dose to water calibration factor of the dosimeter. The results of the measurements are shown in Table 4.3 below:

Table 4.3: Measurements obtained using absorbed dose to water calibration factor

Readings	R_1	R_2	R_3	R_4	R_{Av}
Charge (nC)	65.459	65.445	65.481	65.483	65.467

Using the same equations as used above, the following is the calculation for the source air kerma strength on that particular time and date:

$$S_{k'} = \frac{(65.467nC \cdot 1.011 \cdot 1 \cdot 1 \cdot 1 \cdot 1.006 \cdot 5.412\ X\ 10^7\ \cdot 1 \cdot 0.999 \cdot (0.10)^2)}{0.1667}$$

$$= \mathbf{21.595\ cGy\ h^{-1}\ m^2}$$

4.4 In-Phantom Calibration

On the same day and time, the air kerma strength was obtained using a customized PTW 9193 acrylic phantom (Fig 3.5(a)). The calibration setup in Fig 3.5(b) was used to measure the exposure in terms of charge that was used to calculate the air kerma strength using the air kerma strength and absorbed dose calibration factors as shown in sections 4.4.1 and 4.4.2 below.

4.4.1 Air Kerma Strength from Air Kerma Strength Measurements

Results of measurements obtained using the air kerma calibration factor are shown in Table 4.4 below.

Table 4.4: Measurements obtained using the air kerma strength calibration factor

Readings	R_1	R_2	R_3	R_4	R_{Av}
Charge (nC)	96.235	96.271	96.254	96.224	96.246

Equation 3.6 from Chapter 3 was used to calculate the air kerma strength using the average exposure measurement above, i.e.

$$S_k = \{k_{a\to p}.\, k_r\, .\, k_{zp}\}.\, k_\lambda\, .\, N_K\, .\, k_\tau\, .\, k_{pT}\, .\, M$$

$$= 0.0076 \cdot 1 \cdot 4.914\ X\ 10^7 \cdot \left(\frac{60}{10}\right) \cdot 1.011 \cdot 96.246\ X\ 10^{-9}$$

$$= \mathbf{21.804\ cGy\ h^{-1}.m^2}$$

4.4.2 Air Kerma Strength from Absorbed Dose to Water Measurements

The air kerma strength was also calculated using measurements done in the PTW T9193 phantom with absorbed dose to water calibration factors, see Table 4.5.

Table 4.5: Measurements obtained using absorbed dose to water calibration factor

Readings	R_1	R_2	R_3	R_4	R_{Av}
Charge (nC)	97.137	97.122	97.125	97.120	97.126

From equation 3.7 from the previous chapter, the air kerma strength was calculated as follows:

$$S_k = \left\{ \frac{1}{1 - g_w} . \frac{(\mu_{en}/\rho)_a}{(\mu_{en}/\rho)_w} . k_{w \to p} . k_r . k_{zp} \right\} . k_\lambda . N_w . k_\tau . k_{pT} . M$$

$$= 0.0684 \cdot 1 \cdot 5.412\ X\ 10^7 \cdot \left(\frac{60}{10}\right) \cdot 1 \cdot 1.011 \cdot 97.126\ X\ 10^{-9}$$

$$= \mathbf{21.809\ cGy\ h^{-1}.m^2}$$

4.5 Well Chamber Calibration

The local standard against which all local calibrations are checked is the Well chamber. After performing measurements at the maximum-source-strength-position using the method described in section 3.1.2 of the previous chapter, four-radiation exposure readings were taken at the maximum source strength position. Each exposure lasted 600 seconds and the measurements obtained are shown below:

Table 4.6: Measurements done in Well Chamber

Readings	R_1	R_2	R_3	R_4	R_{Av}
Current (nA)	38.273	38.288	38.280	38.279	38.280

Equation 3.5 was then used to calculate the source strength, i.e.

$$S_k = \frac{M.N_k.f_{tr}}{t}.d_{ref}^2$$

$$= \frac{38.280 \cdot 10^{-9} \cdot 9.403\ X\ 10^7 \cdot 1}{0.1667}.1^2$$

$$= \underline{\mathbf{21.592\ cGy\ h^{-1}.m^2}}$$

Where f_{tr} =1, since the duration of the source transport time is negligible for measurement times equal to or greater than six hundred seconds. All the other symbols and values in the above relationship are the same as described in section 3.1.2 of chapter 3.

4.6 Calibration of Semiconductor Probes

After calculation of the source strength, the bladder and rectum diode probes were then calibrated in the custom made cylindrical PMMA calibration phantom, i.e. PTW T9193 phantom as described in section 3.4 of the previous chapter (see Fig 3.5 (b)). A software program (MultiSoft) was used to obtain calibration factors for the individual diodes. The MultiSoft software captured the individual calibration factors into the program and the program used these factors to measure the dose received by the diodes when exposed to radiation.

For all dose measurements obtained using the PTW Farmer ionization chamber, the measurements were corrected for temperature and pressure changes. Calibration factors and corresponding dose measurements were carried out following the procedure described in the previous chapter, i.e. section 3.4. The calibration factors and corresponding dose measurements made are given in Table 4.7 below.

Table 4.7: Calibration factors and corresponding dose measurements made in a PTW T9193 phantom

Calibration factors (e + 005 Gy/C)						0.6 cc Ion Chamber (cGy)		Diode Doses (cGy)						Av. % Error
B	R_1	R_2	R_3	R_4	R_5	D_{uncor}	D_{cor}	B	R_3	R_1	R_2	R_4	R_5	
4.098	4.695	4.073	4.096	4.106	4.217	283.7	284.0	281.9	283.4	251.0	256.0	255.0	244.0	0.47
4.077	4.661	4.055	4.077	4.094	4.202	283.5	283.8	283.5	284.1	248.7	272.9	278.2	248.6	0.10
4.132	4.749	4.118	4.148	4.157	4.274	283.8	284.1	284.0	284.3	250.0	275.0	275.0	249.0	0.07

See Appendix 2 for the output of the MultiSoft computation of calibration factors. The calibration factors collected over the period the study was being carried out are shown below in Table 4.8. From Table 4.8 it is clear to notice that the calibration factors change with time. The sensitivity and characteristics of the semiconductor materials change with time with prolonged exposure to radiation. The standard deviation of the gradual change of the calibration factors ranged from (0.211×10^5) up to (0.710×10^5), while average monthly deviation also ranged from (0.061×10^5) up to (0.256×10^5) over the nine month period over which the study was carried out.

Dose measurements recorded by the 0.6 cc Farmer ionization chamber, bladder diode and rectum diode number 3 were comparable after the third trial for the first set of readings as shown in Table 4.7 above.

Table 4.8: Calibration factors obtained and used during the research

Calibration factors (e + 005 Gy/C)						
Date	Bladder	R_1	R_2	R_3	R_4	R_5
24.10.11	3.966	4.366	4.169	4.270	4.035	4.023
26.10.11	4.132	4.749	4.118	4.148	4.157	4.274
26.10.11	4.098	4.695	4.073	4.096	4.106	4.217
26.10.11	4.077	4.661	4.055	4.077	4.094	4.202
04.11.11	4.013	4.650	4.349	4.521	4.386	4.459
04.11.11	4.463	5.286	4.905	5.007	4.902	5.039
14.11.11	4.463	5.286	4.905	5.007	4.902	5.039
07.03.12	4.151	5.967	5.114	4.359	3.582	3.017
16.04.12	3.988	6.670	5.499	4.760	3.851	3.226
24.07.12	4.513	5.372	5.029	5.190	4.963	4.985

After the correct calibration factors were obtained and loaded into the MultiSoft program, the dose measurements made in the T9193 phantom were accurate, precise and comparable at the reference positions, i.e. 0.6 cc Farmer chamber, bladder diode and rectal diode number 3. The doses registered after exposure to the same amount of dose were comparable to within 0.07 % as shown in Table 4.7.

4.7 Pilot Study in Phantom

After confirming the accuracy of the 0.6 cc PTW 31002 Farmer chamber, obtaining correct calibration factors and consequently calibrating the bladder and rectal diode probes, a pilot study was carried out in a Alderson- Rando phantom. The diode holes in the phantom were too small for the rectal diode probe to be inserted in the phantom; therefore, the pilot studies were only carried out using the bladder probe (see section 3.4.4 for detailed account of pilot study procedure). After the Smit's applicator and bladder diode probe

were inserted into the phantom, anterior- posterior and lateral radiographs were taken and developed. Dose reference points, i.e. ICRU point A (ICRU, 1985) and the measuring volume of the bladder diode B1, were marked on the radiographs. The radiographs were scanned into a treatment planning software program called Flexiplan (see Appendices 3 and 4).

A treatment plan was made to deliver a dose of 2 Gy (as shown in Figure 4.2) at the ICRU point A and the plan exported to the treatment computer and machine where it was delivered to the phantom and measured by the bladder diode. Several dose measurements were made in the phantom and the results are shown in Table 4.9 below and see also Appendix 5 for a dose measurement report from MultiSoft produced after the dose delivery. B1 is the expected bladder diode reading obtained from treatment planning (Figure 4.2) and obtained after measuring in the Alderson-Rando phantom (Table 4.9)

Table 4.9: Bladder Diode Dose Measurements in Alderson-Rando phantom

Readings	R1	R2	R3	Rav
Bladder diode measurement, B1 (Gy)	1.142	1.141	1.143	1.142

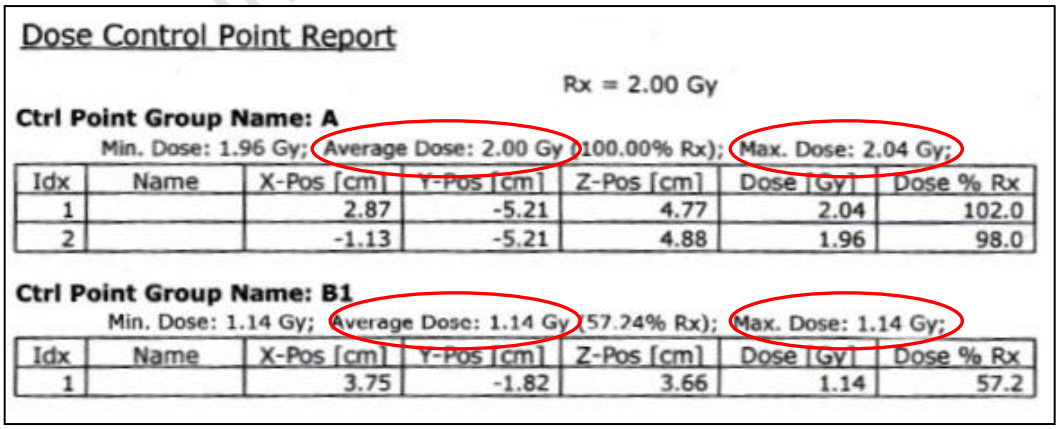

Dose Control Point Report

Rx = 2.00 Gy

Ctrl Point Group Name: A

Min. Dose: 1.96 Gy; Average Dose: 2.00 Gy (100.00% Rx); Max. Dose: 2.04 Gy;

Idx	Name	X-Pos [cm]	Y-Pos [cm]	Z-Pos [cm]	Dose [Gy]	Dose % Rx
1		2.87	-5.21	4.77	2.04	102.0
2		-1.13	-5.21	4.88	1.96	98.0

Ctrl Point Group Name: B1

Min. Dose: 1.14 Gy; Average Dose: 1.14 Gy (57.24% Rx); Max. Dose: 1.14 Gy;

Idx	Name	X-Pos [cm]	Y-Pos [cm]	Z-Pos [cm]	Dose [Gy]	Dose % Rx
1		3.75	-1.82	3.66	1.14	57.2

Figure 4.2: Dose control point report for the treatment plan of 2 Gy at point A in Rando phantom

4.8 *In-vivo* and *In-vitro* Dosimetry

Table 4.10 Ring and Tandem applicator dose results

			TPS Doses Planned from X-rays [Gy]						Measured Diode dose [Gy]			
			ICRU Dose Reference Points				Patient Diode Doses		Patient Diode Doses		Phantom Doses	
	Study	Applicator	A Dose	Bladder	R1	R2	Rectum	Bladder	Bladder	Rectum	Bladder	Rectum
1	1	R2T7	7.0	6.20	4.05	4.55	2.06	5.63	5.400	2.145	4.378	2.588
2			6.0	5.74	4.11	4.72	3.04	4.58	4.675	3.404	4.094	3.024
3	2	R2T5	6.5		4.13	4.22	2.25			2.375		2.507
4	3	R2T7	7.5	4.66	6.40	5.20	2.20	3.04	3.350	2.486	2.690	2.900
5	4	R2T5	6.0	5.61	3.26	3.10	1.14			1.410		1.478
6	5	R2T5	9.0	9.03	6.09	5.95	3.06		4.060	2.935		4.121
7	6	R2T7	9.0	7.75	5.97	5.84	2.81	7.15	7.162	3.994	5.512	2.810
8	7	R2T7	9.0	9.11	6.28	6.07	3.09	4.74	4.027	4.576	4.499	3.694
9	8	R2T5	8.5	6.36	4.83	4.74	3.26			4.905		3.308
10	9	R2T5	7.0	4.10	4.49	3.52	1.71	3.04	3.060	2.631	2.718	2.519
11			7.0	3.96	4.58	4.33	1.94	5.25	3.458	2.737	4.601	2.258
12	10	R2T7	7.0	5.50	3.83	4.77	2.38	3.34	2.852	3.820	2.737	3.095
13			6.0	4.66	3.39	4.35	1.97	3.71	3.114	3.025	3.321	2.586
14			6.5	7.18	3.52	4.37	2.43	3.87	3.157	4.390	3.532	3.025
15	11	R2T5	6.0	3.45	3.60	3.90	2.00	3.36	2.930	3.000	2.869	2.509
16			6.0	5.32	3.15	3.82	1.87	3.04	2.735	3.128	2.470	2.075
17			6.0	4.45	2.92	4.32	2.11	3.95	3.434	3.664	3.576	2.707
18	12	R2T5	6.5	6.55	4.50	4.30	1.65	5.84	4.487	2.443	4.297	1.995
19			5.5	7.42	3.16	3.28	1.80	4.01	3.558	2.897	4.028	2.79
20	13	R2T5	7.0	3.66	3.47	4.70	2.04	5.03	5.000	3.600	4.505	2.568
21			6.0		2.96	3.79	2.24			3.464		2.986
22	14	R2T5	7.0	6.73	5.13	4.91		2.18	1.787	2.903	2.148	2.400
23			6.0	4.41	3.91	3.98	1.86	3.50	3.841	3.097	3.440	2.301
24	15	R2T7	7.0	4.39	4.38	4.27	1.67	7.34	3.301	2.375	6.197	2.129
25			7.0	4.8	3.92	4.20	2.18	2.71	2.797	4.011	2.457	2.824
26	16	R2T7	7.0	4.73	4.34	4.29	1.64	5.63	5.263	2.565	5.373	2.267
27			6.0	5.00	3.09	3.59	1.88		1.963	3.326	1.690	2.934
28			6.0	3.79	3.74	3.9	2.45	1.92	1.841	3.722		
	17	R2T5	7.0	4.21	4.62	4.84	2.45	4.34	5.808	3.549	3.946	3.000
29	18	R2T5	7.0	4.44	3.89	3.58	1.73	5.03	4.482	2.787	8.531	2.377
30			7.0	3.39	4.23	4.44	2.15	4.20	4.025	3.074	4.097	2.928
31			7.0	2.43	4.68	5.5	3.57	2.15			3.496	2.676
32	19	R2T5	7.0	7.51	4.47	4.35	2.05	0.98	0.886	3.194	1.037	2.943
33			6.0	2.95	3.09	4.04	2.49	1.00	1.053	4.144	1.005	3.014
34			7.0	3.24	4.05	4.95	2.51	1.09	1.329	3.486	0.989	3.546
35	20	R2T5	7.0	4.82	4.72	4.75	2.03	2.95	3.091	3.058	2.911	2.962
36			6.5	3.86	4.69	4.4	1.70	3.13	2.587	2.478	3.138	2.038
37			6.5	3.53	4.61	5.32	1.63	5.36	4.845	2.356	4.520	2.276
38	21	R2T7	7.0	10.14	4.36	4.33	1.67	5.60	4.498	2.716	4.090	1.957
39			6.0	5.74	3.96	4.19	2.30	2.93	2.822	3.783	2.498	2.884
40			6.0	3.12	4.90	5.38	1.99	4.19	3.823	3.479	3.451	2.332
41	22	R2T3	6.0	7.21	4.50	5.5	2.24			4.140		2.972

In-vivo dosimetry in patients was carried out following the procedure described in the previous chapter (section 3.5).

A total number of 30 patients participated in the study. The ring and rigid tandem applicator was used on twenty-two patients and forty-one insertions had sufficient data captured in the study (see Table 4.10 above). The vaginal cylinder-rigid tandem combination (combo) applicator was used on eight patients and data from 11 insertions was successfully recorded in the study as shown in Table 4.11 below.

Table 4.11 Vaginal Cylinder – Tandem Applicator dose results

			TPS Doses Planned from X-rays [Gy]						Measured Doses [Gy]			
			ICRU Dose Reference Points				TPS Diode		Patient doses		Phantom Doses	
	Study	Applicator	A Dose	Bladder	R2	Surface	Bladder	Rectum	Bladder	Rectum	Bladder	Rectum
1	5	3cmCyl4cmTan	5.00	3.99	5.89			2.22		2.365		2.365
2	6	3cmCyl6cmTan	5.00	5.07	5.20			2.01		2.420		2.420
3			5.00	5.79	4.73			2.57		2.420		2.970
4	8	3cmCyl6cmTan	5.00	3.67	4.92		2.67	2.32	2.960	2.770	2.720	2.816
5	10	3cmCyl6cmTan	5.00	3.57	5.54		4.10	2.56	4.040	4.430	5.018	4.870
6			5.00	5.05	5.11	7.03	2.51	3.20	2.609	4.901	2.510	3.200
7	14	3cmCyl4cmTan	5.00	4.63	5.49	9.50	2.85	2.66	2.694	3.533	2.683	3.561
8			5.00	8.43	4.36	5.93	9.50	2.14	12.17	3.192		3.192
9	17	3cmCyl6cmTan	5.00	1.82	5.04	7.70	2.96	2.59	2.682	3.866	3.095	3.558
10	20	3cmCyl4cmTan	5.00	3.43	5.41		2.60				2.526	1.880
11	21	3cmCyl4cmTan	6.00	4.62	9.27		5.33	1.70	5.052	2.758	4.999	2.272

The orientation of the treatment setup of the treatment applicators relative to the bladder and rectum diodes in each patient was reproduced in a water phantom as described in section 3.5.3 of the previous chapter. *In-vitro* dose measurements were done for each insertion that had been done in patients and the results obtained tabulated as shown in Tables 4.12 and 4.13 below.

Table 4.12 TPS, *in-vivo* and *in- vitro* doses for Ring &Tandem applicator

			TPS Doses [Gy]						Measured Doses [Gy]				Ratios					
			ICRU Dose Reference Points				Patient Doses		Patient Doses		Phantom Doses		$ICRU_B$/	$\underline{ICRU_{Rectum}}$	$\underline{TPS_{Bladde}}$	$\underline{TPS_{Rectum}}$	$\underline{Bladder_D}$	$\underline{Rectum_D}$
No.	study	Aplctr	A	Bladder	R1	R2	$Rectum_d$	$Bladder_d$	$Bladder_p$	$Rectum_d$	$Bladder_w$	$Rectum_w$	$TPS_{Bladder}$	TPS_{Rectum}	$Bladder_D$	$Diode_D$	$Bladder_w$	$Rectum_w$
1	1	R2T7	7.0	6.20	4.05	4.55	2.06	5.63	5.400	2.450	5.630	2.060	1.148	1.857	1.043	0.841	1.000	1.000
2			6.0	5.74	4.11	4.72	3.04	4.58	4.675	3.404	4.580	3.040	1.228	1.387	0.980	0.893	1.000	1.000
3	2	R2T5	6.5		4.13	4.22	2.25			2.375		2.507		1.777		0.947		0.897
4	3	R2T7	7.5	4.66	6.40	5.20	2.20	3.04	3.350	2.486	2.521	2.900	1.391	2.092	0.907	0.885	1.206	0.759
5	4	R2T5	6.0			3.10	1.14	3.26		1.410		1.478		2.199		0.809		0.771
6	5	R2T5	9.0	9.03	6.09	5.95	3.06		4.060	2.935		4.121	2.224	2.027		1.043		0.743
7	9	R2T7	9.0	7.75	5.97	5.84	2.81	7.15	7.162	3.994	7.150	2.810	1.082	1.462	0.998	0.704	1.000	1.000
8	11	R2T7	9.0	9.11	6.28	6.07	3.09	4.74	4.027	4.576	4.499	3.694	2.262	1.326	1.177	0.675	1.054	0.836
9	12	R2T5	8.5	6.36	4.83	4.74	3.26			4.905		3.308		0.966		0.665		0.985
10	13	R2T5	7.0	4.10	4.49	3.52	1.71	3.04	3.060	2.631	2.718	2.519	1.340	1.338	0.993	0.650	1.118	0.679
11			7.0	3.96	4.58	4.33	1.94	5.25	3.458	2.737	4.601	2.258	1.145	1.582	1.518	0.709	1.141	0.859
12	15	R2T7	7.0	5.50	3.83	4.77	2.38	3.34	2.852	3.82	2.737	3.095	1.928	1.249	1.171	0.623	1.220	0.769
13			6.0	4.66	3.39	4.35	1.97	3.71	3.114	3.025	3.321	2.586	1.496	1.438	1.191	0.651	1.117	0.762
14			6.5		3.52	4.37	2.43	3.87		4.390	3.532	3.025		0.995		0.554	1.096	0.803
15	16	R2T5	6.0	3.45	3.60	3.90	2.00	3.36	2.930	3.000	2.869	2.509	1.177	1.300	1.147	0.667	1.171	0.797
16			6.0	5.32	3.15	3.822	1.87	3.04	2.735	3.128	2.47	2.075	1.945	1.222	1.112	0.598	1.231	0.901
17			6.0	4.45	2.92	4.32	2.11	3.95	3.434	3.664	3.576	2.707	1.296	1.179	1.150	0.576	1.105	0.779
18	18	R2T5	6.5	6.55	4.50	4.30	1.65	5.84	4.487	2.443	4.297	1.995	1.460	1.760	1.302	0.675	1.359	0.827
19			5.5		3.16	3.28	1.80	4.01		2.897	4.028	2.790		1.132		0.621	0.996	0.645
20	19	R2T5	7.0	3.66	3.47	4.70	2.04	5.03	5.000	3.600	4.505	2.568	0.732	1.306	1.006	0.567	1.117	0.794
21			6.0		2.96	3.79	2.24			3.464		2.986		1.094		0.647		0.750
22	22	R2T5	7.0		5.13	4.91		2.18		2.903	2.148	2.400		1.691			1.015	
23			6	4.41	3.91	3.98	1.86	3.50	3.841	3.097	3.440	2.301	1.148	1.285	0.911	0.601	1.017	0.808
24	23	R2T7	7.0	4.39	4.38	4.27	1.67	7.34	3.301	2.375	6.197	2.129	1.330	1.798	2.224	0.703	1.184	0.784
25			7.0	4.80	3.92	4.20	2.18	2.71	2.797	4.011	2.457	2.824	1.716	1.047	0.969	0.544	1.103	0.772
26			7.0	4.44	4.63	4.59	1.91	1.45	1.930	2.215				2.072	0.751	0.862		
27	24	R2T7	7.0	4.73	4.34	4.29	1.64	5.63	5.263	2.565	5.373	2.267	0.899	1.673	1.070	0.639	1.048	0.723
28			6.0		3.09	3.59	1.88			3.326	1.690	2.934		1.079		0.565		0.641
29	25	R2T5	6.0	3.79	3.74	3.90	2.45			3.722	3.946	3.000		1.048		0.658		0.817
30			6.0	3.90	3.93				2.385	3.440			1.635					
31	26	R2T5	7.0	4.44	3.89	3.58	1.73	5.03	4.482	2.787	8.531	2.377	0.991	1.285	1.122	0.621	0.590	0.728
32			7.0	3.39	4.23	4.44	2.15	4.20	4.025	3.074	4.097	2.928	0.842	1.444	1.043	0.699	1.025	0.734
33											3.496	2.676						
34	27	R2T5	7.0	7.51	4.47	4.35	2.05			3.194	1.037	2.943		1.362		0.642		0.697
35			6.0	2.95	3.09	4.04	2.49			4.144	1.005	3.014		0.975		0.601		0.826
36			7.0	3.24	4.05	4.95	2.51			3.486	0.989	3.546		1.420		0.720		0.708
37	28	R2T5	7.0	4.82	4.72	4.75	2.03	2.95	3.091	3.058	2.911	2.898	1.559	1.553	0.954	0.664	1.013	0.700
38			6.5	3.86	4.69	4.40	1.70	3.13	2.587	2.478	3.138	2.038	1.492	1.776	1.210	0.686	0.997	0.834
39			6.5	3.53	4.61	5.32	1.63	5.36	4.845	2.356	4.520	2.276	0.729	2.258	1.106	0.692	1.186	0.716
40	29	R2T7	7.0		4.36	4.33	1.67	5.60		2.716	5.102	2.253		1.594		0.615	1.098	0.741

Table 4.13 TPS, *in-vivo* and *in-vitro* doses for Vaginal Cylinder-Tandem applicator

			TPS Planned Doses [Gy]					Measured Doses [Gy]				Ratios					
			ICRU Reference Dose			Patient Doses		Patient Doses		Phantom Doses		$\frac{ICRU_{Bladder}}{Bladder_{TPS}}$	$\frac{ICRU_{Rectum}}{Rectum_{TPS}}$	$\frac{Bladder_{TPS}}{Bladder_{p}}$	$\frac{Rectum_{TPS}}{Rectum_{p}}$	$\frac{Bladder_{p}}{Bladder_{w}}$	$\frac{Rectum_{p}}{Rectum_{w}}$
	Study	Applicator	A	Bladder	Rectum	$Bladder_{p}$	$Rectum_{p}$	$Bladder_{w}$	$Rectum_{w}$	Bladder	Rectum						
1	5	3Cyl4Tan	5	3.99	5.89		2.22		2.365		2.365		2.490		0.939		1.000
2	6	3Cyl6Tan	5	5.07	5.20		2.01		2.420		2.420		2.149		0.831		1.000
3			5	5.79	4.73		2.57		2.420		2.970		1.955		1.062		0.815
4	8	3Cyl6Tan	5	3.67	4.92	2.67	2.32	2.960	2.770	2.720	2.816	1.240	1.776	0.902	0.838	1.088	0.984
5	10	3Cyl6Tan	5	3.57	5.54	4.10	2.56	4.040	4.430	5.018	4.870	0.884	1.251	1.015	0.578	0.805	0.910
6			5	5.05	5.11	2.51	3.20	2.609	4.901	2.510	3.200	1.936	1.043	0.962	0.653	1.039	1.531
7	14	3Cyl4Tan	5	4.63	5.49	2.85	2.66	2.694	3.533	2.683	3.561	1.719	1.554	1.058	0.753	1.004	0.992
8			5	8.43	4.36	9.50	2.14	12.170	3.192		3.192	0.693	1.366	0.781	0.670		1.000
9	17	3Cyl6Tan	5	1.82	5.04	2.96	2.59	2.682	3.866	3.095	3.558	0.679	1.304	1.104	0.670	0.867	1.087
10	20	3Cyl4Tan	5	3.43	5.41	2.60				2.526	1.880						
11	21	3Cyl4Tan	6	4.62	9.27	5.33	1.70	5.052	2.758	4.999	2.272	0.914	3.361	1.055	0.616	1.011	1.214

CHAPTER 5 ANALYSIS OF RESULTS

5.1 Basic Principles and Terminology of Measurements

"*A measurable quantity (briefly - measurand) is a property of phenomena, bodies, or substances that can be defined qualitatively and expressed quantitatively*." (Rabinovich, 2005). Measurable quantities are also known as physical quantities. Three important features describe a measurement (Rabinovich, 2005);

1. A measurement is a numerical number that corresponds to a property of an object;
2. Measuring instruments are used to perform a measurement;
3. Measurement is at all times an experimental course of action;

Measurement is the process that estimates a value of a quantity (NASA, 2010). Measurements are always accompanied by errors. Measurement uncertainty expresses the lack of knowledge and need to quantify the magnitude and sign of a measurement error. A measurement result must always include a statement of uncertainty in the estimate.

5.1.1 Uncertainty Analysis

Performing general uncertainty analysis usually follows the steps below:

i. Defining the measurement process,
ii. Identification of the sources of error,
iii. Estimation of uncertainties,
iv. Combining uncertainties,
v. Reporting the analysis of the results.

In any uncertainty analysis procedure, the measurand whose value is being estimated through measurement is identified. The test setup, environmental conditions, technical information about the instruments, reference standards and other instruments used and the procedure for performing the measurements are described in detail. The measurement process information

is used to identify possible sources of error. When the sources of error are found, statistical properties of the measurement errors are derived from the distributions of the data and estimates of the uncertainties are obtained (NASA, 2010).

Uncertainty describes the inaccuracy of a measurement result, while ***error*** describes the components of the uncertainty. A ***measurement error*** is defined as the variation of a measurement from the true value of the measurable quantity, expressed in absolute or relative form (Rabinovich, 2005). Uncertainty expresses the magnitude of the measurement error in a measurement result (IAEA-TECDOC-1585, 2008), e.g.

$$A = A_m \pm U_\tau \quad \ldots (5.1)$$

Where,

A is the true value,

A_m is the measured value, and

U_τ is the range and represents the measurement uncertainty.

In the above relationship, the true value of the measurement, A is between $A_m + U_\tau$ and $A_m - U_\tau$ (IAEA-TECDOC-1585, 2008)

5.1.2 Experimental Errors and Uncertainty

Experimental error is the difference between a measurement and the true value. ***Accuracy*** and ***precision*** are used to measure experimental error. No physical quantity can be measured with perfect certainty; errors are always present in any measurement (Taylor, 1997). If a quantity is measured and then the measurement is repeated again, it is most likely that a different value will be measured the second time. This makes it difficult to obtain the "true" value of a physical quantity. However, if refined experimental methods are used and great care is exercised in making measurements, errors can be reduced. In common speech, the words accuracy and precision are often used interchangeably. However, scientifically there is distinction between the meanings of the two words.

5.1.2.1 Accuracy

Accuracy refers to the relationship between a measured quantity and the real value of that quantity. The accuracy of a single measurement can be defined as the difference between the measured value and the true value of the quantity. The accuracy of a measurement is therefore limited by such things as the calibration and sensitivity of the instruments used, the ability to read the meters and mistakes made in recording the measurements (Bevington & Robinson, 1992).

5.1.2.2 Precision

Precision measures how close a measured value is to the true or accepted value. Precision also refers to the amount of scatter in a series of measurements of the same quantity. It is possible for a measurement to be very precise, but at the same time not very accurate. For example, if a voltage is measured using a digital voltmeter that is incorrectly calibrated, the answer will be precise (repeated measurements will give almost the same result to several decimal places) but the measurements will be inaccurate (all of the measurements will be wrong). By making a series of measurements of some quantity, we can obtain an estimate of the precision of each individual measurement (Bevington & Robinson, 1992).

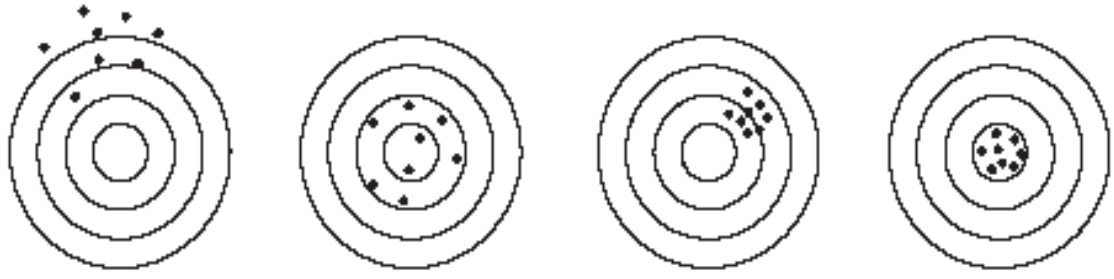

Not accurate	Accurate	Not accurate	Accurate
Not Precise	Not precise	Precise	Precise

Figure 5.1: An illustration of accuracy and precision of measurements in a game of darts

Error and uncertainty are also often used interchangeably. Nevertheless, it is important to be aware of the distinction between the actual error in a given measurement (i.e. in the amount by which the measured value differs from the true value) and the uncertainty in a measurement. In many experiments, the true value of the quantity being measured is not known, and therefore the actual error in the result is not definite. Usually both the systematic and random error of the error must be estimated. The systematic error is estimated *priori* while the random error is estimated *posteriori* (Rabinovich, 2005).

When n single measurements are repeated to account for random errors, $\{x_i\}$ values of the measured quantity will be obtained i.e. $\{x_i\}$, i = 1, . . . , n. This can be written as (Rabinovich, 2005),

$$x_i = A + \varepsilon_i \qquad \ldots (5.2)$$

Where,

A is the actual value of the measured quantity,

ε_i is the error in the measured quantity.

The error ε_i, has both the random and systematic components, i.e.

$$\varepsilon_i = \varphi_i + \vartheta_{ij} \qquad \ldots (5.3)$$

Where,

φ_i is the random error, and

ϑ_{ij} is the systematic error.

Repeating measurements collects information about the random error. Information about the systematic error is obtained from properties of the measuring instrument, the method of measurement and the conditions present during the measurement process. The systematic error cannot be directly obtained from the measurements.

However, it is still possible to make an estimate of the uncertainty (or the probable error) in the measurement based on what is known about the

properties of the measuring instruments. The precision of any individual measurement can be determined by calculating the standard deviation of the mean, also known as the standard uncertainty of the mean, $S_{\bar{x}}$ (Rabinovich, 2005, p. 31):

$$S_{\bar{x}} = \sqrt{\frac{\sum_{i=1}^{n}(x_i - \bar{x})^2}{n(n-1)}} \quad \ldots (5.4)$$

Where $\bar{x}$ is the average value of x and where n is the number of measurements. The standard error can be taken as an estimate of the uncertainty or probable error since any individual measurement has a reasonable probability of being in error by at least that amount. However, the actual error in a measurement can be much larger than the standard deviation if there are systematic errors, e.g. errors in calibration of measuring instruments that affect measurements the same way. It is good practice to compare measured values of quantities with given or theoretical values and the estimate the percentage error (Taylor, 1997).

Additional to the measured quantity A, a confidence interval that determines the confidence of the limits of the random error in the measurement results can be made, i.e.

$$\tilde{A} - \Psi_\alpha \leq A \leq \tilde{A} + \Psi_\alpha ,$$

Where $\Psi_\alpha = t_q S_{\bar{x}}$, and t_q represents the q percent point of the t- distribution and relies on the confidence probability α and the number of degrees of freedom, $v = n - 1$ (Rabinovich, 2005)

5.2 Classification of Measurement Errors

In performing measurements for calibration of measuring instruments, high levels of accuracy and precision are maintained to obtain the measurable quantity so that it can be used for this purpose instead of the true value of the quantity (Rabinovich, 2005). This is the reason why measurement errors are

estimated using indirect data. In carrying out measurements, there are fundamental components that constitute any measuring system, i.e.

- the method of measurement,
- the measuring instrument; and
- the person making the measurements.

Any imperfection inherent in each of the fundamental components of measurement contributes directly to the measurement error. This can be expressed as, in the general form,

$$E = E_m + E_i + E_p \quad \text{... (5.3)}$$

Where,

E is the measurement error,
E_m is the methodological error,
E_i is the instrumental error and
E_p is the personal error.

Several factors can give rise to each separate measurement error component stated above (IAEA-TECDOC-1585, 2008).

5.2.1 Outlying Results

Gross (outlying) errors are errors that considerably surpass the acceptable error margins for a given set of conditions in which the measurements are done (Rabinovich, 2005). The conditions under which the measurements are done may include the properties of the measuring instrument used, the method of measurement, the qualifications and expertise of the experimenter and the physical conditions, i.e. the temperature, humidity and pressure. For a given experiment, a sudden change in temperature may drastically affect measurements for an experiment that has to be carried out at constant temperature. Statistical methods are used to identify o*utlying* or gross errors in

multiple measurements and it is possible to remove the outliers from the data analysis.

For a given ordered series, $X_1 < X_2 < X_3 < - - - < X_n$, from all X_i, the mean x and the standard deviation is calculated and then T is calculated using the following formula:

$$T = \frac{\max|x_i - \bar{x}|}{\delta} \quad \text{... (5.4)}$$

Where δ is calculated using the formula for calculating the standard deviation above (equation (5.1)). The outcome of the calculation will either be,

$$T_1 = \frac{|x_i - \bar{x}|}{\delta} \quad \text{... (5.5)}$$

or,

$$T_n = \frac{|x_i - \bar{x}|}{\delta} \quad \text{... (5.6)}$$

When experiments are done and measurements recorded, it is difficult to predict if x_1 or x_n will be checked. Appendix 6 shows the 0.5, 1, and 5 percentage points of T_q of the corresponding unilateral check of the series $X_1 < X_2 < X_3 < - - - < X_n$. A critical value T_q (taken from Appendix 6), for which the significance level is half of the level used for checking the data was adopted (Rabinovich, 2005). For a calculated value of $T_{1,n}$ in equations 5.5 and 5.6 above, greater than T_q, a subsequent value of x_1 or x_n was removed from the data that was considered in the analysis. This procedure was used to identify outliers from results of measured data as shown in the Appendices 7 and 8.

Table 5.1: Ring and Tandem Applicator Raw data general statistics

(Gy)	Point A Dose	ICRU Bladder	R1	R2	TPS $Bladder_D$	Patient $Bladder_D$	Phantom $Bladder_D$	TPS $Rectum_D$	Patient $Rectum_D$	Phantom $Rectum_D$
Mean	6.762	5.279	4.237	4.489	3.880	3.514	3.567	2.177	3.202	2.690
Std Dev	0.850	1.824	0.865	0.696	1.579	1.356	1.503	0.503	0.721	0.501
Median	7.000	4.765	4.180	4.350	3.870	3.392	3.496	2.060	3.097	2.707
Minimum	5.500	2.430	2.920	3.100	0.980	0.886	0.989	1.140	1.410	1.478
Maximum	9.000	10.140	6.400	6.070	7.340	7.162	8.531	3.570	4.905	4.121

Table 5.2: Statistics of Raw Data Ratios of doses obtained using Ring and Tandem Applicator

	$\frac{ICRU_{Bladder}}{Bladder_{Ptn}}$	$\frac{Bladder_{TPS}}{Bladder_{Ptn}}$	$\frac{Bladder_{TPS}}{Bladder_{Water}}$	$\frac{Bladder_{Ptn}}{Bladder_{Water}}$	$\frac{ICRU_{Rectum}}{Rectum_{Ptn}}$	$\frac{Rectum_{TPS}}{Rectum_{Ptn}}$	$\frac{Rectum_{TPS}}{Rectum_{Water}}$	$\frac{Rectum_{Ptn}}{Rectum_{Water}}$
Mean	1.825	1.129	1.095	1.015	1.456	0.679	0.805	1.191
Std Dev	1.357	0.241	0.165	0.187	0.351	0.119	0.122	0.196
Median	1.476	1.109	1.105	1.044	1.387	0.661	0.782	1.171
Min	0.729	0.820	0.590	0.525	0.966	0.544	0.641	0.712
Max	8.476	2.224	1.369	1.344	2.258	1.043	1.334	1.507

However, it can also be true that an *abnormal* observation may in fact be an indication of an unknown property of the subject under study (Rabinovich, 2005). Below are reasons that may merit an experimenter to remove an outlier from measured data (Rabinovich, 2005):

1. Real measurements generally are comprised of a small number of observations and the chances of obtaining more than two outliers in the results will be very small. Therefore, the outlier under concern may not be cancelled out by another one having an opposite sign in the data set.

2. An outlier is considerably different from the majority of the measured data and hence skews the average value of the data set, thereby increasing the inaccuracy of measurements.

In this study the experimenter eliminated outliers using the unilateral check i.e. eliminating data entries above certain critical values of distribution , $T_n = \frac{\max|x_n - \bar{x}|}{\delta}$ or $T_1 = \frac{\max|\bar{x} - x_1|}{\delta}$ (Rabinovich, 2005) (Appendices 6). A few *in-vitro* dose data entries for ring and tandem applicator dose were identified and eliminated as outliers using upper 5% significance level identification of outliers (Appendix 7). Almost half of all the dose data for the vaginal cylinder and tandem combination (combo) was identified as outliers using the same method as above (Appendix 8). The outliers were not eliminated from the combo results and the data was processed as-it-was without any alterations. Removal of the 'outliers' would have further reduced the sample size. This would have made it very difficult for the data to be effectively used in data analysis.

5.2.2 Blunders

Blunders arise from errors made by the experimenter. For instance, a slip of the pen while writing up results of observations or recording a measurement that is not corrected for temperature and pressure for experiments that are influenced by environmental conditions could result in a blunder. Non-statistical methods are used to identify and remove blunders from measured data sets (IAEA-TECDOC-1585, 2008). In carrying out this research, it was observed that on certain occasions, the positions of placement of bladder and rectal diode probes used for planning were different compared to the final position of the diode probes after treatment. This was as a result of bladder and rectal diode probes slipping out from placement positions (where they would have been secured) inside the patient during treatment. On such incidents, the measured doses were different from the dose computed from the x-ray radiographs. These values were regarded as blunders and were

excluded in the data analysis. Tables 5.3 and 5.4 below show general statistics of processed data without outliers and blunders.

Table 5.3: Ring and tandem processed data statistics without blunders and outliers

(Gy)	Point A Dose	ICRU Bladder	R1	R2	TPS $Bladder_D$	Patient $Bladder_D$	Phantom $Bladder_D$	TPS $Rectum_D$	Patient $Rectum_D$	Phantom $Rectum_D$
Mean	6.795	4.990	4.227	4.414	4.204	3.780	3.731	2.124	3.135	2.679
Std Dev	0.864	1.610	0.886	0.670	1.407	1.156	1.682	0.472	0.719	0.522
Median	7.000	4.450	4.120	4.340	3.950	3.446	3.532	2.040	3.058	2.676
Minimum	5.500	2.950	2.920	3.100	1.450	1.930	0.989	1.140	1.410	1.478
Maximum	9.000	9.110	6.400	6.070	7.340	7.162	8.531	3.260	4.905	4.121

Ratios of TPS planned doses at ICRU reference points to *in-vivo* and *in-vitro* measured doses were also computed to further analyse the data (see Appendices 8 and 9). Tables 5.4 and 5.5 show results for ratios of processed data obtained for the two applicators considered in this study.

Table 5.4 Statistics of ratios for processed data without blunders and outliers for ring and tandem applicator

	$\frac{ICRU_{Bladder}}{Bladder_{Ptn}}$	$\frac{Bladder_{TPS}}{Bladder_{Ptn}}$	$\frac{Bladder_{TPS}}{Bladder_{Water}}$	$\frac{Bladder_{Ptn}}{Bladder_{Water}}$	$\frac{ICRU_{Rectum}}{Rectum_{Ptn}}$	$\frac{Rectum_{TPS}}{Rectum_{Ptn}}$	$\frac{Rectum_{TPS}}{Rectum_{Water}}$	$\frac{Rectum_{Ptn}}{Rectum_{Water}}$
Mean	1.368	1.127	1.082	0.980	1.475	0.689	0.773	1.182
Std Dev	0.418	0.278	0.134	0.183	0.358	0.115	0.160	0.177
Median	1.330	1.088	1.098	1.021	1.403	0.664	0.772	1.189
Minimum	0.729	0.751	0.590	0.525	0.966	0.544	0.641	0.712
Maximum	2.262	2.224	1.359	1.329	2.258	1.043	1.000	1.507

Table 5.5: Statistics of raw data ratios for vaginal cylinder and tandem applicator

	$\frac{ICRU_{Bladder}}{Bladder_{Ptn}}$	$\frac{Bladder_{TPS}}{Bladder_{Ptn}}$	$\frac{Bladder_{TPS}}{Bladder_{Water}}$	$\frac{Bladder_{Ptn}}{Bladder_{Water}}$	$\frac{ICRU_{Rectum}}{Rectum_{Ptn}}$	$\frac{Rectum_{TPS}}{Rectum_{Ptn}}$	$\frac{Rectum_{TPS}}{Rectum_{Water}}$	$\frac{Rectum_{Ptn}}{Rectum_{Water}}$
Mean	1.152	0.982	0.988	0.969	1.825	0.761	0.788	1.053
Std Dev	0.501	0.111	0.085	0.109	0.701	0.155	0.136	0.197
Median	0.914	1.015	1.000	1.007	1.665	0.712	0.786	1.000
Minimum	0.679	0.781	0.817	0.805	1.043	0.578	0.526	0.815
Maximum	1.936	1.104	1.066	1.088	3.361	1.062	1.000	1.532

Statistical values of raw and processed data for the ring and tandem applicator doses are almost the same. However, from Tables 5.2 and 5.4, comparison between raw and processed data ratios of planned ICRU to *in-vivo* doses show that the outliers grossly skew the data, i.e. raw data ratio of $ICRU_{Bladder}/Bladder_{Ptn}$ = 1.825 and processed data ratio of $ICRU_{Bladder}/Bladder_{Ptn}$ = 1.368.

5.2.2.1 Frequencies and Descriptive Statistics of Processed Data

Since most of the data obtained for the combo applicator was identified as outliers using the procedure in section 5.2.1, only data acquired from using the ring and tandem applicator was used for the further analyses.

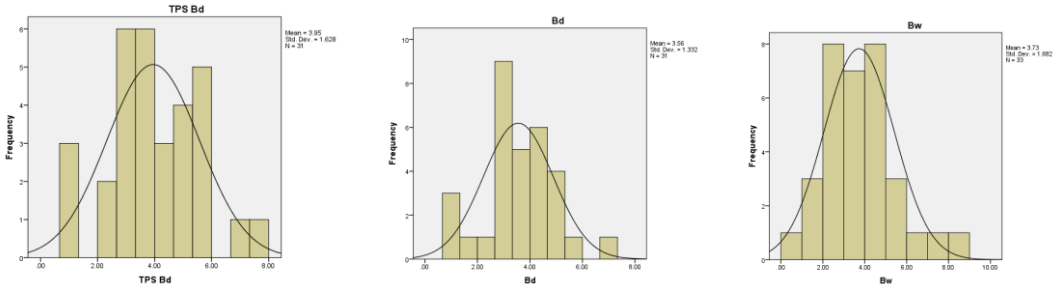

(a) (b) (c)

Figure 5.2: Frequency distributions of (a) TPS planned, (b) *In-vivo*, and (c) *In-vitro* Bladder doses

5.2.2.1.1 Skewness

Skewness occurs when one tail of a frequency distribution is longer than the other, and when the mean and median are different, then the curve is said to be skewed (Rabinovich, 2005). Most common inferential statistical tests assume that the dependent variable is normally distributed. Therefore, it is imperative to have knowledge on how the data is skewed. A perfect normal distribution curve has a skewness of zero.

Figure 5.2 shows the frequency distributions of the TPS planned together with in-vivo and in-vitro measured doses showing differing degrees of skewness. The skewness values range from 0.066 (for TPS bladder) to 0.872 (for TPS Rectum) as shown in Table 5.6 below.

The shapes of the TPS planned and in-vivo bladder doses are almost similar in appearance although the values of the skewness are different, i.e. 0.066 and 0.200 for the TPS and *in-vivo* bladder doses respectively. Similar analysis of the rectum doses show almost similar frequency distributions for the TPS planned and *in-vivo* doses although they also have different skewness values of 0.872 and 0.356 for the TPS planned and *in-vivo* doses respectively. For

both the bladder and rectum, the shapes of frequency distributions of *in-vitro* measured doses look very different from the TPS and *in-vivo* measured doses.

Table 5.6 SPSS Output for general statistics for processed data

		TPS Bladder Diode	TPS Rectum Diode	*In-Vivo* Bladder Diode	*In-Vivo* Rectum Diode	*In-Vitro* Bladder Diode	*In-Vitro* Rectum Diode
N	Valid	31	37	31	37	33	38
	Missing	7	1	7	1	5	0
Std. Deviation		1.628	0.527	1.332	0.721	1.682	0.515
Variance		2.651	0.278	1.774	0.520	2.831	0.265
Skewness		0.066	0.872	0.200	0.356	0.700	0.399
Std. Error of Skewness		0.421	0.388	0.421	0.388	0.409	0.383
Kurtosis		-0.253	0.585	0.907	0.362	1.070	0.901
Std. Error of Kurtosis		0.821	0.759	0.821	0.759	0.798	0.750
Range		6.360	2.430	6.280	3.500	7.540	2.640
Percentiles	25	3.040	1.765	2.852	2.599	2.611	2.274
	50	3.870	2.050	3.434	3.058	3.532	2.692
	75	5.250	2.440	4.487	3.632	4.550	2.990

5.2.2.1.2 Kurtosis

When a frequency distribution has greater peaks than the normal curve, it has positive kurtosis and is said to be **leptokurtic**. If a data distribution is fairly flat with well pronounced tails, it will have negative kurtosis and is said to be **platykurtic**. Kurtosis does not greatly affect the results of most statistical

analyses and therefore was not used in the analysis of the results in this study.

5.2.3 Methodological Errors

Methodological errors arise due to lack of sufficient knowledge on the theory of the phenomena on which the measurement is based on and using incorrect principles to obtain the estimate of the measurable quantity. In particular, the error caused by the threshold discrepancy between the model of a specific object and the object itself is also a methodological error (IAEA-TECDOC-1585, 2008). In this study, ratios were calculated to determine the methodological error for doses at ICRU (ICRU, 1985) reference points, in patients and in a water phantom. This was done to investigate and to prove the validity of the method used to obtain doses received by the bladder and rectum during gynaecological HDR brachytherapy (see Appendices 8 and 9). Doses at reference points obtained through computerised treatment planning were compared with doses measured in patients and doses measured in a water phantom to confirm the validity of computerised treatment planning and *in-vivo* doses as shown in the tables of results (see Appendices 8 and 9) and Tables 5.4 and 5.5 above. The average ratio of ICRU rectal point to *in-vivo* rectum dose was 1.475 ± 0.358 (range: 0.966-2.258) while ICRU bladder point to *in-vivo* bladder dose was 1.368 ± 0.418 (range: 0.729 -2.262) for ring and tandem applicator. The ratios of ICRU point to *in-vivo* dose for the rectum and bladder when using the vaginal combo applicator were 1.825 ± 0.701 (range: 1.043 - 3.361) and 1.152 ± 0.501 (range: 0.679 – 1.936) respectively. The TPS algorithm used to compute the dose is based on using water as tissue-equivalent material. Therefore, the relationship between TPS planned doses, *in-vivo* and *in-vitro* doses was expected to be very close to unity (one), since all the three dosimetry methods all computed or measured dose at the 'same' point. The mean ratios of TPS to *in-vivo* dose for the bladder and rectum were 1.127 ± 0.278 (range: 0.751 – 2.224) and 0.689 ± 0.115 respectively for ring and tandem applicator insertions. Average TPS to *in-vivo* dose ratios for the bladder and rectum were 1.016 ± 0.073 (range: 0.902 – 1.104) and 0.761 ± 0.155 (range: 0.578 – 1.062) in that order for vaginal

combo applicator insertions. Average ratios of TPS to *in-vitro* dose were 0.988 ± 0.085 (range: 0.817 – 1.066) and 0.788 ± 0.136 (range: 0.526 – 1.000) for the bladder and rectum respectively for vaginal combo insertions. While mean ratios of TPS to *in-vitro* dose for the bladder and rectum were 1.082 ± 0.134 (range: 0.590 – 1.359) and 0.773 ± 0.160 (range: 0.641 – 1.000) respectively for ring and tandem applicator insertions.

The average ratios for bladder doses were 'reasonably' close to unity i.e. TPS to *in-vivo*, TPS to *in-vitro*, *in-vivo* to *in-vitro* were 1.127, 1.082 and 0.98 respectively as compared to the average ratios for rectum doses, i.e. TPS to *in-vivo*, TPS to *in-vitro*, *in-vivo* to *in-vitro* were 0.689, 0.773 and 1.181 respectively. The ratios for the bladder doses confirm the methodological validity of the methods used in the study. However, there were large error margins observed in results obtained from computations and measurements in the rectum had which suggests the unfitness of the data to be used for useful *in-vivo* – TPS dose comparisons. The *in-vitro* measurements were useful in confirming the relationship patterns between TPS and *in-vivo* doses.

5.2.4 Personal Errors

These errors arise due to the mere fact that humans perform the measurements. "*A measure of the non-reproducibility of a measurement permitted by the experimenter is the limits of measurement error or uncertainty estimated by the experimenter*." (IAEA-TECDOC-1585, 2008). Measurement errors can also be classified based on their properties. In this respect, systematic and random errors are distinguished.

5.2.5 Systematic Errors

"*A measurement error is said to be systematic if it remains constant or changes in a regular fashion in repeated measurements of one and the same quantity*" (IAEA-TECDOC-1585, 2008). Corrections can be employed to remove errors from measurements. However, it is very difficult to remove all systematic errors using corrections in a measurement. There is always a

fraction of error that will be present in measurements and this becomes the systematic component of the measurement error. Systematic errors are obtained experimentally either:

- by evaluating a measurement against another measurement of the same quantity obtained using a different method, or
- by using a measuring instrument that is more accurate.

However, systematic errors are usually obtained by theoretical analysis (see Table 5.3) of the measurement conditions, relying on information on known properties of the measurable quantity and of measuring instruments.

5.2.5.1 Instrumental Errors

Instrumental errors are caused by using faulty measuring instruments in making measurements. The normal/intrinsic error of instruments, i.e. the error obtained under reference conditions is usually differentiated from additional errors that may arise because of variations in the values of influence quantities from reference conditions (IAEA-TECDOC-1585, 2008). For modern instruments, advances in the reading and regulating mechanisms of measuring instruments have greatly reduced personal errors such that they are normally insignificant. The equipment that was used during this study is regularly calibrated and monitored through frequent consistency quality control checks. Corrective measures are applied as and when necessary to keep the instrument up to specifications and reasonable error margins.

From chapter 4, section 4.1, the average value of the dosimeter stability over the duration of the study was found to be ± 0.52%. The uncertainty in the calibration/stability of the dosimeter contributes directly to the uncertainty in the measurements and therefore is included in determining the overall error in the dose measurement. The stability uncertainty term is shown below (IAEA-TECDOC-1585, 2008):

$$Dose_{True} = Dose_{Raw} \pm \Delta_S \quad \ldots (5.4)$$

$$= Dose_{Raw}\left(1 + \frac{\Delta_S}{Dose_{Raw}}\right)$$

$$= Dose_{Raw} . N_s$$

where:

$\frac{\Delta_S}{Dose_{Raw}}$ is the uncertainty in the stability of the dosimeter and the average value of this uncertainty is $\pm$0.52 % in this study.

Therefore, in the above equation, the factor N_S = 1.0052,

$Dose_{Raw}$ is the unprocessed *in-vivo* or *in-vitro* measured dose,

$Dose_{True}$ is the processed true dose at a given point which incorporates the errors.

Measurements done to confirm the reference dosimetric quantity, i.e. the air kerma strength, were done using the in-air, in-phantom methods and in a Well chamber. This was done to obtain the uncertainty in the calibration of the diode probes. An analysis of values of air kerma strength obtained using the three different methods is shown in Table 5.7 below. From Table 5.7, all the methods used to calculate the air kerma strength produced values close to the Well Chamber measurement (see Appendix 9), i.e. the values were on average within 2 % of the local standard. Since this study was concerned with determining the dose received by organs at risk during gynaecological HDR brachytherapy, air kerma strength was calculated based on the absorbed dose to water factors in this study.

Table 5.7: Comparison of source strength measured using different methods

Method		Air Kerma Strength ($cGyh^{-1}.m^{2)}$	% Error $= \left[\frac{WC - K}{WC}\right] X100\%$
Well Chamber (WC)		21.592	0.000
In Air (IA)	i Exposure	21.790	- 0.917
	ii Absorbed Dose	21.595	- 0.014
In Phantom (IP)	i Exposure	21.804	- 0.982
	ii Absorbed Dose	21.809	-1.010

where,

K is exposure or absorbed dose based air kerma values obtained using the in-air or in-phantom method.

A comparison between measurements obtained using the well chamber and the decay adjusted manufacturers value (on the certificate) was done using MS Excel spreadsheet and was found to be -2.2% (see Appendices 1 and 13).

5.2.5.2 Static and Dynamic Errors

Measurement errors can also be grouped into static and dynamic errors. All of the errors described in the previous sections above are static errors.

"Dynamic errors are caused by the inertial properties of measuring instruments." (IAEA-TECDOC-1585, 2008).

"*The inertial properties of an instrument can be such, however, that the changes in the measurable quantity over the measurement time will give rise to a definite error in the results of measurements of the instantaneous values*." (IAEA-TECDOC-1585, 2008).

The resultant data set of instantaneous values gathered from the experiments will not be concurrent with the change of the measurand in time because of the dynamic error.

Table 5.8: Change in the diode calibration factors with time (dynamic error)

Calibration Factors (e + 005 Gy/C)						
Date	B	R1	R2	R3	R4	R5
24.10.11	3.966	4.366	4.169	4.270	4.035	4.023
26.10.11	4.132	4.749	4.118	4.148	4.157	4.274
26.10.11	4.098	4.695	4.073	4.096	4.106	4.217
26.10.11	4.077	4.661	4.055	4.077	4.094	4.202
04.11.11	4.013	4.650	4.349	4.521	4.386	4.459
04.11.11	4.463	5.286	4.905	5.007	4.902	5.039
14.11.11	4.463	5.286	4.905	5.007	4.902	5.039
07.03.12	4.151	5.967	5.114	4.359	3.582	3.017
16.04.12	3.988	6.670	5.499	4.760	3.851	3.226
24.07.12	4.513	5.372	5.029	5.190	4.963	4.985
Minimum	3.966	4.366	4.055	4.077	3.582	3.017
Maximum	4.513	6.670	5.499	5.190	4.963	5.039
Mean	4.186	5.170	4.622	4.544	4.298	4.248
Range	0.547	2.304	1.444	1.113	1.381	2.022
Standard deviation	0.211	0.710	0.526	0.419	0.478	0.703
Monthly deviation	0.061	0.256	0.160	0.124	0.153	0.225
Weekly deviation	0.015	0.064	0.040	0.031	0.038	0.056
% Weekly deviation	0.363	1.238	0.868	0.680	0.893	1.322

The **instantaneous dynamic error** occurs because of variation in the rate of change of a measurable quantity and inertial properties of an instrument with respect to a separate instantaneous quantity being measured at a given time.

If a varying quantity is measured using a measuring instrument, the difference between a measurement obtained and the actual process of variation of the recorded quantity in time gives the dynamic error of the given dynamic measurement. (IAEA-TECDOC-1585, 2008). In this research, the instantaneous dynamic error arose from calibrating the diode probes at given time intervals. This was necessitated by the fact that the response of the diode semiconductor material (used to make the diode) changes with time because of exposure to radiation (Huyskens, et al., 2001). The rate at which periodical calibrations of the diode probes were made, influenced the magnitude of the dynamic error that is present in the measurements. Table 5.8 above shows an MS Excel spreadsheet output for computing the variation of the calibration factors of the *in-vivo* diodes with time. The calibration factors vary weekly from at least 0.36% to 1.32% due to the change in the measuring properties of the diodes.

For independent sources of error, the combined error is calculated as by equation 5.5 below (NASA, 2010),

$$\mu_x = \sqrt{\mu_1^2 + \mu_2^2 + \mu_3^2 + \cdots} \qquad \ldots (5.5)$$

Therefore, combining the instrumental errors above to get the expected Systematic error gives,

$$= \sqrt{(0.45^2 + 2.2^2 + 1.01^2 + 1.32^2)}$$

$$= 2.8\%$$

5.2.6 Random Error

"*If there are differences between the results of separate measurements, and these differences cannot be predicted individually and any regularities inherent to them are manifested only in many results, then the error from this*

scatter of the results is called the ***random error****"* (IAEA-TECDOC-1585, 2008).

Table 5.9: Random error (intra-patient) for TPS, *in-vivo* and *in-vitro* measurements using ring and tandem applicator

Std	ICRU Pnt ADose (Gy)	TPS (Gy)		*In-Vivo* (Gy)		*In-vitro* (Gy)		INTRA Patient Dose Variation (Gy)					
		Rectum	Bladder	Bladder	Rectum	Bladder	Rectum	B_{TPS}	B_d	B_w	R_{TPS}	R_d	R_w
13	7	1.71	3.04	3.060	2.631	2.718	2.519	2.21	0.398	1.883	0.23	0.106	0.261
	7	1.94	5.25	3.458	2.737	4.601	2.258						
16	6	2.00	3.36	2.930	3.000	2.869	2.509	0.32	0.195	0.399	0.13	0.128	0.434
	6	1.87	3.04	2.735	3.128	2.470	2.075	0.59	0.504	0.707	0.11	0.664	0.198
	6	2.11	3.95	3.434	3.664	3.576	2.707	0.91	0.699	1.106	0.24	0.536	0.632
23	7	1.67	7.34	3.301	2.375	6.197	2.129	4.63	0.504	3.740	0.51	1.636	0.695
	7	2.18	2.71	2.797	4.011	2.457	2.824	1.37	1.371		0.24	0.16	
	7	1.91	1.45	1.930	2.215			1.26	0.867		0.27	1.507	
25	6	2.45			3.722	3.946	3.000					0.282	
	6			2.385	3.440								
26	7	1.73	5.03	4.482	2.787	8.531	2.377	0.83	0.457	4.434	0.42	0.287	0.551
	7	2.15	4.20	4.025	3.074	4.097	2.928						
27	7	2.05			3.194	1.037	2.943			0.048	0.46	0.292	0.603
	7	2.51			3.486	0.989	3.546						
28	6.5	1.7	3.13	2.587	2.478	3.138	2.038	2.23	2.258	1.382	0.07	0.122	0.238
	6.5	1.63	5.36	4.845	2.356	4.520	2.276						
							Mean	1.595	0.806	1.712	0.268	0.520	0.452
							St Dev	1.316	0.641	1.583	0.151	0.549	0.197
							Max	4.630	2.258	4.434	0.510	1.636	0.695
							Min	0.320	0.195	0.048	0.070	0.106	0.198

where the subscripts $_{TPS}$, $_d$ and $_w$ represent TPS planned, *in-vivo* and *in-vitro* doses respectively.

Performing measurements of the same quantity repeatedly makes it possible for random errors to be identified in a measurement system. From section 5.1, the random error Ψ with probability equal to the confidence probability α has limits $\pm\Psi_\alpha$ (Rabinovich, 2005):

$$\Psi_\alpha = t_q S_{\bar{x}}$$

In this study, the treatment planning and *in-vivo* dosimetry measurement procedures for each fraction were done only once on each patient for each treatment fraction. It was only the *in-vitro* measurements that could be repeated (at most) three times in order to establish the random error (see Appendices 10 and 11)

"*The quality of measurements that reflects the closeness of the results of measurements of the same quantity performed under the same conditions is called the repeatability of measurements*" (IAEA-TECDOC-1585, 2008).

Random errors are small when there is good repeatability of measurements. Data processing to obtain the intra-patient random error per critical organ was done and the results are shown in Table 5.9 above. Data for patients who had unchanged prescription dose for at least two insertions was selected for this type of analysis. Data from seven patients fitted this criterion and was used in the intra-patient dose variation investigation. The differences between individual doses recorded per each insertion per critical organ per patient were calculated and tabulated as shown in Table 5.9. The standard deviation of the variation of intra-patient dose for the entire population sample was regarded as the random error. This random error was the expected dose difference between insertions.

The same analysis could not be done for the vaginal combo applicator since only data from three patients matched the selection criterion and the sample was too small for a valid analysis to be done on the data. A separate analysis was also done to obtain the uncertainty in the bladder and rectum doses from

patient-to-patient, i.e. inter-patient dose variation. The same data sample from the previous analysis was used for this investigation. In order to calculate the inter-patient dose variation per critical organ, the mean intra-patient variation for the entire sample (from the previous analysis) was subtracted from each individual dose value recorded for each critical organ and the results obtained are shown in Table 5.10 below.

Table 5.10: Random error (inter-patient) for TPS, *in-vivo* and *in-vivo* measurements using ring and tandem applicator

Std	ICRU Pnt A Dose (Gy)	TPS (Gy)		*In-Vivo* (Gy)		*In-vitro* (Gy)		INTER-Patient Dose Variation (Gy)					
		Rectum	Bladder	Bladder	Rectum	Bladder	Rectum	B_{TPS}	B_d	B_w	R_{TPS}	R_d	R_w
13	7	1.71	3.04	3.060	2.631	2.718	2.519	0.62	0.408	0.171	0.04	0.414	0.191
	7	1.94	5.25	3.458	2.737	4.601	2.258						
16	6	2.00	3.36	2.930	3.000	2.869	2.509	4.31	2.063	4.035	0.38	1.508	0.261
	6	1.87	3.04	2.735	3.128	2.47	2.075	0.27	0.309	0.659	0.04	0.558	
	6	2.11	3.95	3.434	3.664	3.576	2.707	0.91	0.699	1.106	0.24	0.536	0.632
23	7	1.67	7.34	3.301	2.375	6.197	2.129	4.63	0.504	3.740	0.51	1.636	0.695
	7	2.18	2.71	2.797	4.011	2.457	2.824	1.37	1.371		0.24	0.16	
	7	1.91	1.45	1.930	2.215			1.26	0.867		0.27	1.507	
25	6	2.45			3.722	3.946	3.000					0.282	
	6			2.385	3.440								
26	7	1.73	5.03	4.482	2.787	8.531	2.377	0.83	0.457	4.434	0.42	0.287	0.551
	7	2.15	4.20	4.025	3.074	4.097	2.928						
27	7	2.05			3.194	1.037	2.943			0.048	0.46	0.292	0.603
	7	2.51			3.486	0.989	3.546						
28	6.5	1.70	3.13	2.587	2.478	3.138	2.038	2.23	2.258	1.382	0.07	0.122	0.238
	6.5	1.63	5.36	4.845	2.356	4.520	2.276						
							Mean	1.825	0.993	1.947	0.267	0.664	0.453
							Std Dev	1.598	0.735	1.821	0.175	0.586	0.214
							Max	4.630	2.258	4.434	0.510	1.636	0.695
							Min	0.270	0.309	0.048	0.038	0.122	0.191

The standard deviation of this process was regarded as the expected inter-patient dose variation. In this study, although a patient usually received HDR

brachytherapy treatment three times for a full treatment course, only one *in-vivo* dosimetry procedure was possible per insertion. During the following insertions/treatments, it is difficult to reproduce the ICRU dose reference points and diode probes positions and there is little that can be done about this except to perform the procedure in such a way that it will be as painless, comfortable and technically adequate as required by the treatment protocols. Therefore, only the *in-vitro* dose measurements could be repeated at least twice as shown in Appendices 10 and 11. Table 5.10 and 5.11 below show a summary of the data processing results obtained using MicroSoft Excel spreadsheet for *in-vitro* measurements. The mean standard deviation for the bladder and rectum, i.e. $Bladder_{Std}$ and $Rectum_{Std}$ were regarded as the random error. This random error is the intra-measurement expected error, i.e. the personal error or reproducibility of the *in-vitro* measurements.

Table 5.11: Determining Random Error from repeated *in-vitro* measurements for ring and tandem applicator (intra-measurement)

	$Bladder_{Std}$ (Gy)	$Rectum_{Std}$ (Gy)
Mean	0.150	0.111
Std Dev	0.150	0.135
Median	0.075	0.059
Min	0.002	0.000
Max	0.513	0.468

Table 5.12: Determining random error from repeated *in-vitro* measurements for vaginal cylinder and tandem applicator (intra-measurement)

	$Bladder_{Std}$ (Gy)	$Rectum_{Std}$ (Gy)
Mean	0.083	0.299
Std Dev	0.094	0.441
Median	0.030	0.107
Min	0.008	0.018
Max	0.211	0.966

In performing *in-vitro* measurements using the ring and tandem applicator, the resultant dose variation due to random errors was ± 0.150 Gy and ± 0.135 Gy for the bladder and rectum respectively. Dose variations observed after using the combo applicator were ± 0.094 Gy and ± 0.441 Gy respectively. From the results, it is clear that a greater random error was obtained in carrying out *in-vitro* measurements for the combo applicator rectum dose. One of the contributing factors may be the fact that since the radiation sources are close to the surrounding tissue when using the combo applicator, the dose to the rectum wall and the dose gradient within the surrounding tissue will be very high. Therefore, a slight displacement in the reference dose point position results in a marked dose difference from the expected dose.

5.3 Combining Uncertainties

The methodological error was not included in the final error expressions in this study. However, measures were taken to periodically monitor and correct for these errors in order to prevent these errors from affecting the dose computations and measurements. Instrumental and personal errors were used to estimate the uncertainty in the *in-vivo* and *in-vitro* measured doses.

From equation 5.3,

$$E = E_m + E_i + E_p$$

The combined error in measuring the *in-vitro* doses can be expressed as follows:

5.3.1 Ring and Tandem

(a) Expected error in bladder dose measurements

$$E = (0.028A\ Gy) + (0.150\ Gy)$$

where A is the true value of the quantity as given in equation 5.1.

(b) Expected error in rectum dose measurements

$$E = (0.028A\ Gy) + (0.111\ Gy)$$

5.3.2 Combo Applicator

(a) Expected error in bladder dose measurements

$$E = (0.028A\ Gy) + (0.083\ Gy)$$

(b) Expected error in rectum dose measurements

$$E = (0.028A\ Gy) + (0.441\ Gy)$$

5.4 Correlations between TPS Planned, In-vivo and In-vitro Diode Doses

This type of test was done to establish the strength of the linear relationship between two sets of data that was under comparison. A correlation coefficient was computed to indicate how the variability of the data obtained in the study was affected by the association between the two sets of data concerned. SPSS software was used to compute correlation coefficients for the paired samples shown in the output table below.

This is the sample coefficient of determination r^2. The coefficient of determination has the following interpretation:

$$\left\{\begin{matrix}The\ proportion\ of\ variability \\ in\ y\ unexplained\ by\ the \\ linear\ relationship\end{matrix}\right\} = \frac{\sum(y-\hat{y})^2}{\sum(y-\bar{y})^2}$$

$$= \frac{\sum(y-\bar{y})^2[(x-\bar{x})(y-\bar{y})]^2/\sum(x-\bar{x})^2}{\sum(y-\bar{y})^2}$$

$$= 1 - \frac{S_{xy}^2}{S_{xx}S_{yy}} = 1 - r^2$$

and so,

r^2 = 1 – the proportion of unexplained variability in the population,

= the proportion of variability in y which is explained by the linear relationship,

A large r^2, i.e. r^2 close to 1, means that most of the variability is explained by the relationship, and having knowledge of the numerical value of the x variable is more or less as efficient as knowledge of y. If r^2 is close to zero, then there is a poor relationship between the two variables x and y. There are studies in which r^2 is the most significant statistic that can be computed

explaining the relationship between variables. The r^2 statistic is used also in regression analysis to determine whether a regression equation will be useful for predicting one variable using data from another. (Dowdy, et al., 2004)

Table 5.13: SPSS output table for correlations of paired TPS planned, *in-vivo* and *in-vitro* doses for the bladder and rectum

		N	Correlation	Sig.
Pair 1	TPS Bd & Bd	30	0.860	0.000
Pair 2	TPS Bd & Bw	31	0.877	0.000
Pair 3	Bd & Bw	30	0.828	0.000
Pair 4	TPS Rd & Rd	36	0.757	0.000
Pair 5	TPS Rd & Rw	37	0.745	0.000
Pair 6	Rd & Rw	37	0.682	0.000

From Table 5.13, all the paired samples had significant correlations, i.e. $p = 0.00$ for all the pairs. Correlation coefficients for the bladder doses were more pronounced, i.e. all greater than 0.82 as compared to rectum doses with highest correlation coefficient 0.757. The highest correlation was between TPS planned and *in-vitro* measured dose for the bladder, which confirms the verity that the TPS dose computing algorithm is based on water as a tissue equivalent material.

5.5 Differences in Means of TPS planned, In-vivo and In-vitro Doses

The paired samples test or **T- test** was carried out to compare the means of two sets of data at any given time. The null hypothesis for this test was:

$$H_0: \mu_d = 0 \text{ and } H_a: \mu_d \neq 0$$

Where μ_d was the population mean for the difference of the dose computed by the TPS, measured *in-vivo* and *in-vitro*. The tests were carried out using SPSS for a 95% confidence interval or p = 0.05 significance level and Table 5.14 below gives a summary of the output results.

Table 5.14: SPSS Output results for paired sample T-test of TPS planned, in-vivo and in-vitro doses for the bladder and rectum

		Paired Differences					t	df	Sig. (2-tailed)
		Mean	Std. Deviation	Std. Error Mean	95% Confidence Interval of the Difference				
					Lower	Upper			
Pair 1	TPS B_d - B_d	0.470	0.827	0.151	0.161	0.779	3.110	29	0.004
Pair 2	TPS B_d - B_w	0.160	0.827	0.149	-0.144	0.463	1.075	30	0.291
Pair 3	B_d - B_w	-0.260	0.971	0.177	-0.622	0.103	-1.466	29	0.153
Pair 4	TPS R_d - R_d	-1.029	0.482	0.080	-1.192	-0.865	-12.780	35	0.000
Pair 5	TPS R_d - R_w	-0.518	0.374	0.062	-0.643	-0.394	-8.427	36	0.000
Pair 6	R_d - R_w	0.472	0.529	0.087	0.296	0.648	5.433	36	0.000

From Table 5.14, the null hypothesis could not be rejected, i.e. the means of the sets of the data were the same except for comparisons that included the

bladder *in-vitro* dose data. This also means that the TPS computes valid *in-vivo* doses for the bladder and rectum.

Where,

B_d is the *in-vivo* bladder diode dose measured,
TPS B_d is the bladder diode dose calculated by the treatment planning system

B_w is the *in-vitro* bladder diode dose measured

R_d is the *in-vivo* rectum diode dose measured,

TPS R_d is the rectum diode dose calculated by the treatment planning system,

R_w is the *in-vitro* rectum diode dose measured.

5.6 Regression Analysis

It was difficult to formulate a relationship between the TPS planned and the *in-vivo* measured doses. Therefore, regression analysis was done using MS Excel software to attempt to describe the relationships. The MS Excel Regression analysis tool performs linear regression analysis by using the "least squares" method to fit a line through a set of observations. Regression makes it possible to analyze how a single dependent variable is affected by the values of one or more independent variables and then the results are used to predict future values using results from the regression process.

Regression analyses of *in-vivo* against ICRU point doses for both the bladder and rectum was done and produced identical R-squared values of 0.096. These values were too low for any conclusion to be drawn from them. Table 5.15 above gives a regression summary output for the comparison between patient bladder diode dose and the TPS bladder dose for the ring and tandem applicator.

Table 5.15: Summary output for regression of bladder *in-vivo* dose against ICRU bladder dose

SUMMARY OUTPUT								
Regression Statistics								
Multiple R	0.774							
R Square	0.599							
Adjusted R Square	0.581							
Standard Error	0.756							
Observations	24							
ANOVA								
	df	*SS*	*MS*	*F*	*Significance F*			
Regression	1	18.749	18.749	32.831	9.19E-06			
Residual	22	12.563	0.571					
Total	23	31.312						
	Coefficients	*Standard Error*	*t Stat*	*P-value*	*Lower 95%*	*Upper 95%*	*Lower 95.0%*	*Upper 95.0%*
Intercept	1.149	0.492	2.336	0.029	0.129	2.170	0.129	2.170
X Variable 1	0.624	0.109	5.730	9.19E-06	0.398	0.850	0.398	0.850

From the output, the R-squared value of 0.5988 is not sufficient (ideally it should be close to unity, i.e. 1). Therefore, the regression model was not good enough to accurately predict the patients' *in-vivo* doses from TPS doses as further proved by graph 5.1 below. From graph 5.1, the relationship between the series and predicted data is not good enough to give good predictions of the *in-vivo* diode doses.

Figure 5.3: Regression line plot of the series and predicted data of bladder *in-vivo* versus ICRU reference point doses

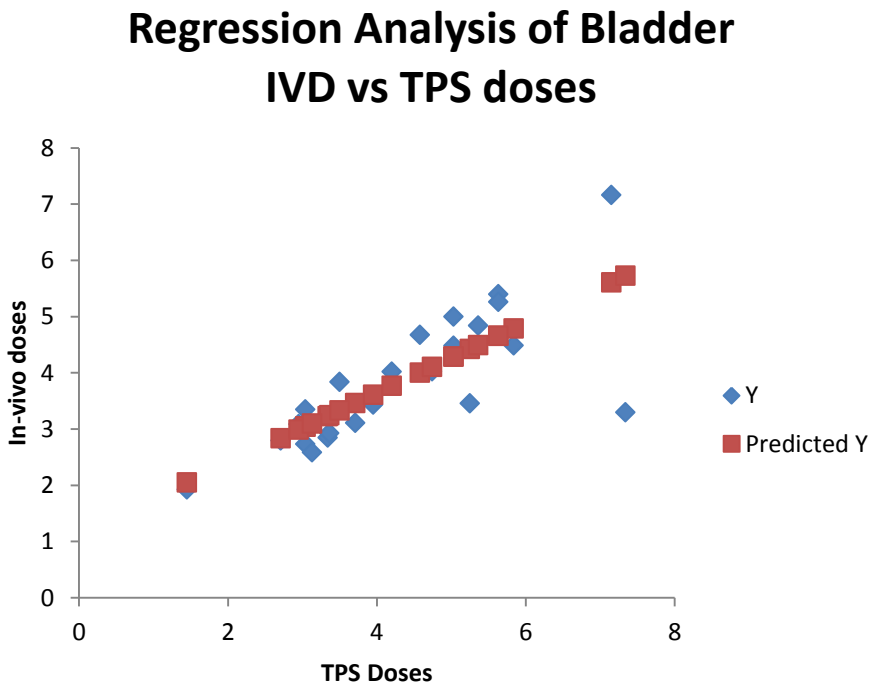

Even without any regression being done on the data, the spread or scatter does not clearly show a linear relationship.

Another regression analysis was done using patient rectum *in-vivo* and rectum ICRU reference point doses. The output of this analysis is shown below in Table 5.16. A graph of the regression of the patient diode against TPS doses data was plotted together with the predicted dose data as shown in graph 5.2.

From the output table, the R-squared value of 0.5685 is not good enough and strongly indicates the unreliability of the data for prediction purposes. Graph 5.2 plotted to show the relationship between *in-vivo* and TPS planned doses reveals that there was no relationship between the two sets of data. The R-squared values suggest the failure of regression analysis to fully explain the relationship between the rectum *in-vivo* and TPS doses. Therefore, as was recommended by previous investigators in HDR brachytherapy (Wäldhausl, et al., 2005) and (Hassouna, et al., 2011), all clinical decisions must based on the TPS and *in-vivo* dosimetry must be done to confirm the TPS doses.

Table 5.16: Regression output for rectum *in-vivo* doses and ICRU reference point doses

Regression Statistics								
Multiple R	0.754							
R Square	0.569							
Adjusted R Square	0.556							
Standard Error	0.491							
Observations	37							
ANOVA								
	df	*SS*	*MS*	*F*	*Significance F*			
Regression	1	11.097	11.097	46.116	7.13E-08			
Residual	35	8.422	0.241					
Total	36	19.518						
	Coefficients	*Standard Error*	*t Stat*	*P-value*	*Lower 95%*	*Upper 95%*	*Lower 95.0%*	*Upper 95.0%*
Intercept	0.636	0.376	1.690	0.100	-0.128	1.400	-0.128	1.400
X Variable 1	1.176	0.173	6.791	7.13E-08	0.824	1.527	0.824	1.527

Figure 5.4 Regression line plot of the series and predicted data of rectum *in-vivo* versus ICRU reference point doses

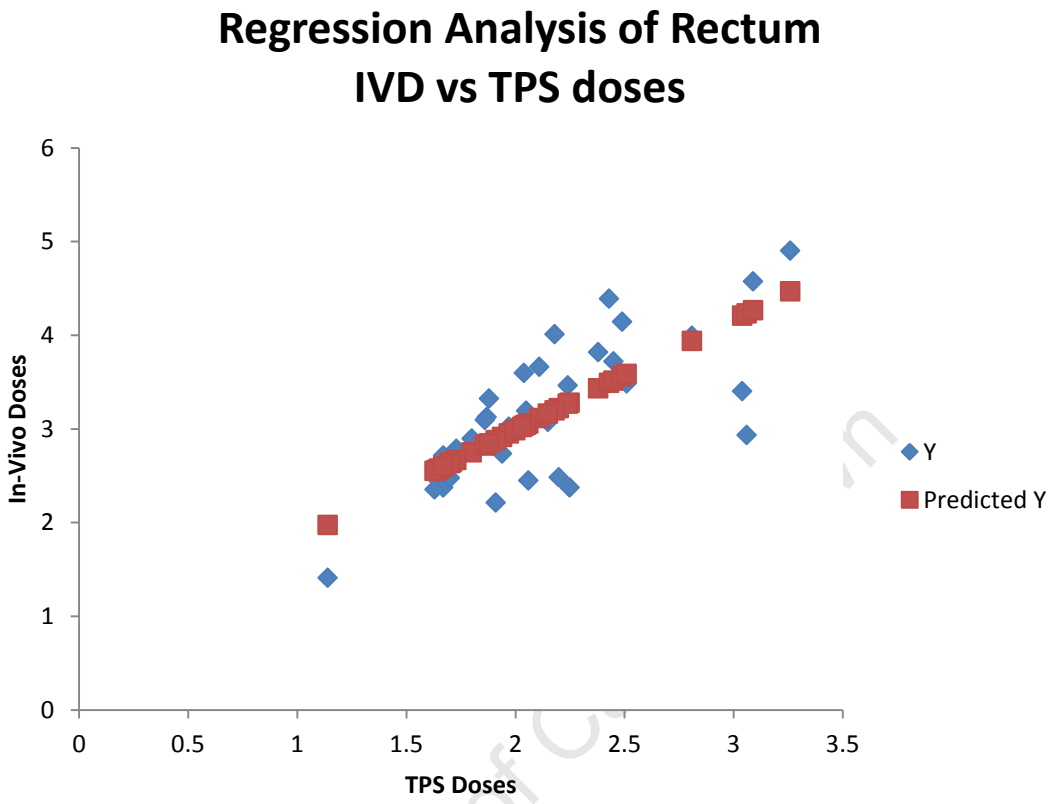

CHAPTER 6 DISCUSSION AND CONCLUSION

6.1 Summary

From Chapter 1, the main aim of this research was to establish a complimentary and reliable method of performing *in-vivo* dosimetry during gynaecological high-dose rate (HDR) afterloading brachytherapy at Groote Schuur Hospital. This was necessitated by the need to verify the '*in-vivo*' doses computed by the TPS using orthogonal radiographs. The study was also carried out to justify recommendations in literature that advise that *in-vivo* dosimetry should be done on patients using rectal and bladder dosimeters, additional to the computed dose calculations made by the TPS (Wäldhausl, et al., 2005).

Commissioning and acceptance of the *in-vivo* diodes was a rigorous process that was carried out based on manufacturer instructions and guidelines, as well as by using recommendations made by previous investigators (Wilkinson, 2010). Calibrating the source strength in the Well chamber, in the PTW T9193 phantom and using the in-air method produced results that varied by a maximum of 1.01 %. The average combined systematic error during the study was found to be 2.8 %. The *in-vivo* diode probes were calibrated based on measurement of source strength. Verification of the calibration process in a Rando phantom produced accurate and precise results that confirmed the computerised TPS planned doses. In order to preserve accurate and precise measuring properties of the *in-vivo* diode dosimetry system, regular calibrations of the system had to be done, i.e. at least once every fortnight (Wäldhausl, et al., 2005). The weekly percentage deviation in the calibration factors ranged from 0.36 % to 1.32 %. Calibrating the *in-vivo* dosimetry system once every two weeks is likely to keep the dynamic error under control. The PTW 3D MP3 tank made a good phantom in which valid measurements were done. A water filled tank provided an equivalent patient scatter volume in which *in-vivo* measurements were replicated as shown in Tables 5.4 and 5.5.

To a large extent the in-phantom measurements successfully replicated real clinical situations under which patients were treated as reflected by the pattern of the relationships between TPS, *in-vivo* and *in-vitro* comparisons.

Initially, inserting diode probes into patients took an additional seven to ten minutes. However, as more insertions were done and practical experience was gained, the additional time reduced roughly to an average time of four to five minutes. The radiation oncologists were able to clearly distinguish and mark the ICRU dose reference points together with the bladder and rectum diode positions in the patients on most of the radiographs. From the data analysis, ratios of ICRU to *in-vivo* doses were 1.4 ± 0.4 and 1.5 ± 0.4 for the bladder and rectum respectively for the ring and tandem applicator. For the combo applicator the corresponding ratios were 1.2 ± 0.5 and 1.8 ± 0.7 for the bladder and rectum. The results are very similar to results that were obtained by (Hassouna, et al., 2011), i.e. 1.2 ± 0.5 and 1.7 ± 0.5 for the bladder and rectum respectively using the ring and tandem applicator. The ratios confirm that the ICRU reference point dose system overestimates the dose that is measured in the OARs during HDR brachytherapy, similar to (Datta, et al., 2006). However, when comparing the TPS planned to *in-vivo* doses, ratios obtained using the ring and tandem applicator were 1.1 ± 0.3 and 0.7 ± 0.1 for the bladder and rectum respectively. Ratios obtained using the combo applicator were correspondingly 1.0 ± 0.1 and 0.8 ± 0.2 for the bladder and rectum. The *in-vivo* bladder doses closely confirmed the TPS planned doses. However, for the rectum, the *in-vivo* doses were higher than the TPS calculated doses similar to what was also observed by (Kim & Pareek, 2003). Ideally all the ratios should be equal to one.

Ratios of the TPS calculated to *in-vitro* dose measurements for the ring and tandem applicators were correspondingly 1.1 ± 0.1 and 0.8 ± 0.2 for the bladder and rectum, while for the vaginal combo applicator were 1.0 ± 0.1 and 0.8 ± 0.1 for the bladder and rectum respectively. From Tables 5.4, 5.5 and 6.1, it is evident that for the rectum, ratios of TPS planned to *in-vivo* doses are less than unity by an almost similar magnitude for both applicators. This

phenomenon is further confirmed by the ratios of the TPS planned to *in-vitro* doses.

Table 6.1: Comparison of ratios of computed and measured doses

	Bladder				Rectum			
Applicator	ICRU *In-vivo*	TPS *in-vivo*	TPS *In-vitro*	*In-vivo* *In-vitro*	ICRU *In-vivo*	TPS *in-vivo*	TPS *In-vitro*	*In-vivo* *In-vitro*
R & T	1.4 ± 0.4	1.1 ± 0.3	1.1 ± 0.1	1.0 ± 0.2	1.5 ± 0.4	0.7 ± 0.1	0.8 ± 0.2	1.2 ± 0.2
Combo	1.2 ± 0.5	1.0 ± 0.1	1.0 ± 0.1	1.0 ± 0.1	1.8 ± 0.5	0.8 ± 0.2	0.8 ± 0.1	1.1 ± 0.2

The TPS underestimates the dose received by the rectum by roughly 20 %. This difference may be attributed to the inability to make corrections for inhomogeneities when using orthogonal radiographs for treatment planning purposes. This shortfall may be overcome by using computerised tomography (CT) based images for planning purposes (Datta, et al., 2006). However, *in-vivo* doses for the bladder closely confirm the TPS calculated doses since ratios for all comparisons regarding the bladder except ICRU comparisons are close to unity.

Since ICBT brachytherapy consists of several treatments on different days, data analysis was done to obtain the expected dose variation within the OARs in a patient (intra-patient) on different insertions during the course of treatment. This dose variation was regarded as being the intra-patient random error. The highest intra-patient random errors were obtained while measuring *in-vivo* bladder doses, i.e. TPS, *in-vivo* and *in-vitro* random errors were ±1.3 Gy, ±0.6 Gy and ±1.6 Gy respectively for the ring and tandem applicator as shown in table 6.2 below.

Table 6.2 Intra-patient random errors

	Intra-patient random errors (Gy)					
	Bladder			Rectum		
Applicator	TPS	*In-vivo*	*In-vitro*	TPS	*in-vivo*	*in-vitro*
Ring & Tandem	±1.3	±0.6	±1.6	±0.3	±0.5	±0.2

This may be due to the proximity of the bladder to the 'ring' and the radiation sources. A slight displacement in the position of the *in-vivo* diode or ICRU reference point results in a marked dose change due to the high dose gradients close to the radiation source. The rectum intra-patient random errors were lower using both applicators with the highest dose being ±0.6 Gy for both applicators. The random error is smaller for the rectum since it is further away from the radiation source and changes in the displacement of diode or ICRU dose reference point positions do not produce large dose variations as compared to closer to the applicator and radiation sources.

There were differences in doses that were observed for patients administered with the same treatment parameters, i.e. dose and applicator. This variation in dose from patient to patient (inter-patient) variation was regarded as the inter-patient random error. The average inter-patient errors obtained using the ring and tandem applicator are shown in Table 6.3. Maximum expected random error was observed for the bladder and lower random error observed in the rectum for the same reasons given above.

For the *in-vitro* measurements, the average intra-measurement random error was obtained as ±0.2 Gy and ±0.1 Gy for the bladder and rectum respectively using the ring and tandem applicator while for the combo the random error was correspondingly ±0.1 Gy and ±0.4 Gy for bladder and rectum. See (Tables 5.10 and 5.11).

Table 6.3 Inter-patient random errors

	Intra-patient random errors (Gy)					
	Bladder			Rectum		
Applicator	TPS	*In-vivo*	*In-vitro*	TPS	*in-vivo*	*in-vitro*
Ring & Tandem	±1.6	±0.7	±1.8	±0.2	±0.6	±0.2

Data analysis was done to compare the relationship between TPS, *in-vivo* and *in-vitro* doses and all the correlations were significant, i.e. $p = 0.00$. A paired T-test ($p < 0.05$) was done using SPSS to compare the means of TPS, *in-vivo* and *in-vitro* doses; the means were the same except for comparisons that included bladder *in-vitro* doses. The bladder diode's proximity to the radiation sources probably magnified personal errors during *in-vitro* measurements and in the process distorted the data. This resulted in the T-test detecting different sample means for the bladder TPS – *in-vitro* and *in-vivo* - *in-vitro* dose inter-comparisons.

Regression analysis was done to compare TPS and *in-vivo* dose data. The regression analysis was done to confirm the following (Tyrell, 2009):

- whether variables were related or not,
- provide information about the relationship between the data,
- describe (quantify) the strength of the relationship, and
- ascertain whether it was possible to predict one variable from the other.

The correlation coefficients showed that the TPS and *in-vivo* data are closely related, i.e. correlation coefficient for TPS-*in-vivo* was 0.86 for the bladder and 0.75 for the rectum. Non-linear relationships with poor r-squared values were obtained after regression analysis of *in-vivo* against TPS dose data, i.e. 0.60 and 0.57 for the bladder and rectum doses respectively. The relationship between the TPS and *in-vivo* doses observed in the study confirmed what was also observed by (Hassouna, et al., 2011) for both the bladder and rectum. This means that contrary to the results of the investigation carried out by

(Samiei, et al., 2006), regression analysis may not be used to effectively predict *in-vivo* doses from TPS doses.

6.2 Uncertainties and Limitations

Only the bladder diode could be verified in the Rando phantom because the diode holes in the phantom were too small for the rectum diode probe to fit in. However, since the bladder diode position and dose are analogous to the position and dose of the central diode of the rectum probe (diode number 3) in the PTW T9193 phantom, a confirmation of the bladder dose in Rando would have been confirmed by the central rectum diode if it were to be put in the same position to measure dose under the same conditions. Dose measurements done in the PTW T9193 confirmed the similarity of the bladder diode and central rectum diode measured doses. This reasoning and exercise was regarded as sufficient to substantiate the use of the rectum diode probe without verification in Rando or any other additional phantom.
There was an intention to use ultrasound imaging (US) techniques to position applicators and diode probes in patients for treatment planning purposes (Barillot, et al., 1994); however, due to logistical problems and patients' unmet demand for diagnostic US procedures, it was not possible to carry out US investigations in the study.

The use of computerised tomography (CT) patient images was also not possible in this study. Since the CT scanner at the institution was a considerable distance away from the HDR brachytherapy treatment theatre, the radiation oncologist responsible raised concerns about possible movement of applicators during transfer of patients between the treatment couch and CT bed and moving to and from the CT scanner. The situation was made worse by the unavailability of scanning slots for HDR brachytherapy patients since it was a radiology dedicated CT.

Positioning of the diodes in the water was critical for reproducing the measurements made in the patient for both the bladder and rectum. This was

more critical for the bladder since for most setups, the bladder was nearer to the source. Small displacements in diode positioning resulted in large dose deviations due to the steep dose gradient close to the radiation source. Although patients have varying anatomies, a standard tissue equivalent volume was used in the study. This may have introduced uncertainties in the *in-vitro* dose measurements.

Occasionally it was difficult to identify the bladder diode on lateral radiographs after insertion. Large patient anatomies and double exposures made in acquiring images resulted in poor lateral radiographs, from which neither the Foley balloon nor bladder diode could be identified. Inserting a bladder probe through a urethra that already has a contrast balloon inserted is not easy. Often, the *in-vivo* bladder diode and could not be inserted because of this challenge.

In certain events where dose measurements were done without clear identification of the organ at risk or *in-vivo* diode, the data was disregarded in the data analysis. In carrying out this research, every now and then the bladder and rectal diodes probes slipped out from positions where they should have been secured inside the patient. This was also experienced in previous studies (Hassouna, et al., 2011). On such occasions, the measured doses were different from the doses computed from the x-ray radiographs. These values were regarded as blunders and were excluded in the data analysis.

6.3 Merits of the *in-vivo* dosimetry system

In-vivo dosimetry is practiced in a relatively small number of institutions worldwide (Essers & Mijnheer, 1999). The low practice of *in-vivo* dosimetry around the world may be attributed to the perception that "*the gain in patient treatment accuracy as a result of in-vivo dosimetry will be small compared to the additional workload and costs involved*" (Essers & Mijnheer, 1999). A lot of research has been done to justify *in-vivo* dosimetry in gynaecological HDR brachytherapy. In carrying out this investigation, it was realised that *in-vivo*

dosimetry in gynaecological HDR brachytherapy is critical and goes a long way to improve the quality assurance and outcomes of treatment.

Calibrating the *in-vivo* dosimetry equipment once every fortnight helps to manage the dynamic error of the dose measuring instruments. The TPS and *in-vivo* dosimetry data for the bladder had a high correlation coefficient that confirmed the validity of both the TPS and *in-vivo* doses as true reflections of the actual dose received by the bladder. For the rectum, *in-vivo* dose measurements were higher when compared to TPS doses.

(Yaparlvi, et al., 2008) findings suggest a strong relationship between the ICRU rectal reference dose with volumetric rectal doses. This information is useful in determining tolerance levels for the rectum during HDR brachytherapy treatment for gynaecological conditions. Recommendations from (Pötter, et al., 2006) suggest that using 3D image based clinical target volumes will most likely increase the therapeutic ratio, including target coverage and sparing of OARs.

In-vivo dosimetry is a useful means of evaluating actual dose received by patients and avoid misadministration during HDR brachytherapy. Knowledge of the dose received by OARs during one treatment fraction enables radiation oncologists to adjust the prescription dose and treatment parameters for the subsequent treatments. *In-vivo* dosimetry allows verification measurements of the dose delivered to be done, thereby making a confidence check of the treatment (Alecu & Alecu, 1999). This study confirms previous *in-vivo* dosimetry studies made by (Wäldhausl, et al., 2005), that *in-vivo* diode accuracy and reproducibility is good enough for clinical use. In other words, computerised treatment planning and *in-vivo* dosimetry are separate complementary procedures that may be done simultaneously and separately to monitor dose received by OARs during HDR brachytherapy (Wäldhausl, et al., 2005). However,(Hassouna, et al., 2011) suggested that 3D image based dose calculations were a more accurate and reliable means of evaluating dose received by OARs compared to *in-vivo* diode dosimetry.

(Hassouna, et al., 2011) recommended therefore that clinical decisions must be based on 3D image based dose calculations.

In South Africa, The Hazardous Substances Act, 1973 (Act 15 of 1973) and Regulations (No R1332 of 3 August 1973) governs the safe use of medical x-ray equipment in the country. This Act has a provision that guides *in-vivo* dosimetry during external beam radiotherapy. In the current Act, there is no provision guiding *in-vivo* dosimetry in brachytherapy. In order to enhance medical practices that safeguard patients' health and exploit the benefits of *in-vivo* dosimetry (Podgorsak, 2005), the Radiation Control Directorate, Department of Health ,South Africa may want to consider formulating *in-vivo* dosimetry guidelines to be practiced during brachytherapy.

6.4 Future Work

During this study it was observed that there are many errors associated with patients' movement during the treatment procedure. There is need to evaluate current methods and devices used to immobilize patients during gynaecological HDR brachytherapy. Ideal immobilizing techniques and devices should be able to immobilize patients from the waist-down and simultaneously hoist and secure the thighs and legs during HDR brachytherapy. Such devices must be fixed to the operating couch/table and ensure that the patient is comfortable, allowing no or only limited movement. This may assist in reducing patient movement during treatments, since it is very difficult for a person to remain motionless for long periods of times. Very often patients have to endure treatment durations of more than ten minutes, especially when the Iridium-192 source is no longer as active as right after a source change. Immobilisation may enable repeat insertions to be quicker, more reproducible and make patients more 'comfortable' during insertions. An additional graduated accessory (to be attached to the main immobilizing device) to secure source applicators and possibly the *in-vivo* diode probes in position may also be necessary.

Future studies may also be done to investigate change in applicator positions as a result of transferring patients to and from CT scanners that are located in

different bunkers. Transferring patients between the treatment and CT scanner bunkers is done at some centres that do not have gynaecological-HDR-brachytherapy-dedicated CT scanners, but want to exploit the advantages of 3D image based treatment planning.

APPENDIX

APPENDIX 1: Ir-192 July 2011 Source Certificate

Certificate For sealed Sources

G2-00223G

Issue Date: 2011-07-27 (1) Source number: NLF 01 D85A-701

Product Code: REF 09-00-001 (DRN 07785)
Serial number: SN n.a.
Production Code: LOT 87812/03

Serial no. Transport Container: 00072
Serial no. Check Cable: T0588
Customer name: GROOTE SCHUUR HOSPITAL

SOURCE SPECIFICATIONS

Reference Air Kerma Rate: 46.08 mGy h^{-1} +/- 5% at 1 m (2)
Measured at: 2011-07-22 11:01 hh:mm CET (1)
Apparent Activity: 418.86 GBq (11.32 Ci) at date of measurement (3,4)

Source Type: FLEXISOURCE IR192, 10 CI
Capsule dimensions: 0.86 mm diameter, 4.60 mm length
Source pellet dimensions: 0.60 mm diameter, 3.50 mm length
Source pellet form: solid Iridium
Radionuclide: Ir192
Encapsulation: single
Capsule material: stainless steel, AISI 316L
ISO Classification: ISO/99/C63411

QUALITY CONTROL

Laser Weld Visual Check: passed
Leakage test: leakfree (5)
Surface contamination test: < 185 Bq (5 nCi) (6)

The undersigned, authorized officer of Mallinckrodt Medical B.V., certifies that this source complies with the requirements of ISO2919 and that all of the information given in this certificate is true and correct.

QUALITY CONTROL SUPERVISOR .....

(1) Date format yyyy-mm-dd
(2) At Confidence level of 99.7%
(3) The apparent Activity is determined by applying a conversion factor (0.110 mGy m^2 h^{-1} GBq^{-1}) to the measured gamma radiation output of the sealed source determined with a calibration instrument. The instrument is calibrated against the standard of the Physikalisch-Technische Bundesanstalt (PTB), Braunschweig, Germany.
(4) The Apparent Activity is the Iridium-192 activity; other radionuclides not detectable
(5)Leakage test method according to ISO9978 method Liquid nitrogen bubble test (8.2.4)
(6) Surface contamination test according to ISO9978 method Wet wipe test (8.3.1)

Manufactured by Mallinckrodt Medical B.V. * Westerduinweg 3 * NL-1755 LE Petten * Telephone +31 224 567890
Manufacturer's code in accordance with Council Directive 2003/122/EURATOM: NLF 01
On behalf of Nucletron B.V. * Waardgelder 1 * NL-3900AX Veenendaal

APPENDIX 2: Calibration factors computed from MultiSoft Software program

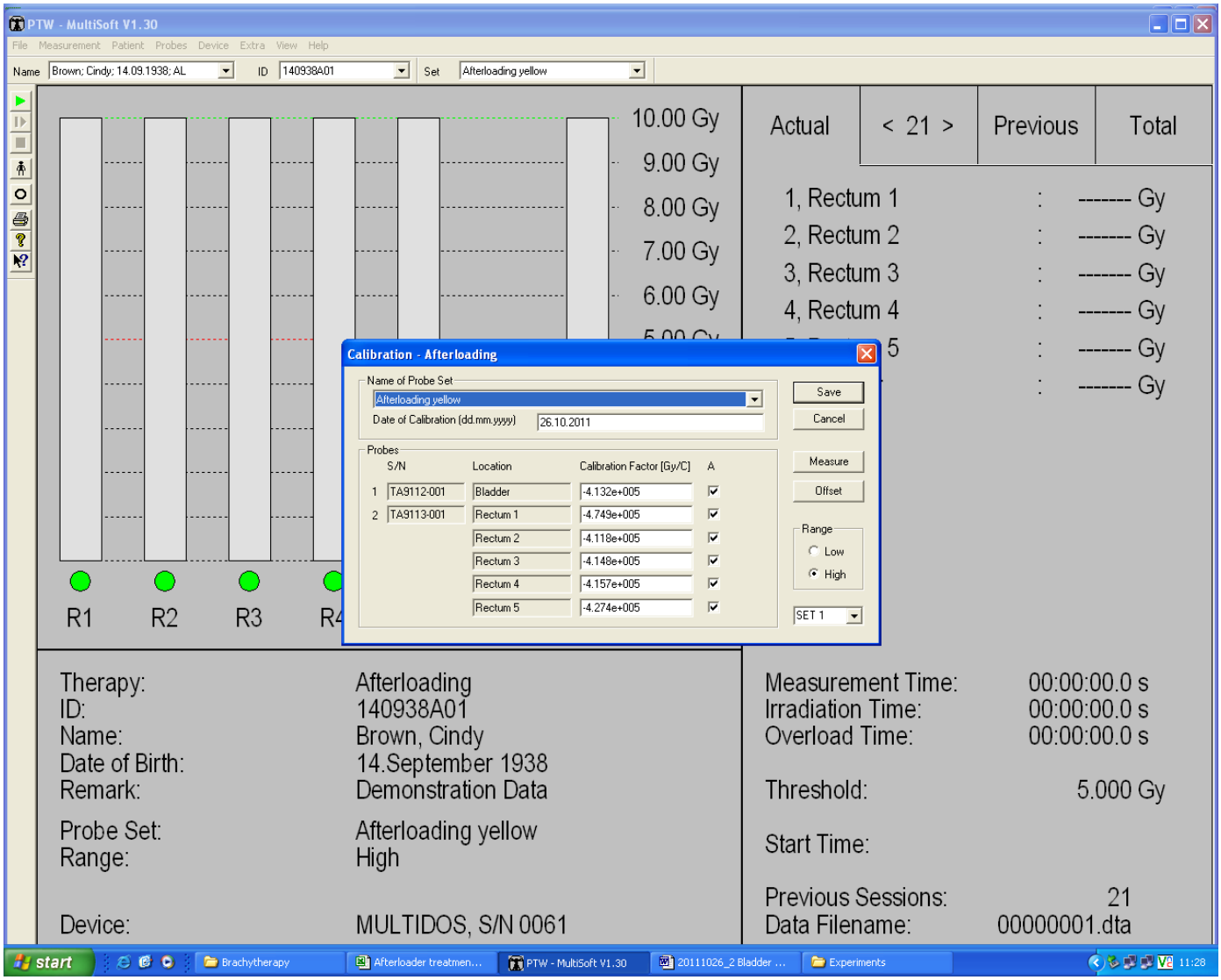

APPENDIX 3: Anterior- Posterior x-ray Plan of Alderson-Rando phantom from Flexiplan Treatment Planning System

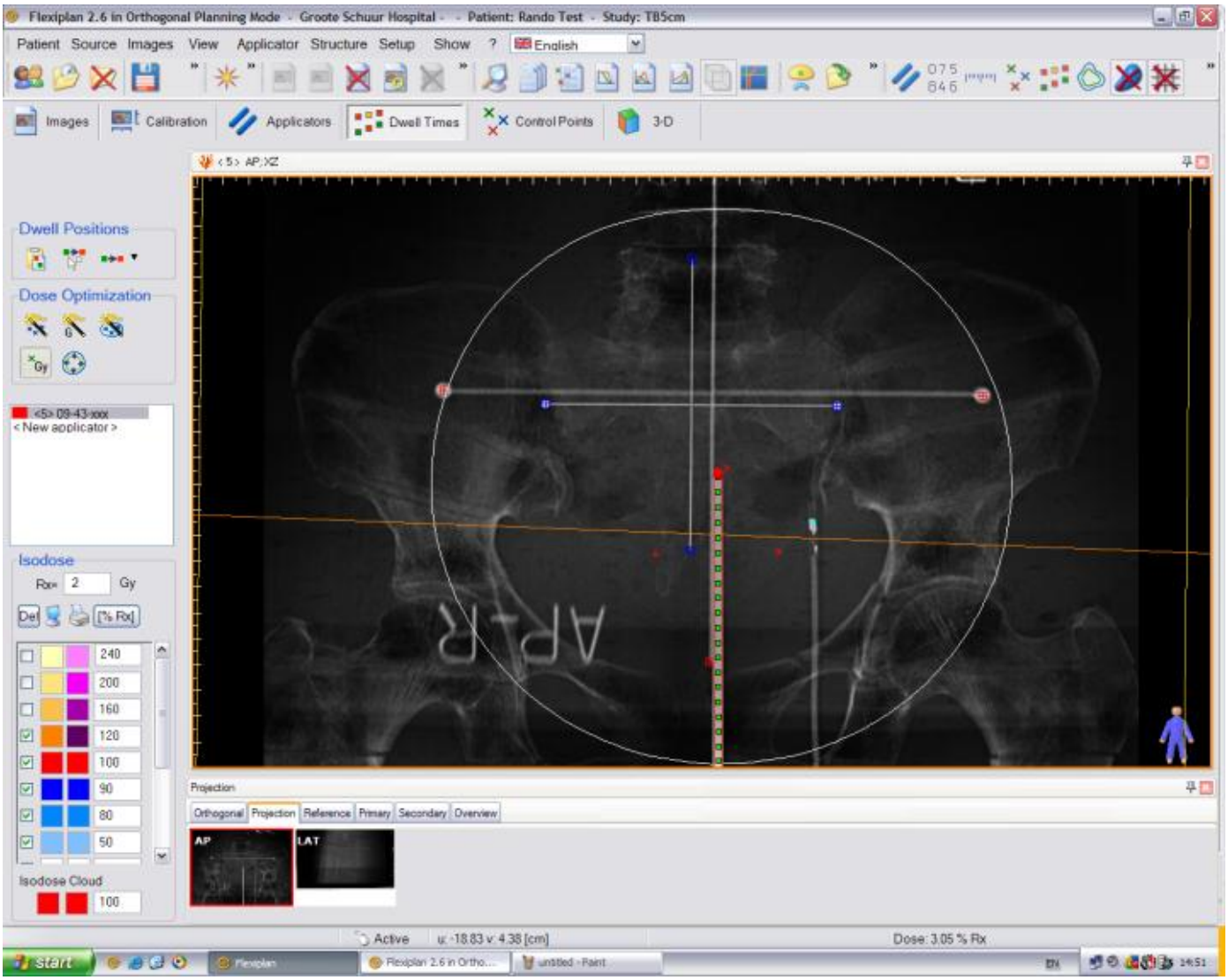

APPENDIX 4: Lateral x-ray Plan for Alderson-Rando phantom from Flexiplan Treatment Planning System

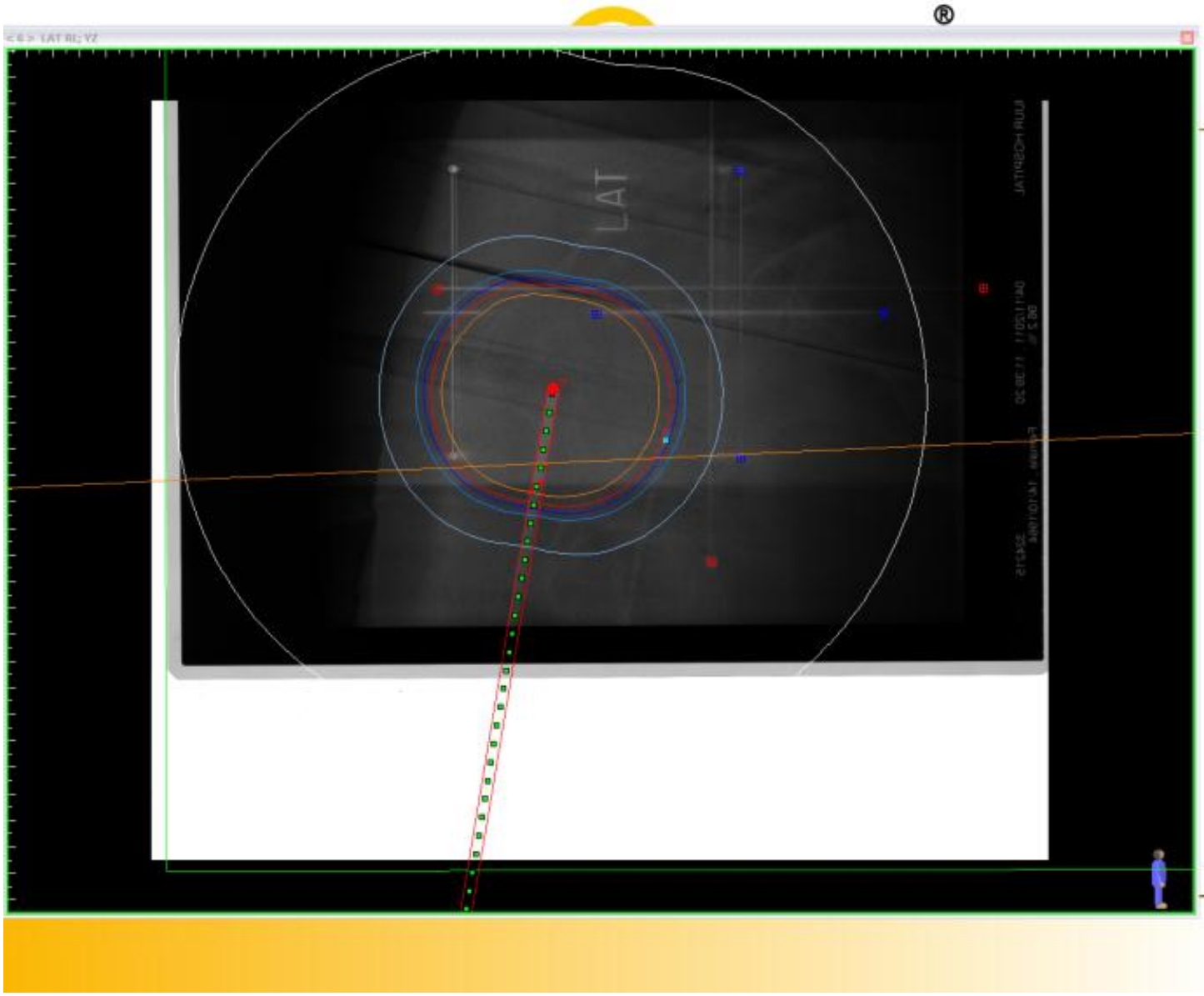

APPENDIX 5: Bladder diode dose measurement in Alderson-Rando obtained using MultiSoft Software Program

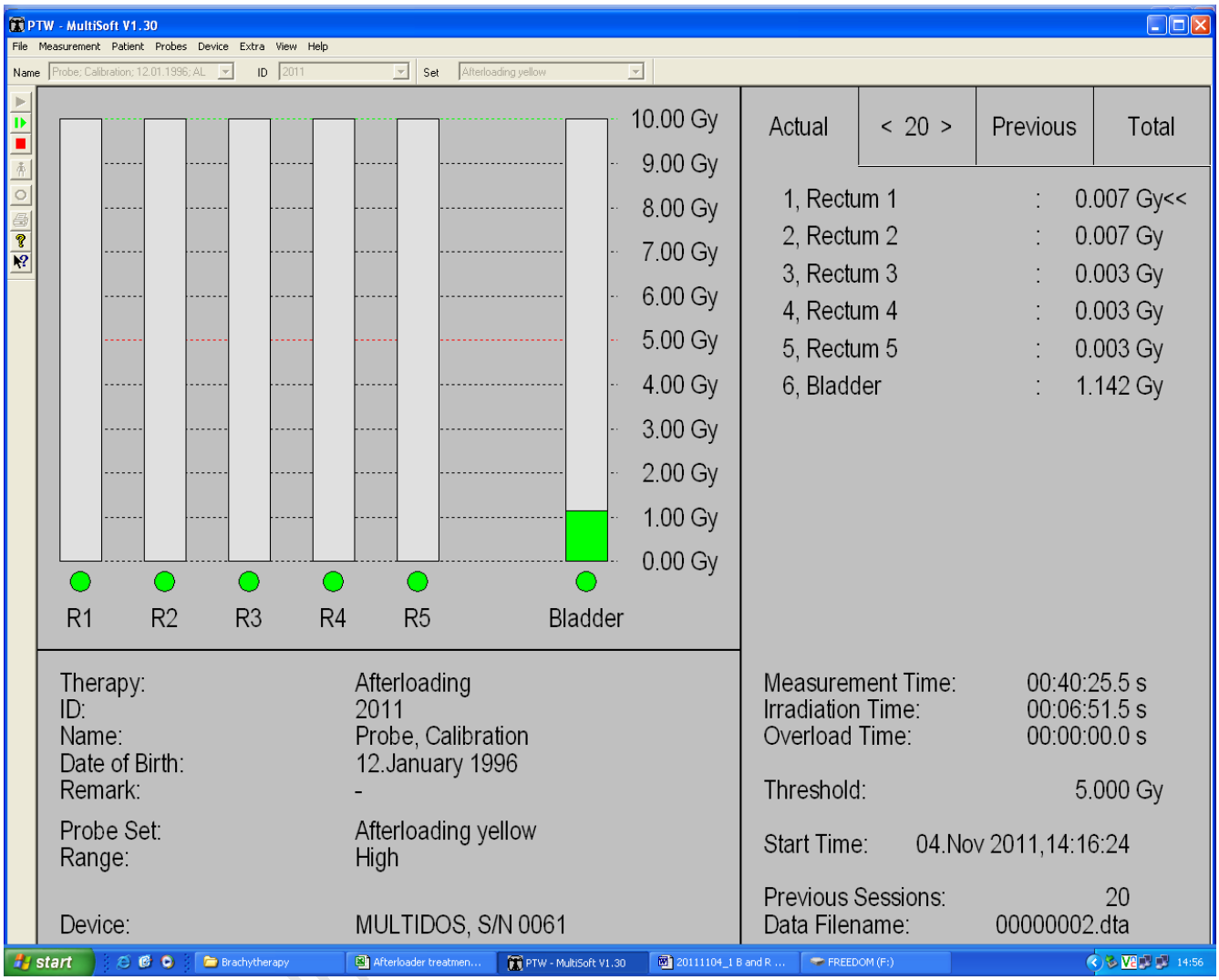

APPENDIX 6:

Table.1 Critical values of the distribution of $T_n = \frac{\max|x_n - \bar{x}|}{\delta}$ or $T_1 = \frac{\max|\bar{x} - x_1|}{\delta}$ (using unilateral check) (Rabinovich, 2005)

Number of Observation,*n*	Upper 0.5% Significance level	Upper 1% Significance level	Upper 5% Significance level
3	1.155	1.155	1.153
4	1.496	1.492	1.463
5	1.764	1.749	1.672
6	1.973	1.944	1.822
7	2.139	2.097	1.938
8	2.274	2.221	2.032
9	2.387	2.323	2.110
10	2.482	2.410	2.176
11	2.564	2.485	2.234
12	2.636	2.550	2.285
13	2.699	2.607	2.331
14	2.755	2.659	2.371
15	2.806	2.705	2.409
16	2.852	2.747	2.443
17	2.894	2.785	2.475
18	2.932	2.821	2.504
19	2.968	2.854	2.532
20	3.001	2.884	2.557
21	3.031	2.912	2.580
22	3.060	2.939	2.603
23	3.087	2.963	2.624
24	3.112	2.987	2.644
25	3.135	3.009	2.663
26	3.157	3.029	2.681
27	3.178	3.049	2.698
28	3.199	3.068	2.714
29	3.218	3.085	2.730
30	3.236	3.103	2.745

APPENDIX 7: Table 2 Upper 5% significance level Identification of Outliers,

-2.745 < $T_n = \frac{\max|x_n - \bar{x}|}{\delta}$ < 2.745 , from Ring and Tandem applicator results

Study	Applicator	$Bladder_{icru}$	$R1_{icru}$	$R2_{icru}$	$Rectum_{tps}$	$Bladder_{tps}$	$Bladder_{d}$	$Rectum_{d}$	$Bladder_{w}$	$Rectum_{w}$
1	R2T7	0.505	-0.217	0.087	-0.232	1.108	1.391	-1.466	0.540	-0.204
		0.253	-0.147	0.331	1.716	0.443	0.857	0.281	0.351	0.666
2	R2T5		-0.124	-0.387	0.146	-2.458	-2.592	-1.147	-2.373	-0.366
3	R2T7	-0.339	2.501	1.021	0.047	-0.532	-0.121	-0.993	-0.583	0.418
4	R2T5	0.182	-1.130	-1.995	-2.060	-2.458	-2.592	-2.486	-2.373	-2.419
5	R2T5	2.057	2.143	2.098	1.755	-2.458	0.403	-0.370	-2.373	**2.855**
6	R2T7	1.355	2.004	1.940	1.259	2.071	2.691	1.099	1.294	0.239
7	R2T7	2.101	2.362	2.270	1.815	0.545	0.379	1.907	0.620	2.003
8	R2T5	0.593	0.685	0.360	2.153	-2.458	-2.592	2.363	-2.373	1.233
9	R2T5	-0.646	0.292	-1.392	-0.927	-0.532	-0.335	-0.792	-0.565	-0.342
		-0.723	0.396	-0.229	-0.470	0.868	-0.041	-0.645	0.688	-0.863
10	R2T7	0.121	-0.471	0.403	0.404	-0.342	-0.488	0.858	-0.552	0.808
		-0.339	-0.980	-0.200	-0.411	-0.108	-0.295	-0.245	-0.164	-0.208
		1.043	-0.830	-0.171	0.504	-0.007	-0.263	1.649	-0.023	0.668
11	R2T5	-1.003	-0.737	-0.846	-0.351	-0.330	-0.431	-0.280	-0.464	-0.362
		0.023	-1.258	-0.958	-0.609	-0.532	-0.575	-0.102	-0.730	-1.228
		-0.454	-1.524	-0.243	-0.132	0.044	-0.059	0.641	0.006	0.033
12	R2T5	0.697	0.304	-0.272	-1.046	1.241	0.718	-1.053	0.486	-1.388
		1.174	-1.246	-1.737	-0.748	0.082	0.033	-0.423	0.307	0.199
13	R2T5	-0.888	-0.888	0.303	-0.271	0.728	1.096	0.553	0.624	-0.244
			-1.477	-1.004	0.126	-2.458	-2.592	0.364	-2.373	0.590
14	R2T5	0.796	1.032	0.604		-1.077	-1.274	-0.415	-0.944	-0.579
		-0.476	-0.379	-0.731	-0.629	-0.241	0.241	-0.145	-0.084	-0.777
15	R2T7	-0.487	0.165	-0.315	-1.007	2.192	-0.157	-1.147	1.750	-1.120
		-0.263	-0.367	-0.415	0.007	-0.741	-0.529	1.123	-0.738	0.267
16	R2T7	-0.301	0.119	-0.286	-1.066	1.108	1.290	-0.884	1.202	-0.845
		-0.153	-1.327	-1.291	-0.589	-2.458	-1.144	0.172	-1.249	0.486
		-0.816	-0.575	-0.846	0.543	-1.242	-1.234	0.722	-2.373	**-5.369**
17	R2T5	-0.586	0.443	0.504	0.543	0.291	1.692	0.482	0.252	0.618
18	R2T5	-0.460	-0.402	-1.306	-0.887	0.728	0.714	-0.576	**3.303**	-0.625
		-1.036	-0.009	-0.071	-0.053	0.203	0.377	-0.177	0.353	0.474
19	R2T5	1.224	0.269	-0.200	-0.252	-1.837	-1.939	-0.011	-1.683	0.504
		-1.277	-1.327	-0.645	0.623	-1.825	-1.815	1.307	-1.704	0.646
		-1.118	-0.217	0.662	0.663	-1.768	-1.612	0.394	-1.715	1.708
20	R2T5	-0.252	0.558	0.374	-0.291	-0.589	-0.312	-0.199	-0.436	0.542
		-0.778	0.523	-0.128	-0.947	-0.475	-0.684	-1.004	-0.285	-1.302
		-0.959	0.431	1.193	-1.086	0.937	0.982	-1.174	0.634	-0.827
21	R2T7	2.666	0.142	-0.229	-1.007	1.089	0.726	-0.674	0.348	-1.464
		0.253	-0.321	-0.430	0.245	-0.602	-0.510	0.807	-0.711	0.387
		-1.184	0.766	1.279	-0.371	0.196	0.228	0.385	-0.077	-0.715
22	R2T3	1.059	0.304	1.451	0.126	-2.458	-2.592	1.302	-2.373	0.562

APPENDIX 8: Table 3 Upper 5% significance level Identification of Outliers, -2.234 < $T_n = \frac{\max|x_n - \bar{x}|}{\delta}$ < 2.234 , from cylinder and tandem (combo) applicator results

							$T_n = \frac{\max\|x_n - \bar{x}\|}{\delta}$					
	Study	Applicator	$Bladder_{icru}$	$R2_{icru}$	Surface	$Bladder_{tps}$	$Rectum_{tps}$	$Bladder_{d}$	$Rectum_{d}$	$Bladder_{w}$	$Rectum_{w}$
1	5	3cmCyl4cmTan	-0.336	0.267	-4.246	**-4.246**	**-2.545**	**-4.246**	**-2.434**	**-4.246**	**-2.434**
2	6	3cmCyl6cmTan	0.310	-0.262	-4.246	**-4.246**	**-2.706**	**-4.246**	**-2.392**	**-4.246**	**-2.392**
3			0.742	-0.622	-4.246	**-4.246**	**-2.277**	**-4.246**	**-2.392**	**-4.246**	-1.970
4	8	3cmCyl6cmTan	-0.528	-0.476	-4.246	-2.200	**-2.468**	-1.978	-2.124	-2.162	-2.088
5	10	3cmCyl6cmTan	-0.588	-0.001	-4.246	-1.105	**-2.284**	-1.151	-0.852	-0.401	-0.515
6			0.298	-0.331	1.140	**-2.323**	-1.794	**-2.247**	-0.491	**-2.323**	-1.794
7	14	3cmCyl4cmTan	0.047	-0.040	3.032	-2.062	-2.208	-2.182	-1.539	-2.190	-1.518
8			**2.323**	-0.905	0.297	**3.032**	**-2.606**	**5.078**	-1.800	**-4.246**	-1.800
9	17	3cmCyl6cmTan	-1.636	-0.384	1.653	-1.978	**-2.261**	-2.191	-1.284	-1.875	-1.520
10	20	3cmCyl4cmTan	-0.672	-0.101	-4.246	**-2.254**	**-4.246**	**-4.246**	**-4.246**	**-2.310**	**-2.805**
11	21	3cmCyl4cmTan	0.041	**2.856**	-4.246	-0.162	**-2.943**	-0.375	-2.133	-0.416	**-2.505**

APPENDIX 9: Calibration checks for Well chamber (MS Excel Spreadsheet)

DIVISION OF MEDICAL PHYSICS

Ir-192 HDR Afterloader Source Change: Calibration and checks for Well-chamber

Date of measurement:	15/08/2011 11:15

Dose meter
PTW4

Temp.	Pressure	T&P Fact
20.0 °C	1013.3 hPa	1.0000

Ionization Chamber	Serial number
Well-type chamber Type No. 077.091	0348

Polarizing voltage
Note: +300 V

Apparent Activity Calibration Factor (From chamber calibration certificate)	8.548 GBq/nA
Dose Rate measured in nA	38.280 nA

	Source Activity	Date
Measured Activity	8.8437 Ci	15/08/2011 11:15
Apparent Activity (in GBq) (Given by manufacturer)	418.8600 GBq	22/07/2011 11:01
Apparent Activity (in Ci) (Given by manufacturer)	11.3205 Ci	`

Date	Measured Source Activity (A)	Apparent Activity of source (B) [Manufacturer]	% Correlation (<2% and >-2%): 100*(A-B)/B
15/08/2011 11:15	8.8437 Ci	9.0411 Ci	-2.2%
	0 days	24.010 days	

Comments:

Developed Checkfilm	Changed Console Activity	Changed Planning Activity	Filed Certificate and Documents	Filled Log Book

Calculated By **Medical Physicist**

APPENDIX 10: Ring and Tandem *In-vitro* Bladder and Rectum Dose Measurements

Ring & Tandem			*In-vivo* doses [Gy]		*In-Vitro* Measurements [Gy]											
	Study	Applicator	Bladder	Rectum	R_1	R_2	R_3	R_4	R_{av}	R_{std}	B_1	B_2	B_3	B_4	B_{av}	B_{std}
1	1	R2T7	5.400	2.450	2.060	2.066	2.061	2.063	2.063	0.003	4.378	4.344	4.325	4.326	4.343	0.025
2			4.675	3.404	3.024				3.024		4.094				4.094	
3	2	R2T5		2.375	2.516	2.509	2.497		2.507	0.010						
4	3	R2T7	3.350	2.486	2.635	2.637	2.637	3.299	2.802	0.331	2.782	2.785	2.786	2.575	2.732	0.105
5	4	R2T5		1.410	1.479	1.441	1.513		1.478	0.036						
6	5	R2T5	4.060	2.935	4.151	4.090			4.121	0.043						
7	6	R2T7	7.162	3.994	2.374	3.279	2.621		2.758	0.468	5.166	5.987	5.391		5.515	0.424
8	7	R2T7	4.027	4.576	3.806	3.581			3.694	0.159	4.451	4.546			4.499	0.067
9	8	R2T5		4.905	3.295	3.336	3.293		3.308	0.024						
10	9	R2T5	3.060	2.631	2.448	2.590			2.519	0.100	2.834	2.602			2.718	0.164
11			3.458	2.737	2.252	2.273	2.249		2.258	0.013	4.253	4.872	4.678		4.601	0.317
12	10	R2T7	2.852	3.820	3.139	3.050			3.095	0.063	2.665	2.809			2.737	0.102
13			3.114	3.025	2.505	2.666			2.586	0.114	3.307	3.334			3.321	0.019
14				4.390	3.004	3.046			3.025	0.030	3.414	3.649			3.532	0.166
15	11	R2T5	2.930	3.000	2.467	2.551			2.509	0.059	2.856	2.881			2.869	0.018
16			2.735	3.128	2.065	2.085			2.075	0.014	2.501	2.438			2.470	0.045
17			3.434	3.664	2.684	2.730			2.707	0.033	3.548	3.603			3.576	0.039
18	12	R2T5	4.487	2.443	1.947	2.042			1.995	0.067	4.351	4.242			4.297	0.077
19				2.897	2.594	2.986			2.790	0.277	3.818	4.238			4.028	0.297
20	13	R2T5	5.000	3.600	2.467	2.515	2.421		2.468	0.047	4.268	4.532	4.714		4.505	0.224
21				3.464	2.986	2.986			2.986	0.000						
22	14	R2T5		2.903	2.251	2.548			2.400	0.210	2.163	2.132			2.148	0.022
23			3.841	3.097	2.295	2.307			2.301	0.008	3.487	3.401			3.444	0.061
24	15	R2T7	3.301	2.375	2.115	2.130	2.129		2.125	0.008	5.899	6.435	6.258		6.197	0.273
25			2.797	4.011	2.810	2.837			2.824	0.019	2.443	2.470			2.457	0.019
26	16	R2T7	1.930	2.215	2.282	2.201	2.317		2.267	0.060	4.789	5.751	5.580		5.373	0.513
27			5.263	2.565												
28				3.326	2.975	2.893			2.934	0.058	1.698	1.681			1.690	0.012
	17	R2T5		3.722	2.980	2.952	3.067		3.000	0.060	4.011	3.894	3.946		3.950	0.059
29	18	R2T5	2.385	3.440	2.373	2.295	2.463		2.377	0.084	8.487	8.356	8.750		8.531	0.201
30			4.482	2.787	2.836	3.020			2.928	0.130	3.681	4.097			3.889	0.294
31			4.025	3.074	2.817	2.535			2.676	0.199	3.547	3.445			3.496	0.072
32	19	R2T5			2.928	2.957			2.943	0.021	1.029	1.045			1.037	0.011
33				3.194	3.029	3.005			3.017	0.017	1.003	1.006			1.005	0.002
34				4.144	3.546				3.546		0.969				0.969	
35	20	R2T5		3.486	3.355	2.634	2.898		2.962	0.365	2.869	2.954	2.911		2.911	0.043
36			3.091	3.058	2.096	1.985			2.041	0.078	3.119	3.156			3.138	0.026
37			2.587	2.478	2.276				2.276		4.520				4.520	
38	21	R2T7	4.845	2.356	2.253	1.660			1.957	0.419	5.102	4.517			4.810	0.414
39				2.716	3.204	2.564			2.884	0.453	2.190	2.805			2.498	0.435
40					2.645	2.713	2.690		2.683	0.035	3.288	3.582	3.068		3.313	0.258
41	22	R2T3			2.972				2.972							

APPENDIX 11: Vaginal Cylinder and Tandem *in-vitro* Bladder and Rectum Dose Measurements

Vaginal Cylinder and Tandem			TPS Doses [Gy]			*In-vivo* doses [Gy]		*In-Vitro* Measurements [Gy]								
	Study	Applicator	Point A	Bladder	Rectum	Bladder	Rectum	B_1	B_2	B_{av}	B_{st}	R_1	R_2	R_3	R_{av}	R_{st}
1	5	3Cyl4Tan	5.0		2.22		2.365					2.512	2.510	2.505	2.509	0.004
2	6	3Cyl6Tan	5.0		2.01		2.420					2.410	2.435		2.423	0.018
3			5.0		2.57		2.420					2.967	2.969	2.974	2.970	0.004
4	8	3Cyl6Tan	5.0	2.67	2.32	2.960	2.770	2.722	2.711	2.717	0.008	2.869	2.762		2.816	0.076
5	10	3Cyl6Tan	5.0	4.10	2.56	4.04	4.430	5.167	4.869	5.018	0.211	4.089	4.284		4.187	0.138
6			5.0	2.51	3.20	2.609	4.901	2.300	2.304	2.302	0.003	4.055	4.183		4.119	0.091
7	14	3Cyl4Tan	5.0	2.85	2.66	2.694	3.533	2.726	2.683	2.705	0.030	2.195	3.561		2.878	0.966
8			5.0	9.50	2.14	12.17	3.192					2.818	3.152		2.985	0.236
9	17	3Cyl6Tan	5.0	2.96	2.59	2.682	3.866	3.117	3.073	3.095	0.031	3.528	3.598	3.549	3.558	0.036
10	20	3Cyl4Tan	5.0	2.60				2.555	2.497	2.526	0.041	2.476	2.370		2.423	0.075
11	21	3Cyl4Tan	6.0	5.33	1.70	5.052	2.758	4.981	5.017	4.999	0.025	2.231	2.313		2.272	0.058

APPENDIX 12: Ethics Approval

UNIVERSITY OF CAPE TOWN

Health Sciences Faculty
Human Research Ethics Committee
Room E52-24 Groote Schuur Hospital Old Main Building
Observatory 7925
Telephone [021] 406 6338 • Facsimile [021] 406 6411
e-mail: shuretta.thomas@uct.ac.za

07 December 2011

HREC REF: 545/2011

Mr F Hliziyo
c/o Dr T Kotze
Medical Physics
L-Block

Dear Mr Hliziyo

PROJECT TITLE: DOSE INTERCOMPARISONS BETWEEN COMPUTER PLANNING, IN-VIVO AND PHANTOM MEASUREMENTS FOR IRIDIUM-192 HDR BRACHYTHERAPY.

Thank you for responding to the issues raised by the Faculty of Health Sciences Human Research Ethics Committee.

It is a pleasure to inform you that the HREC has **formally approved** the above-mentioned study.

Approval is granted for one year till the 15th December 2012.

Please submit a progress form, using the standardised Annual Report Form (FHS016), if the study continues beyond the approval period. Please submit a Standard Closure form (FHS010) if the study is completed within the approval period.

Please note that the ongoing ethical conduct of the study remains the responsibility of the principal investigator.

Please quote the HREC. REF in all your correspondence.

Yours sincerely

Wesley Brooks

pp **PROFESSOR M BLOCKMAN**
CHAIRPERSON, HSF HUMAN ETHICS
Federal Wide Assurance Number: FWA00001637.
Institutional Review Board (IRB) number: IRB00001938

This serves to confirm that the University of Cape Town Human Research Ethics Committee complies to the Ethics Standards for Clinical Research with a new drug in patients, based on the Medical Research Council

s.thomas

REFERENCES

Alecu, R. & Alecu, M., 1999. In-vivo rectal dose measurements with diodes to avoid misadministrations during intracavitary high dose rate brachytherapy for carcinoma of the cervix. *Medical Physics,* 26(5), pp. 768-770.

Anon., 2012. *Wikipedia.* [Online]
Available at: http://en.wikipedia.org/wiki/Brachytherapy
[Accessed 15 February 2012].

Baltas, D., Sakelliou, L. & Zamboglou, N., 2007. *The Physics of Modern Brachytherapy for Oncology.* 1st ed. New York London: Taylor and Francis.

Barillot, I., Horiot, J. & Maingon, P., 2000. Impact on treatment outcome and Late Effects of Customized Treatment Planning in Cervix Carcinomas. *International Journal of Radiation Oncology, Biology and Physics,* Volume 48, pp. 189-200.

Barillot, I., Horiot, J., Maingon, P., Bone-Lepinoy, M., Vaillant, D., Feutray, S., 1994. Maximum and mean bladder dose defined from ultrasonography. Comparison with the ICRU reference in gynaecological brachtytherapy. *Radiotherapy and Oncology,* Volume 30, pp. 231-238.

Battermann, J., Boon, T. & Moerland, M., 2004. Results of permanant prostate brachytherapy, 13 years of experience at a single institution.. *Radiotherapy and Oncology,* 71(1), pp. 23-28.

Bevington, P. R. & Robinson, K. D., 1992. *Data Reduction and Error Analysis for the Physical Sciences.* 2nd ed. s.l.:WCB/McGraw-Hill.

Bochud, F., Leemann, B., Linder, R., Moeckli, R., Münch, K., Nemec, H. Sassowsky, M., Stucki, G., 2005. *Dosimetry and Quality Assurance in High Dose Rate Brachytherapy with Iridum-192, Recommendation N0. 13,* s.l.: Swiss Society for Radiobiology and Medical Physics.

Datta, N., Srivastava, A., Das, J., Gupta, A., Rastogi, N., 2006. Comparative assessment of doses to tumor, rectum, and bladder as evaluated by orthogonal radiographs vs. computer enhanced computed tomography-based intracavitary brachytherapy in cervical cancer. *Brachytherapy ,* Volume 5, pp. 223-229.

Devlin, P., 2007. *Brachytherapy Applications and Techniques.* 1st ed. s.l.:Lippincott Williams & Wilkins.

Dowdy, S., Weardon, S. & Chilko, D., 2004. *Statistics for Research.* Third ed. New Jersey: John wiley & Sons, Inc.,.

Dutreix, A., 1984. When and how can we improve precision in radiotherapy. *Radiotherapy Oncology,* Volume 2, pp. 275-292.

Esche, B., Crook, J. & Horiot, J., 1987. Dosimetric methods in the optimization of radiotherapy for carcinoma of the uterine cervix. *International Journal of Radiation Oncology, Biology and Physics,* Volume 13, pp. 1183-92.

Essers, M. & Mijnheer, B., 1999. In vivo dosimetry during external photon beam radiotherapy. *International Journal of Radiation Oncology Biology and Physics,* 43(2), pp. 245-259.

Galalae, R., Martinez, A., Mate, T., Mitchell, C., Edmundson, G.,Nuernberg, N., Eulau, S, Gustafson, G. , 2004. Long-term outcome risk factors using conformal high-dose-rate brachytherapy (HDR-BT) boost without neoadjuvant androgen suppression for localized prostate cancer. *International Journal of Radiation Oncology, Biology and Physics,* 58(4), pp. 1048-1055.

Gerbaulet, A., Pötter, R., Mazeron, J.J., Meertens, H.' Van Limbergen, E., 2005. *The GEC Estro Handbook of Brachytherapy.* Vienna: IAEA.

Godden, T., 1988. *Physical aspects of Brachytherapy.* Bristol: Adam Hilger/International Organisation of Physicists (IOP) Publishing.

Haie-Meder, C., Chargari, C., Rey, A., Dumas, I, Morice, P., Magne, N. , 2009. DVH parameters and outcome for patients with early-stage cervical cancer treated with preoperative MRI-based low dose rate brachytherapy followed by surgery. *Radiotherapy and Oncology,* 93(2), pp. 316-321.

Haie-Meder, C., Kramar, A. & Lambin, P., 1993. Analysis of complications in a prospective randomized trial comparing two brachytherapy low dose rates in cervical carcinoma. *International Radiation Oncology, Biology and Physics,* 29(5), pp. 419-24.

Hareyama, M., Sakata, K., Oouchi, A., Nagakura, H., Shido, M., Someya, M., Koito, K., et al., 2002. High-dose-rate versus low-dose-rate intracvitary therapy for carcinoma of the uterine cervix: a randomized trial.. *Cancer,* 94(1), pp. 117-124.

Hassouna, A., Bahadur, Y., Constantinescu, C., El Sayed, M., Naseem, H., Naga, A., 2011. In vivo diode dosimetry vs. computerized tomography and digitally reconstructed radiographs for critical organ dose calculation in high-dose-rate brachytherapy of cervical cancer. *American Brachytherapy Society.*

Huh, H.,WooChul, K., Loh, J., Lee, S., Kim, C., Lee, S., Shin, D.,; Shin, D., Cho, S., Lim, S., Cho, K., Kwon, S., Kim, S., 2007. Rectum Dose Analysis Employing a Multi-purpose Brachytherapy Phantom;. *Japan Journal of Clinical Oncology,* 37(5), pp. 391-398.

Huyskens, D., Bogaerts, R., Verstraete, J., Loof, M., Nystrom, H., Fiorino, C., Broggi, S., Jornet, N., Ribas, M., Thwaites, D., 2001. *Practical Guidleines For The Implementation of In Vivo Dosimetry with Diodes In External Radiotherapy With Photon Beams (Entrance Dose).* 1st ed. s.l.:ESTRO.

IAEA-TECDOC-1585, 2008. *Measurement Uncertainty: A Practical guide for Secondary Standards Dosimetry Laboratories,* Vienna: IAEA.

ICRU, 1954. London: British Journal of Radiology.

ICRU, 1962. *Radiation Quantities and Units Report 10a ,* Washington: International Commision on Radiological Units.

ICRU, 1976. *Determination of absorbed dose in a patient irradiated by beams of X- and Gamma raysin radiotherapy procedures,* Washington D.C.: International Commission on Radiation Units and Measurements.

ICRU, 1979. *Average Energy Required to Produce an Ion Pair Report No.31 ,* Washington: ICRU.

ICRU, 1980. *Radiation Quantities and Units Report No. 33,* Washington DC: International Commission on Radiological Units.

ICRU, 1985. *Dose and Volume Secification for Reporting Intracavitary Therapy in Gynecology, Vol. 38,* Bethesda,MD: International Commision on Radiation Units and Measurements.

ICRU, 1989. *Tissue Substitutes in Radiation Dosimetry and Measurement,* Bethesda: International Commission on Radiation Units and Measurements.

ICRU-38, 1985. *Dose and Volume Specification for Reporting Intracavitary Therapy in Gynecology, Vol. 38,* Bethesda,MD: International Commision on Radiation Units and Measurements.

ICRU-44, 1989. *Tissue Substitutes in Radiation Dosimetry and Measurement,* Bethesda: International Commission on Radiation Units and Measurements.

Khan, F. M., 2010. *Physics of Radition Therapy.* s.l.:Lippicott Williams & Wilkins.

Kim, R. & Pareek, P., 2003. Radiography based treatment planning compared with computed tomography (CT)-based treatment planning for intracavitary brachytherapy in cancer of the cervix:Analysis of dose-volume histograms. *Brachytherapy* , Volume 2, pp. 200-206.

Kim, W. C., Kim, G. E., Suh, C. O. & Loh, J. J., 2001. High Versus Low Dose Rate Intracavitary Irradiation for Adenocarcinoma of the Uterine Cervix. *Japanese Journal of Clinical Oncology,* 31(9), pp. 432-437.

Kondo, S. & Randolph, M., 1960. Effect of finite size of ionization chambers on measurements of small photon sources.. *Rad.Research,* Volume 13, pp. 37-60.

Kutcher, G., Coia, L., Gillin, M., Hanson, W., Leibel, S., Morton, R., Palta, J., Purdy, J., Reinsten, L., Svensson, G., Weller, M., Wingfield, L., 1994. Comprehensive QA for Radiation Oncology : Report of AAPM Radiation Therapy Committee Task Group 40. *Medical Physics*, 21(4), pp. 581-618.

Nag, S., Erickson, B., Thomadsen, B., Orton, C., Demanes, J., Petereit, D.., 2000. The American Brachytherapy Society Reccommendations for High-Dose-Rate Brachytherapy for Carcinoma of the Cervix. *International Journal of Radiation Oncology, Biology and Physics*, 48(1), pp. 201-211.

NASA, N. A. S. A., 2010. *Measurement Uncertainty Analysis Principles and Methods:NASA Measurement Quality Assurance Handbook-ANNEX 3*. Washington,USA: NASA.

Nath, R.,Anderson, L., Luxton, G., Weaver, K., Meigooni, A.,., 1995. *Dosimetry of Interstitial Brachytherapy Sources: Recommendations of the AAPM Radiation Therapy Committee Task Group No. 43,* New York: American Institute of Physics.

Newman, G., 1996. Increased morbidity following the introduction of remote afterloading, with increased dose rate, for cancer of the cervix. *Radiotherapy Oncology*, Volume 39, pp. 97-103.

Perez, C., Breaux, S. & Bedwinek, J., 1991. Impact of dose outcome of irradiation alone in carcinoma of the uterine cervix:analysis of two different methods.. *International Journal of Radiation Oncology, Biology and Physics,*, Volume 21, pp. 885-98.

Perez, C., Grigsby P.W., & Nene, S., 1999. Radiation morbidity in carcinoma of the uterine cervix: dosimetric and clinical correlation. *International Journal of Radiation Oncology, Biology and Physics*, Volume 44, pp. 855-66.

Pickles, T., Keyes, M. & Morris, W., 2009. Brachytherapy or Conformal External Radiotherapy for Prostate Cancer: A Single-Institution Matched-Pair Analysis. *International Journal of Radiation Oncology, Biology and Physics*, 76(1), pp. 43-49.

Podgorsak, E., 2005. *Radiation Physics: "A handbook for Teachers and students".* 1st ed. Vienna: International Atomic Energy Agency.

Pötter, R.,Haie-Meder, C., Van Limbergern, E., Barillot, I., De Brabandere, M., Dimopoulos, J., Dumas, I., Erickson, B., Lang, S., Nulens, A., Petrow, P., Rownd, J., Kirisitis, C., 2006. Recommemndations from gynaecological (GYN) GEC ESTRO working group (II): Concepts and terms in 3D image-based treatment planning in cervix cancer brachytherapy-3D dose volume parameters and aspects of 3D image-based anatomy, radiation physics, radiobiolog. *Radiotherapy and Oncology,* Volume 78, pp. 67-77.

Pötter, R., Knocke, T., Fellner, C., Baldass, M., Reinthaller, A., Kucera, H., 2000. Definitive radiotherapy based on HDR brachytherapy with Iridium 192 in uterine crevic carcinoma: report on the Vienna University Hospital findings (1993-1997) compared to the preceding period in the context of ICRU recommendations. *Cancer Radiothérapie,* 4(2), pp. 159-172.

Qi, Z., Deng, X., Huang, S., Lu, J., Lerch, M.,; Cutajar, D.,; Rosenfeld, A.,., 2007. Verification of the plan dosimetry for high dose rate brachytherapy using metal-oxide-semiconductor field effect transistor detectors.. *Medical Physics,* 34(6).

Rabinovich, S. G., 2005. *Measurement Errors and Uncertainties, Theory and Practice.* Third Edition ed. New York: Springer.

Samiei, F., Dehghan Manshadi, H.., Jaberi, R., Sharafi, A., Meysami, A.P., Gharaati,H.., 2006. Rectal Dose Evaluation and comparison between in-vivo and planning dosimetry in patients with cervical and endometrial cancer whho received brachytherapy treatment. *Journal of Iran University of Medical Sciences,* 12(49).

Stewart, A. J. & Viswanathan, A. N., 2006. Current controversies in high-dose-rate versus low-dose-rate brachytherapy for cervical cancer.. *Cancer,* 107(5), pp. 908-915.

Tamaka, T., Ishikawa, H., Takahashi, T., Tamaki, Y., Kitamoto, Y.,Okamoto, M., Noda, S., Katoh, H., Shirai, K., Sakurai, H., Nakano, T.,., 2012. Comparison of efficacy and safety of low-dose-rate vs. high-dose-rate intraluminal brachtherapy boost in patients with superficial esophagal cancer. *Brachytherapy,* Volume 11, pp. 130-136.

Taylor, J. R., 1997. *An Introduction to Error analysis: The Study of Uncertainties in Physical Measurements.* 2nd ed. s.l.:University Science Books.

Tyrell, S., 2009. *SPSS :Stats Practically Short and Simple.* 1st ed. s.l.:Sidney Tyrell and Ventus Publishing ApS.

Venselaar, J.,Aalbers, A., Brouwer, W., Meertens, H., Petersen, J., Schaeken, B.,Visser, A., 1994. *Recommendations for the Calibration of Iridium-192 High Dose Rate Sources,* s.l.: Netherlands Commission on Radiation Dosimetry.

Venselaar, J., Perez-Calatayud, J., Tolli, H., Teixeira, N., Roue, A., Rijnders, A., Marchetti, C., Kawszynska, M., Kneschaurek, P., Kirisits, C., Grusell, E., Ferreira, I., Briot, E., Bidmead, M., 2004. *A Practical Guide to Quality Control of Brachtherapy Equipment.* 1st ed. Brussels: European Guidelines for Quality Assurance in Radiotherapy.

Viani, A., Manta, G., Stefano, E. & de Fendi, L., 2009. Brachytherapy for cervix cancer: low-dose rate brachtherapy -a-meta-analysis of clinical trials. *Journal for Experimental and clinical Research,* 28(47).

Viswanathan, A. N. & Petereit, D. G., 2007. Gynecologic Brachytherapy. In: P. M. Devlin, ed. *Brachytherapy:Applications and Techniques.* s.l.:Lippincott Williams & Wilkins, pp. 223-267.

Wäldhausl, C., Wambersie, A., Potter, R. & Georg, D., 2005. In-Vivo Dosimetry for Gynaecological Brachytherapy: Physical and Clinical considerations.. *Radiotherapy and Oncology,* Issue 77, pp. 310-317.

Wang, C., Leung, S. & Chen, H., 1997. High-dose-rate intracavitary brachytherapy (HDR-IC) in treatment of cervical carcinoma; 5-year results and implication of increased low-grade rectal complication on inititian of an HDR-IC fractionation scheme. *International Journal of Radiation Oncology Biology Physics,* 38(2), pp. 391-398.

Wang, X., Liu, R., Ma, B, Yang, K., Tian, J., Jiang, L., Bai, Z., Hao, X., Wang, J., Li, J., Sun, S., Yin, H., 2010. High dose rate versus low dose rate intracavitary brachytherapy for locally advanced uterine cervix cancer.. *Cochrane Database System Review,* Issue 7, p. CD007563.

Wikidot, 2012. *www.wikidot.com.* [Online]
Available at: http://electrons.wikidot.com/pair-production-and-annihilation
[Accessed 26 March 2012].

Wilkinson, D., 2010. *Commissionoing of an In-Vivo Dosimetry System for High Dose Rate Gynaecological Brachytherapy.* [Online]
Available at: http://ro.uow.edu.au/theses/3277
[Accessed 20 October 2011].

Williamson, J., 1988. Monte Carlo and analytic calculation of absorbed dose near Caesium-137 intracavitary sources. *Interantional Journal of Radiation Oncology,Biology and Physics,* Volume 15, pp. 227-237.

Yaparlvi, R., Mutyala, S., Gorla, G.,Butler, J.,Mah, D., Garg, M., Kalnincki, S., 2008. Point vs. volumetric bladder and rectal doses in combined intracavitary-interstitial high-dose-rate brachytherapy: Correlation and comparison with published Vienna applicator data. *Brachyhtherapy* , Volume 7, pp. 336-342.

Yorke, E., Alecu, R., Ding, L., Fontenla, D., Kalend, A., Kaurin, D., Masterson-McGary, M., Marinello, G., Matzen, T., Saini, A., Shi, J., Simon, W.,Zhu, T., Zhu, X., Rikner, G., Nilsson, G., 2005. *Diode in vivo dosimetry for patients receiving External Beam Radiation Therapy,* Madison: American Association of Physicists in Medicine (AAPM) Report No. 87, Task Group 62.